

HUNGARIAN

AGRICULTURAL

ENGINEERING





HUNGARIAN
ACADEMY
OF SCIENCES

Hungarian Agricultural Engineering

N^o 31/2017

Editors-in-Chief:
Dr László TÓTH
Dr. László KÁTAI

Managing Editor:
Dr. Csaba FOGARASSY

Secretary of Editorial board:
Dr. László MAGÓ

Editorial Board:

Dr. David C. FINGER
Dr. György SITKEI
Dr. Gábor KESZTHELYI-SZABÓ
Dr. László TÓTH
Dr. János BEKE
Dr. István SZABÓ
Dr. István J. JÓRI
Dr. Béla HORVÁTH
Dr. Péter SEMBERY
Dr. László FENYVESI
Dr. Csaba FOGARASSY
Dr. Zoltán BÁRTFAI
Dr. László MAGÓ
Dr. Bahattin AKDEMIR
Dr. R. Cengiz AKDENİZ
Dr. József NYERS
Dr. Mićo V. OLJAČA
Dr. Zdenek PASTOREK
Dr. Vijaya G.S. RAGHAVAN
Dr. Lazar SAVIN
Dr. Bart SONCK
Dr. Goran TOPISIROVIĆ
Dr. Valentin VLADUT

PERIODICAL OF THE COMMITTEE OF
AGRICULTURAL ENGINEERING OF
THE
HUNGARIAN ACADEMY OF SCIENCES

Published by

Szent István University, Gödöllő
Faculty of Mechanical Engineering
H-2103 Gödöllő, Páter K. u. 1.



Gödöllő
2017

Published online: <http://hae-journals.org>
HU ISSN 0864-7410 (Print)
HU ISSN 2415-9751(Online)

PREFACE

In the name of the Committee of Agricultural and Biosystem Engineering of the Hungarian Academy of Sciences we would like to welcome everyone who is interested in reading our journal. The Hungarian Agricultural Engineering (HAE) journal was published 30 years ago for the very first time with an aim to introduce the most valuable and internationally recognized Hungarian studies about mechanization in the field of agriculture and environmental protection. In the year of 2014 the drafting committee decided to spread it also in electronic (on-line and DOI) edition and make it entirely international. From this year exclusively the Szent István University's Faculty of Mechanical Engineering took the responsibility to publish the paper twice a year in cooperation with the Hungarian Academy of Sciences. Our goal is to occasionally report the most recent researches regarding mechanization in agricultural sciences (agricultural and environmental technology and chemistry, livestock, crop production, feed and food processing, agricultural and environmental economics and energy production) with the help of several authors. The drafting committee has been established with the involvement of outstanding Hungarian researchers who are recognized on international level as well. All papers are selected by our editorial board and a double blind review process by prominent experts which process could give the highest guarantee for the best scientific quality. We hope that our journal provides accurate information for the international scientific community and serves the aim of the Hungarian agricultural and environmental engineering research.

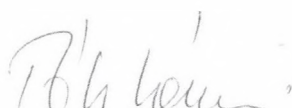
Special issue: Circular Economy

The Circular Economy (CE) is based on a holistic perspective which is built on all long term sustainable planning processes. It summarizes the special business solutions and circulation strategies to establish sustainability. The life cycle of products can be extended, the system can be kept close to a 'zero waste' state, and the material- and energy flows can be organized into mostly closed cycles. The circular economy framework proposes a global economic model that decouples economic growth and development from the consumption of finite resources. The system is based on some key principles related to technological and biological cycles. This includes a clear distinction between technological and biological materials, keeping them at their highest value at all times.

This Special Issue of the Hungarian Agricultural Engineering introduces papers on any of these themes, concepts, principles and technical solutions in cooperation with the Circular Economy: Focus on Renewable Energy Conference and Roundtable program (Project ID: HU03-0005-C1-2014).



Dr. László KÁTAI
editor in chief



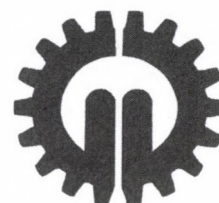
Dr. László TÓTH
editor in chief



Dr. Csaba FOGARASSY
editor of special issue

The "Circular Economy scientific special issue" was supported by the HU03-0005-C1-2014 project which is part of the EEA Grants 2009-2014 Renewable Energy programme area.
www.eeagrants.org, www.egt-newenergy.szie.hu "





THE APPLICATION OF LIFE CYCLE ASSESSMENT IN CIRCULAR ECONOMY

Author(s):

K. Tóth Szita^{1,2}

Affiliation:

¹Faculty of Economics, University of Miskolc, H-3515 Miskolc, Hungary

²LCA Centre, Iglói street 2, H-3519 Miskolc, Hungary

Email address:

regszita@uni-miskolc.hu

Abstract

Circular Economy's concept is becoming more and more widespread in the world. It's fundamental philosophy is that the waste of one system can become the input of another, thereby increasing resource efficiency, and decreasing environmental load. However, the circular economy model does not always mean environmental gains. Therefore, before using it, taking a more in-depth look at the environmental, social, and economic effects of the planned technological solution from the perspective of life cycle, and only introducing it, if their combined effects are more advantageous than the open-chain technological lining. The study takes a look at the basics of circular economy and life cycle, and sheds light on the advantages of realising the economic model via a LCA.

Keywords

circular economy, sustainability, life cycle assessment

1. Introduction

The success of circular economy in Europe and the entire world has become more prominent in recent years, even though the description itself is nothing new. Circular

economy combines multiple theoretic concepts and practical applications. We can find within it the thought of industrial ecology [1], the from cradle to cradle theorem [2], and blue economy [3], even bio-mimicry. The latter one is adapting living, naturally developed solutions into technical practice. The material exchange processes happen in closed systems within the circular model, waste and by-products are nearly 100% recycled. Some authors think that CE combines the thoughts of 3R (reduce, reuse, recycle), even 6R (reduce, reuse, recycle, redesign, remanufacture, recover) with zero emission, LCA and resource efficiency's concepts [4]. Within the European Union, an annual 15 tonnes of material is used per capita, of which 4,5 tonnes per capita becomes waste,

more than half of which is dumped. Changing to a circular economy slows down and prevents waste production, as repair and recycling is put into focus, and waste is considered a resource. If environmental considerations were taken seriously even during the planning phase, "preventing waste production could spare up to 604 billion Euros for the European business life, meanwhile, could decrease GHG emission by 2-4%". The model of circular economy means many advantages for Europe. It helps sustainable economic growth, job establishing, and efficiency increase as well [5]. The Ellen MacArthur Foundation is the frontline warrior in serving the model, but circular economy was integrated into the EU's legislation too [6].

2. Basics of circular economy

Circular economy is based on three basic principles. First is to protect environmental capital, and develop it, through the regulated usage of available resources, and the balance of renewable resource flow. This all suggest a strong decrease in material, and f. e. create the conditions for soil regeneration.

The second principle is to optimise resource extraction by way of circulating products, parts and materials, which maximises their appearance in the technical and biological cycle. This means that remanufacturing, refurbishing and maintenance are well-planned, in order to make materials a part of economic processes for as long as possible.

The third principle is to minimise negative externalities, eliminate toxic substances, by either replacing or reducing them. In the planning phase, waste can be reduced by choosing appropriate materials, which also decreases harmful substance emission. However, fossilised energy resources can only be replaced by renewable ones [7]. The model of circular economy is based on closing opened economic flows [7]. In the case of open processes, intervening in the environment starts with resource extraction, and ends with waste entering the environment as follows:

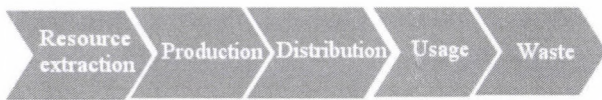


Figure 1. Model of open chain process

However, in circular economy [7]:

- waste is equal to nutrients,
- variety is an important virtue,
- energy has to be extracted from renewable sources,
- prices has to be consistent with reality, and it is important that
- we think in terms of systems.



Figure 2. Model of circular economy [8]

The European Committee, and the Circular Economy

The European Committee accepted the legislation package regarding circular economy on the 2. December, 2015,

which has the goal of "advocating Europe's transition to a circular economic system which increases international competitiveness, helps economic growth, and creates new jobs." [9]. According to the views of the European Committee, the economic model based on circular processes:

- aids recycling and prevents the loss of valuable materials;
- creates jobs and causes economic growth;
- creates new business models, and makes waste-free concepts realisable through eco-design and industrial symbiosis, and
- decreases the emission of greenhouse gases, and detrimental environmental effects.

The package aims to rethink waste management and tries to create a new regulation background by taking long-term conditions into consideration, and by integrating the life cycle perspective in a way that they motivate for the best solutions for the life cycle stages, and make the closure of processes realised. Using circular economy on a company level can spare about 8% costs according to estimates, while the emission of greenhouse gases can be reduced by up to 2-4%.

In order to realise the action plan, many conditions, regulations are needed. For example, environment-friendly planning's principle and regulations related to product requirements, manufacturer responsibility, profession policy requirements, etc.

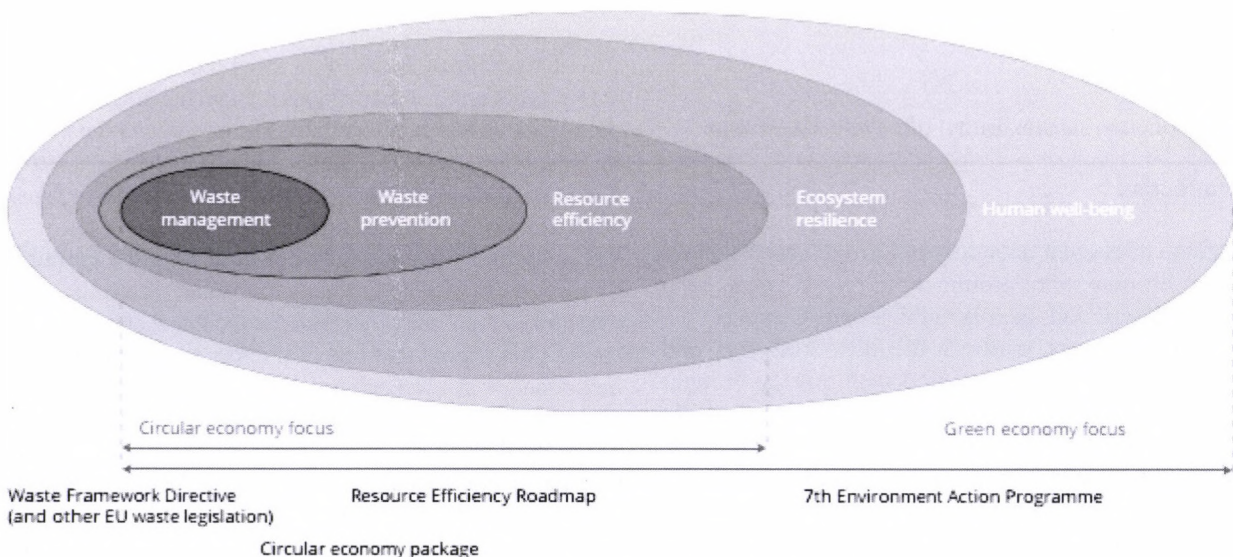


Figure 3. Circular economy and green economy [10]

In Europe, the Netherlands is the most dedicated follower of circular economy. There are many inspirational solutions for the many sectors today, but in order to spread these, there is a need to maintain a continuous knowledge transfer. In order to make CE spread as widely as possible,

people's attitude itself has to be changed. Though sustainable resource management's new solutions are achievable for business life, practical application and creation of motivators acceptable for the task is dependent on the action plans of the State and the EU.

Characteristics of a circular economy

The most notable characteristics of circular economy are [10]:

Less input and natural resource usage:

- minimal and optimised usage of resources,
- producing more value from less material;
- decreasing import dependence of natural resources;
- efficient natural resource utilisation,
- minimal energy and water consumption.

Renewable, recyclable resources and energy have to have their share increased:

- exchanging non-renewable energy resources for renewable ones, and maintaining sustainable supply,
- increasing the share of recycled and recyclable materials, in exchange of new materials,
- closing material loops,
- materials from sustainable sources.

Decreasing emission levels:

- decreased emission compared to the full cycle of less and sustainable material,
- less environment-polluting clean material cycles.

Reduced losses and waste material:

- construction of waste minimisation;
- combustion and waste deposits are minimised;
- dissipative losses of valuable resources are minimised.

Protection of products', their parts' and materials' economic value:

- increased life expectancy,
- re-usage of parts;
- value protection of materials
- high-quality recycling.

Naturally, these require eco-design, and the creation of conditions related to repair and remanufacture, well-organised recycling, which also needs us to make a market for secondary material resources. There is a need for economic regulators, tenders, financial tools for domestic establishment, and innovation is indispensable.

Based on the experiences of already realised processes, it seems that the advantages of circular economy really are apparent in the following areas:

- reduced material- and energy usage,
- reduced unpredictability of material price and supply,
- reduction and diminishing of negative environmental external effects,
- creation of new jobs,
- increase in innovation,
- increase in the economy's international competitiveness,
- conserved advantages for a resistant and sustainable economy.

However, we may question if the principles of production processes and their related quality, green workplaces' protection (labour safety and labour health), and environmental protection are properly held onto, in the face of increasing economic advantages.

In order to create good models, taking the life cycle perspective into consideration is indispensable.

Lieder and Rashin studied many publications, and these made it obvious that using a circular model solution confers advantages and positive economic effects [11].

3. Life cycle assessments for aiding circular economy

Background of life cycle assessments

The description of life cycle relates to economy, more specifically, the cyclicity of micro-economies, and innovation, which became widely used due to the works of Schumpeter. Originally, it described products, and meant the timeframe in which a product, product group lasts from the start of manufacture and appearance on the market, until the end of manufacture, or leaving from the market. Later, it was expanded for technology, and even organisations, entrepreneurship, related to the companies' strategic activities, investments, and their quests, long-term goal changes. The life cycle's analysis and evaluation is meaningful because any intended or realised innovation (be it product, technological or organisational) can be called successful based on the investment's return. One of the most important decision criteria of intended innovation, and basis of evaluating the realised investment is to know the return time and excess profits achieved. The curve which describes product life cycle shows the product quantity or production values sold (or sellable) based on time, and generally shows a logistical, overflow tendency. The life cycle in an economic sense is naturally referring to a total amount of products manufactured during in some cycle, or technology which operates for a determined time, similarly to organisations operating as such. The life cycle description used in environment economy is much newer, it appeared in the early 1990's. The definition's appearance, and it's widespread use was caused by the general change induced by the advancement of environment studies and the attitude towards the environment. The main point of this change can be summarised as thought, action programmes and tasks shifted from environmental protection to environmental economy, from treating detrimental effects and making waste "disappear" towards prevention, and to the general definition of what sustainable development actually is. From this perspective, the life cycle can be related to some product, technological solution or organisation by pinpointing the timeframe "from birth to death", or "from cradle to grave". The analysis of life cycle affects the total environmental load for this period. From the input side, non-renewable and partially renewable energy resource utilisation, from the output side, any kind of environmental load and damage is affected by manufacture and usage, and disposal is determined in its chain, in quantities (natural units and / or money). The life cycle assessment's (LCA for short) meaning and goal is given exactly by finding the products, technological solutions and organisations, which offer the most advantageous, optimal environmental effect for a given demand's supply, with the given conditions, during a given timeframe (usually a year), or in other words, offer the solution with the lowest environmental load [12].

Using LCA for planning circular economy

In order to evaluate the effects of circular economy, using the life cycle assessment is a useful tool. LCA is a robust, scientifically based tool which can measure and evaluate products and business models coming from circular economy. It can strengthen advice on closed circular solutions, or may discard them, based on the results.

The analysis has to be, once again, conducted using the ISO 14040:2006 standard, closely following the methodology determined within. It is important to properly determine the system, to create the circular model, defining the function unit, and data requirements, furthermore, registering allocation. Collecting the input-output data along the life cycle has to be followed by an estimation of environmental effects using some kind of method. An often used environmental effect estimation is CML 2001, and the ReciPe method. As for effect categories, greenhouse effect, acidity potential, eutrophication, and toxicity are the focus areas.

LCA is a good addition, and basis for circular economy, as it helps introducing said economy in three steps. In the first step, the advantages or disadvantages of circular economy are analysed with LCA on a hypothetical product or service level. In the second step, after getting to know the limits, it identifies the possible development alternatives along the life cycle. This also includes rethinking developments. Finally, the third step is to determine the goal along the business strategy, by which we can start advancement towards circular economy.

LCA societies have an important role in introducing and spreading circular economy, as they have to give assurance about the legitimacy of CE solutions based on their objective analyses, and through making product declarations, they can aid the sustainability requirements of products coming from a CE more transparent. Therefore, not only the classic environmental life cycle assessment (eLCA) is advised to conduct, but the analysis conducted along the three principles of sustainability as well: apart from the eLCA, doing the life cycle cost analysis and social life cycle analysis (SLCA) are needed as well. These together give the life cycle sustainability analysis.

Using LCA, we can compare open and closed chain technological solutions, and in case the LCSA's result is better for the closed chain, introducing it is advised and legitimised. Meaning:

$$\frac{LCSA_{OPEN}(eLCA+LCC+SLCA)}{LCSA_{CLOSED}(eLCA+LCC+SLCA)} \geq 1$$

where:

eLCA is environmental life cycle assessment;

LCC is life cycle cost analysis,

SLCA is social life cycle assessment.

The latter two also have well-defined methodologies.

The above formula can be used for both products, manufacture processes, services, on either micro-, macro- or regional level. There are a multitude of publications within the international literature, which analysed the environmental effects of circular processes compared to open chain solutions. There were case studies for recycling foodstuff waste by creating circular models, [13] for renovating or

deconstructing buildings, and for processing the waste material from demolition work [14], and developing models based on the LCA of closed urban material flows, to mention a few examples. These were mostly dealing with the innovative processing of waste material.

The advantages of the circular model can also be explained with personal research results. After the sustainability analysis of a chemistry technological solution that works by producing and reusing a solvent, it was obvious that there was an improvement compared to the open chain technology, as we can see on the figure below.

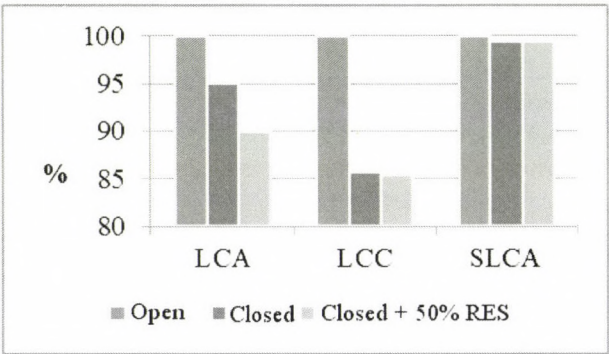


Figure 4. SLCA-based evaluation of technologies [15]

According to the 3D analysis, the highest sparing was at costs, whereas the lowest was from the perspective of social effects, but environmental load also decreased. It was obvious that the technology's material circulation caused advantageous effects. The positive result can be further improved by using renewable resources [15].

4. Conclusions

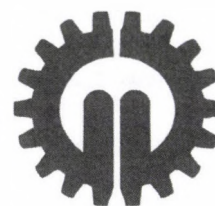
We can find an increasing amount of programmes related to circular economy, which has become more and more prevalent in recent years. Circular economy most notably reaches – with well-chosen technology – the decrease of environmental effects via economic advantages (waste management and material cost decrease). Economic organisations can move towards sustainable production methods by obtaining tender funding with innovative waste management technologies.

It is obviously advantageous if by the workings of circular economy - when waste is used to regain a part of the materials required for the technology - less material has to be procured, and the amount of waste decreases as well, but we cannot forget that such technologies require further resource usage. We have to decide what additive investment is required for the advantages that come with obtaining materials, and if the emissions of the technological solution made this way aren't more than the base technology. Circular technologies have legitimacy if the product manufactured this way have no greater environmental, social and economic effects for its entire life cycle than those of the original technology's. In order to determine this, we need the comparative effect analysis

based on life cycle assessment. If the total energy requirement is increased, its effect may be somewhat decreased, by using renewable energy resources.

References

- [1] **Ayres R. U., Simonis U. E.:** 1994. Industrial Metabolism: Restructuring for Sustainable Development. The United Nations University, pp. 390.
- [2] **Braungart M., McDonough W.:** 2009. Cradle to cradle: Remaking the Way We Make Things. Vintage Publisher, London, UK, pp. 208.
- [3] **Pauli G.:** 2010. Blue Economy – 10 Years, 100 Innovations, 100 Million Jobs. Club of Rome, Winthertur, Switzerland, pp. 336.
- [4] **Winans K., Kendall A., Deng H.:** 2017. The history and current applications of the circular economy concept. Renewable and Sustainable Energy Reviews, Vol. 68 (Part 1), pp. 825-833.
<http://dx.doi.org/10.1016/j.rser.2016.09.123>
- [5] **Ellen MacArthur Foundation.:** 2015. Circular Economy in Europe Towards a new economic model Growth Within: A Circular Economy Vision For a Competitive Europe. Ellen MacArthur Foundation Publisher, UK, pp. 98.
- [6] **European Commission.:** 2015. Closing the loop – An EU action plan for the Circular Economy. pp. 21.
- [7] **Ellen MacArthur Foundation.:** 2015. Towards the Circular Economy. Business rationale for an accelerated transition. Ellen MacArthur Foundation Publisher, UK, pp. 20.
- [8] **Stahel W. R.:** 2016. The Circular Economy, Nature, Vol. 531, pp. 436-438. <http://dx.doi.org/10.1038/531435a>
- [9] **Patrício J., Costa I., Niza S.:** 2015. Urban material cycle closing – assessment of industrial waste management in Lisbon region. Journal of Cleaner Production, Vol. 106, pp. 389-399.
<http://dx.doi.org/10.1016/j.jclepro.2014.08.069>
- [10] **Almut R., de Schoenmakere M., Gillabel J.:** 2016. Circular economy in Europe – Developing the knowledge base EEA Report No 2/2016. European Environment Agency, Luxembourg, pp. 42.
- [11] **Lieder M., Rashid A.:** 2015. Review Towards circular economy implementation: a comprehensive review in context of manufacturing industry. Journal of Cleaner Production, Vol. 115, pp. 36-51.
<http://doi.org/10.1016/j.jclepro.2015.12.042>
- [12] **Tóth Szita K.:** 2009. Az életciklus-elemzés kialakulása, fejlődése, értelmezése dióhéjban. Eco-Matrix, Vol 1, No. 1, 5-8.
- [13] **Corrado S., Ardente F., Sala S., Saouter E.:** 2017. Modelling of food loss within life cycle assessment: From current practice towards a systematisation. Journal of Cleaner Production, Vol. 140 (Part 2), pp. 847-859.
<http://dx.doi.org/10.1016/j.jclepro.2016.06.050>
- [14] **Assefa G., Ambler C.:** 2017. To demolish or not to demolish: Life cycle consideration of repurposing buildings. Sustainable Cities and Society, Vol. 28, pp. 146–153. <http://dx.doi.org/10.1016/j.scs.2016.09.011>
- [15] **Zajáros A., Tóth. Szita K., Matolcsy K., Horváth D.:** 2016. Veszélyes hulladékból történő oldószer-visszanyerés életciklus szemléletű vizsgálata. [Life cycle assessment of solvent-recovery from hazardous waste] in Szilágyi A. (ed) 2016. Életciklus Szemlélet A Körforgásos Gazdaságban [Lifecycle perspective in the Circular Economy], Budapest, Hungary pp. 93-102.



THE DEVELOPMENT OF A CIRCULAR EVALUATION (CEV) TOOL – CASE STUDY FOR THE 2024 BUDAPEST OLYMPICS

Author(s):

Cs. Fogarassy¹ – A. Kovacs² – B. Horvath¹ – M. Borocz¹

Affiliation:

¹Climate Change Economics Research Centre, Szent István University, Páter Károly street 1.,
H-2100 Gödöllő, Hungary

²Department of Operations Management and Logistics, Szent István University, Páter Károly street 1.,
H-2100 Gödöllő, Hungary

Email address:

fogarassy.csaba@gtk.szie.hu, kovacs.attila@gtk.szie.hu, horvath@carbonmanagement.hu, borocz.maria@gtk.szie.hu

Abstract

According to the early candidate intentions, The Budapest 2024 Bid Committee goal was to submit a responsible and sustainable Games plan to the IOC. In doing so, it became evident that a superior approach would be needed than that adopted by cities hosting earlier versions of the Olympic and Paralympic Games. In recent years, Olympic Games were successfully organised from the perspective of handling sustainability. The previously applied low-carbon standards aimed to mitigate the greenhouse gas (GHG) emissions comparing to business-as-usual (BAU) processes. However, the carbon management strategy is still limited to the decarbonization of material stocks assigned to certain functions. This is the reason for the appearance of a new economic perception, Circular Economy which is built on sustainable material flow and reasonable resource utilization. While the low-carbon concept aimed to optimize the application of stocks, circular economy rather applies services for the same functions. Therefore, the mechanism eliminates the potential emission sources in the first place. This paper aims to introduce a calculation method which helps to assess the stock intensity of activities throughout the Olympics lifecycle (preparation, host of games, legacy periods). The outcome of the methodology, the Circular Economic Value (CEV) highlights the main improvement points on the initial BAU plans. This theoretical model will be used for the future evaluation of the Budapest 2024 Olympic Games, where future researches are expected to associate cost-benefit ratios to this value and enable decision makers to apply the accurate circular planning tools to enhance circularity of the long term Olympic programming.

Keywords

circular planning, Budapest Olympic Games, circular economic value, sustainable games, circular economy model, closing loops, priority levels of circularity

1. Introduction

According to the early candidate intentions, The Budapest 2024 Bid Committee goal was to submit a responsible and sustainable Games plan to the IOC. In doing so, it became evident that a superior approach would be needed than that adopted by cities hosting earlier versions of the Olympic and Paralympic Games. To realise this, they wish to make use of the business solutions and methods employed by the planning of circular economic systems.

In recent years, Olympics were successfully organised from the perspective of handling sustainability [1, 2]. The Olympic Games in London and Rio de Janeiro were examples, where resource systems and greenhouse gas (GHG) emission levels were intentionally controlled, and related management systems were expressly established for this purpose [3, 4]. Due to the success of these cases, the International Olympics Committee made it a requirement for any applicants to prepare a 'Carbon Management Strategy' and a 'Resource Management Strategy' to their feasibility study. In the Carbon Management Strategy, they estimate the GHG emission balance, and work out compensational measures [5, 6]. In the Resource Management programme, they calculate the changes in energy-, water-, and material usage, and the waste flows' processes [7]. Regarding the 'Carbon Management Strategy', and the 'Resource Management Strategy', the technical solutions are planned on the applicable technological level, abiding by the given economic conditions [8].

The circular economic perspective is based on the holistic planning, which is built on all long term sustainable planning processes [9, 10, 11]. It summarises the special business solutions and circulation strategies, which can be used to elevate sustainability planning to a higher level [12, 13]. The life cycle of products can be extended [14], the system can be kept close to a 'zero waste' state [15], and the material- and energy flows can be organised into mostly closed cycles (Figure 1).

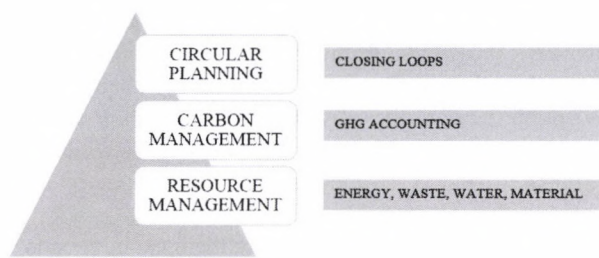


Figure 1. Interconnections of sustainable planning processes, and analysed systems

The carbon footprint calculations made for previous Olympic Games were conducted using the international calculation method, mostly on the Scope1 (direct emissions) analysis level [16, 17]. In this case, the direct energy, material and waste process flows have the most influence [18]. The GHG calculation methodology of earlier Olympic Games simply considered procurement items included in the Olympic host city's operational budget. These are e. g. the emission rates related to the internal transport / traffic, airway travels, internal waste emission rates, construction of roads or other infrastructure related to the Olympics (most of which were demolished after the Olympics), and emission rates related to these [19, 20]. Indirect emissions, which are on the analysis level of Scope2, show the amount of energy purchased, and the ratio of green energy used [21]. This means GHG emissions coming from energy usage which is not under the influence of the organisers (they're produced without control from the perspective of the user). Based on the reduction logic of Scope2 (mitigation of indirect emissions), this volume can be diminished, if we increase the self-produced energy's share within the total energy consumption [22]. The Scope3 analysis level (additional indirect emissions) contains advised elements [23, 24] which are often hard to describe with data. Therefore, this segment is rarely calculated in practice.

Scope2 and Scope3 measurements, and planned decreases had less significance even in the case of earlier (London, Rio) Olympics. This was mainly caused by the timeframe of the GHG footprint measurement which was only extended to the duration of the Olympics. Thus, the precise measurements of the emission rates in the preparation and afterlife phases was impossible to conduct (most notably for indirect services).

Apparently, the hierarchic relations between the low-carbon and the circular economy principles both show the methodological difference between the two evaluation methods. While the carbon footprint calculations focus on decreasing the emission rates related to internally controlled systems (Scope1) [25], the circular economic development concept aims to increase sustainability levels within Budapest's 2024 sustainability procurement policy [26]. These can mainly be found within the Scope2 or Scope3 indicator groups [27, 28]. In other words, the previously applied low-carbon standards aimed to mitigate the GHG emissions comparing to business-as-usual (BAU) processes. The carbon management strategy is still limited

to the decarbonization of material stocks assigned to certain functions [29]. In the case of the circular planning, the applied functions are achieved by the employment of services [30]. The mechanism eliminates the potential emission sources in the first place [31]. The described logic indicates that carbon footprint analyses can only partially, or simply cannot support the mechanisms of circular economic system design. This is the reason for the emerging need of unusual applications throughout the planning of the future Olympics. According to previous research findings, the desired movement of stock and flow rates – to the direction of a higher service content – can be accomplished through the increased utility of stocks. This paper aims to introduce a calculation method which enables decision makers to estimate the possible material and energy flow of certain activities. The elaborated methodology helps to assess the stock intensity of actions throughout the Olympics lifecycle. The outcome of the calculation is supposed to identify the necessary tool to ensure a higher level of utility. The present study determined these tools based on the priorities of circular economy.

2. Scientific background

Priority levels for circular solutions

The approach which gained fame as '3R' has been in the curriculum of public education since 1818, and means the three basic capabilities (Reading, wRiting, aRithmetic), promoting their importance. After a while, environmentalists also created their own 3R - to symbolise their priorities - which means Reducing the quantity of waste (which was on the rise rapidly during the second half of the XX. century), Recycling it, or completely preventing its creation by Reusing products [32, 33].

These 200 years old pillars are the basis of the alternative economic perspective named circular economy [34], a notion that gains more and more ground nowadays. The concept was designed as an answer for the linear economic model which reigned until the beginning of the XXI. century. Linear economy advertises production based on new resources, and throwing products away after their effective life cycle is over (End-of-Life) [35]. In the circulation of natural ecosystems, the waste of one life form is always the nutrient for yet another [36, 37]. It is impossible to imagine that any life form in nature would produce an 'output' which will not become an 'input' for another [38, 39, 40].

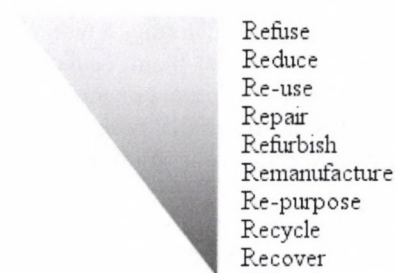


Figure 2. Priority levels of circularity [42]

During the design of circular theses, researchers rely on the previously introduced, 'R-signed' methods. The toolbox of waste treatment and prevention was expanded until 9R nowadays [41, 42], which are called the priority levels of circularity (Figure 2).

The concept seen on Figure 2 is designated in accordance with major two aspects. The first one is the 'function before the material' policy, which aims to lengthen the usage of the product for its intended purpose for as long as possible [43]. The second priority is to minimise the energy used. In other words, after the effective life cycle is finished, the product should be treated with the lowest possible energy requirement [44]. The different levels will also indicate the strength of their role in the various circular mechanisms. It must be stressed, that the hierarchy of the tools may differ in certain countries, due to the deviation in development levels. For instance, some theories might prefer re-use over reduction. Their logic indicates, that while the reduction of production reduces waste as well, reuse at some cases could even prevent its generation [38, 45]. Although, this argument might be valid at some points, it does not apply to the Hungarian conditions. Regarding re-use, the second-hand culture is widely anticipated in the country. However, the products offered at second-hand stores are mostly manufactured in the Britain. Therefore, it is rather a BAU resale process than a resource efficient reusing activity. Another example is the application of maintenance tools (e. g. repair). In the case of Hungarian infrastructure, a lot of transportation and building stocks are over their originally planned life cycle [46, 47]. Even though the circular priorities prefer to maintain the function of products, the improvement of obsolete systems can easily lead to major deadweight losses in the long-term [48, 49, 50]. After the examination of possible logical paradoxes, the detailed introduction of the certain priorities is presented:

Refuse: this method is one of the most effective interpretations for circularity. In this case, the production of a new product does not take place at all, since consumers refuse to purchase it. In general, this is the point which cause hardships to most people who attempt to understand it, and it is also the most critical point of circular economy. Many do not understand how processes can be circular, if the material flow is not even created. Furthermore, others believe that increasing production is indispensable for sustaining economic growth, whereas circularity only has to integrate into the system via recycling. However, critics advertising these requirements fail to take two fundamental aspects into consideration. One is the creation of the many externalities. If experts could arrange a monetized value to all these effects and account them, economic processes would display an entirely different picture [51, 52, 53, 54]. The other aspect is the materialist policy, which constricts most critics into the theoretic framework of the linear economy.

In the recent decades, many notions aiming to move the current stock economy towards the flow economy, which is based on a service thought process, were born [26]. In theory, the concept of 'performance economy' has been designed a long time ago [55], and practical examples for

'sharing economy' has been taking ground steadily nowadays [56]. Though the theoretic background, or the practical implementation may differ, the idea behind these perceptions stresses the same interpretation. Their message is that modern economies need business models which help members of society, so they do not need to own products to gain their services [57].

Reduce: in this case, it refers to reducing at both ends of the product chain. On one hand, the utilization of less resources to produce less products in the beginning of the process. On the other hand, the decreasing consumption of products which leads to less amount of waste. The question remains - which end of the market does the circulation start, from the consumer, or from the producer? Though early, classic economic theories were born on markets where a low amount of products had to deal with over-demand, these trends did change by now. Currently, the demand for products determines the supply, and has done so for the last century. Moreover, supply often goes beyond the demand these days [58]. Thus, tools to artificially stimulate demand became 'popular', such as marketing, loan, or planned obsolescence [59, 60]. These methods induce, create opportunities, or force people to increase their consumption, which in turn increases the waste they produce [39]. Therefore, the answer to the question is obviously on the side of the consumer. People themselves are responsible for the amount of products on the market. If they decide to decrease their consumption, they can force producers to stop creating so many unnecessary products [38].

Reuse: this method has very simple characteristics. It can be applied when someone wants to get rid of a product they own, even though it still fulfils its function. Therefore, they do not discard the product, but take it to a second-hand shop instead [61]. The present, and preceding methods can be considered the most efficient solutions, as these make people capable of preventing the creation of waste.

Repair, Refurbish and Remanufacture: one of the most notable mottos of the XXI. century's consumer society: "I recommend to buy new, it's cheaper than the repair costs". This perspective was, in the beginning, used for the technological products which appeared with the digital age. The society began to realise the intent behind the phenomenon, as the motto was extended even for wares which were easy to repair before. In some terms, this trend can be considered as the extension mechanism of planned obsolescence. This time not only the actual lifetime of the product becomes shortened during production, but it even prevents the consumer from lengthening it. To combat this, circular economy created the definition of 'circular design' [62]. Its essence is for manufacturers to not only make sure of the long lifetime, but also to equip consumers to maintain it. The first variant is when after the product malfunctions, it can simply be repaired. Refurbishing is a bit different, as it focuses on the compatibility attributes of the product. Nowadays, often the malfunction of a single element forces people to throw away the entire product. Therefore, circular design prefers the creation of products that are easy to disassemble, to make the various parts easy to exchange with new ones. Finally, in the case of

remanufacturing, the new product is assembled from the elements of used ones [62].

Up-cycling: this is the first tool which shows some similarity with current trends to some extent. This is caused due to the so-called 'retro' perspective being a fad all around the year, which supports the various methods of reusing already used products. Therefore, this branch managed to take considerable advantage during the last two decades, and multiple companies happily use it during their CSR projects [63]. Its essence is that we find alternative methods of usage for products which lost their original function.

Recycling: regarding the concept of circular economies, this mechanism is the first to come up in people's minds. However, the idea based on circulation is more than simply returning material into the process [64]. During recycling, circularity policies are only implemented in a faded manner, since it does not sustain the product function, or create a new one. Recycling focuses on the material composition of the objects, which can be used in the production processes as secondary resource materials.

Recovery: recovering energy from waste is basically one of the most primitive forms of waste treatment. People usually associate to energy produced in trash combustors when thinking about this method, which may have a significantly different efficiency due to differences in the actual facility [65]. These facilities often cause more negative externalities during their operations – e. g. air pollution – in comparison with the benefits at the end of the process. Nothing is better proof of this than the fact that in the world, there are currently no trash combustion facilities operating with a profit (not even in western countries). This is a perfect example of how the method is simply weak, instead of a difference between the development levels of countries.

The presented circular priorities were all ranked according to their material and energy intensity. The higher the activities are ranked, the better their resource productivity is. This is due to the increased utility achieved by longer lifespan and lower material/energy need of processes. The top of the hierarchy represents not only a novel approach by the prevention of waste but a whole new economic paradigm by indicating the idea of sharing. Although, it has become clear that the top priorities cannot be feasible in all cases. When a system operates only on a low level of circularity, the application of much higher methods might cause serious malfunctions. Therefore, the purpose of the presented calculation methodology will be to determine the current state of circularity and appoint the most applicable tool for development.

3. Material and methods

Ensuring eco-efficiency through the application of the MIPS method

The novelty of circular economy is that while earlier concepts mainly focus on environmentally friendly waste management, this perspective aims to prevent waste in the first place [38, 41]. The most effective method to avoid

producing waste is to not even make the product which would inevitably become waste later [31, 66]. Therefore, of all preferred methods, the most important is where people refuse the consumer attitude leading to the manufacture of new products [65]. In these cases, it is better to repair or reuse older products, by which the manufacturer's side must either produce less, or manufacture products of excelsior quality [62]. An important driving force behind the activities on the top of the hierarchy is the service-based perspective. In this case, the consumer discovers more and more the possible ways to use products, without actually buying them [30, 55].

Therefore, one of the main policies of circular economy is to discard the 'consumer' description, in favour of 'user' [61]. A suitable basis for evaluating service content is the eco-efficiency (Equation 1).

$$EE = \frac{S}{Mi} \quad (1)$$

This basically means the reverse interpretation of the MIPS method (Material Input Per Service), which shows the rate of service by unit of material [67]. The importance of the connection between these two factors was highlighted by the researchers of the German Wuppertal Institute in the 1990's [68]. The logic of Equation 1 shows that an activity will be the most efficient (from an environmental standpoint), if the least possible amount of material resources (and energy, obviously) are used for it [26, 69]. To illustrate this, the best example is the usage of cars. Owning a personal vehicle is considered as the least efficient stocking, as even people who use their car intensively, only utilize it for a short time during a single day [70, 71]. In the remaining time, there is no use for it, its value deteriorates, the owner must consider its placement and safe storage, and taxes have to be paid for it. This is one of the reasons why the platforms related to sharing economy concern the new method to use traffic systems [72]. So, the fact is commonly accepted, that a car – similarly to many other products – satisfies its function in the most efficient manner, if it's always in use [73, 74, 75]. Therefore, based on the logic of eco-efficiency, the travel distance taken via taxi (or other mass transport or vehicle sharing platforms) is much more advantageous than being personally owned by the user.

Tracking the material flow

Recent researches which tried to measure the level of circularity, mostly included the development of metric methods. There are two mainstream branches of the topic. One of them comes from the study conducted by the Ellen MacArthur Foundation [76], while the other was created by a single engineer called Maurits Korse from the University of Twente [77]. Therefore, during the elaboration, the methods will be referred by the names of their creator. The MacArthur concept basically deals with the material flow (Figure 3) during production, and the usefulness of manufactured products.

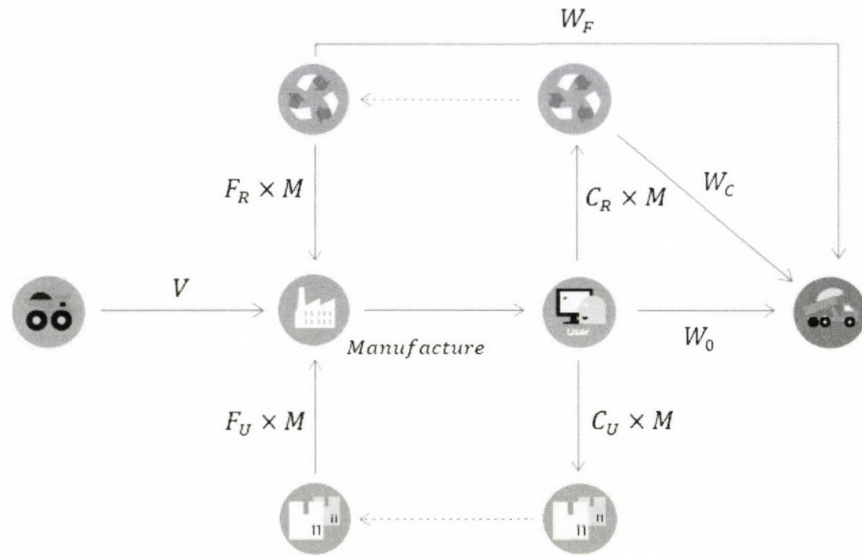


Figure 3. Process draft of the MacArthur-style material flow [76]

where: M: Mass of Product / Amount of products, V: Virgin feedstock / Primary raw material used for the product, W: Waste created with the product, W₀: The amount of waste which is either deposited, or reallocated into energy production systems which is generated during the life cycle of the product. This material isn't included into production. WF: The waste produced during the manufacture of secondary resource material required for the product WC: The waste produced during the recycling of the product, CR: Volume of products which are recycled CU: Volume of products which are reused, FR: Recycled materials used during the manufacturing of the product FU: Reused materials used during the manufacturing of the product

The MacArthur model uses the so-called 'Linear Flow Index' (LFI) for the measurement of the material flow (Equation 2).

$$LFI = \frac{V + W}{2M + \frac{W_F - W_C}{2}} \quad (2)$$

This theory mainly sprouts from the logic focusing on the primary resource materials consumed during the manufacturing of the products, and the waste produced during the latter phases of their life cycle.

While the material flow, and the recycling of material flows are merely parts of the MacArthur mechanism, the Korse calculation (Equation 3) takes explicitly this side into consideration for calculating the circular value [78, 79, 80].

$$C = \frac{\sum_{material} m_{in} (r + v \times (1 - S)) \times \sum_{material} m_{out} r_{pot} (1 - A)}{m_{totin}^2} \quad (3)$$

where:

- C: Circular value
- m: Material volume
- r: Recycled content
- v: Virgin feedstock / Primary raw material content
- S: Scarcity of the raw material
- r_{pot}: Recycling potential
- A: Accumulation factor

As this equation (Equation 3) also shows, the Korse-style material flow suggests a much more diversified train of thought. First, it analyses the ratio of recycled and primary resource materials in the material input (mi) used for production. For the latter, it also accounts how rare is the material on the Earth. A rare resource will obviously impact the value of the indicator negatively. Eventually, it also considers how much of the product's materials (mout) will be recyclable at the end of its efficient life cycle.

The two logic frameworks can be considered as complementary factors of each other. While the MacArthur branch focuses more on the level of primary resource material usage, the Korse method analyses the opportunity for recycling both on the input and output sides. The latter contains a quite sophisticated logic, which naturally needs more data. Therefore, though the calculation presented in this paper uses the elements of the MacArthur method, it sufficiently structures them by keeping the Korse principle.

4. Results and discussion

The method of calculating the circular values for the Olympics

The Circular Economic Value (CEV) calculation [81] used two main components. The first is the material flow which is involved for the integration of the 'closing the loop' principle [82, 83, 84]. Due to the MacArthur and Korse logics' influence, the input side accounts the rate of

primary resource material usage. On the output side, the amount of waste produced from the product gain significance. Therefore, the two components show the areas where system leakages might appear in terms of circularity. In case of the Olympics, not only the material flow, but the sustainable energy consumption is also important. Thus, these two became the focus points of the methodology [85]. The logic used here is similar to the handling of material flows. The input and output side perspective has been applied for describing this process as well. The former is based the amount of energy which comes from fossilized energy resources consumed for

production. For the latter, it is assumed that some elements of the products will be handled through circular (E_c), whereas other elements through linear (E_l) methods. The numerator consisted of the share of linear processes. Furthermore, the denominator represents the amount of energy required for recyclability and the energy produced during the disposal. The separation of input and output sides serves to make the decision process easier. This way, the possible leakage points on both ends of the processes become visible, in addition to the unified CEV value. The calculation method for the indicator value can be seen on Equation 4.

$$CEV\% = 100 - \left(\frac{\left(\frac{M_p}{M_p + M_s} + \frac{M_d}{M_r + M_d} \right) + \left(\frac{E_f}{E_s + E_f} + \frac{E_l}{E_c + E_l} \right)}{4} \right) \times 100 \quad (3)$$

where:

- CEV Circular economic value
- M_{lin} Material volume on the input side (linear)
- M_{lout} Material volume on the output side (linear)
- M_p = The amount of primary raw materials used for the manufacturing of the product
- M_s = The amount of secondary raw materials used for the manufacturing of the product
- M_d = Amount of non-recyclable materials remaining after the product is used (linear)
- M_r = Amount of recyclable materials remaining after the product is used (circular)
- E_{lin} Energy value on the input side (linear)
- E_{lout} Energy value on the output side (linear)
- E_f = Amount of non-renewable energy used during the manufacturing of the product
- E_s = Amount of renewable energy used during the manufacturing of the product
- E_l = Amount of energy produced during disposal, after the product was used (linear)
- E_c = Amount of energy used for the product's recyclability, after the product was used (circular)

The CEV indicator designed for the circular structuring of the Olympics shows how a system element performs in the time of the analysis. In other words, which level of circulation it stands from the perspective of an optimised system. The Circular Economic Value identifies the improvement points of the material and energy usage to enhance circularity. Therefore, it visualizes which areas of the linear material and energy flows must be turned into circular systems. Furthermore, the CEV can be applied at the previously demonstrated circular priorities. The value indicates the most applicable tool which can be utilized in the certain development areas of the Olympics (e. g. transport, building, energy). Figure 4. illustrates a theoretic case when the value resulted in a performance level of 50%. For the association of the CEV with the circular

priorities, the levels have been theoretically identified with oriented percentages.

In the pictured case, the tools which have a higher circularity level than the CEV, can be applied to enhance the system performance. Although, it is important that the activity with the closest value to the CEV will be the most effective to use. As it was stressed at the end of the literature session, the application of too intense interventions would lead to major system malfunctions. The pyramid which narrows on its way to the top of the figure, illustrates the decreasing cost-efficiency of the tools in comparison with the initial CEV. Obviously, the utilization of these aspects is not that simple, and most of the cases will require the combination of the certain activities. This logic shows only the significance of accurate orientation by the definition of the actions.

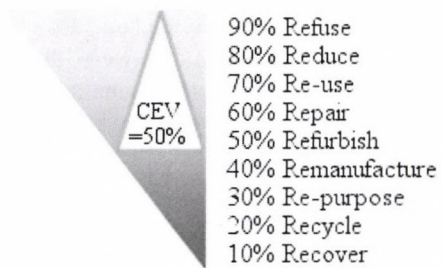


Figure 4. Priority levels of circularity interpreted in terms of CEV percentages

The measurement of the gained circularity level requires a comparison to the state which would be implemented without any circular applications. The latter case is associated as the BAU movement and the CEV must be calculated for that as a baseline for comparison. This value is called CEVBAU. Furthermore, the alternate scenario which includes the tools for circular system planning will be identified as CEVScen. The difference between these two values shows the level of transition to achieve in terms

of circularity. This divergence is defined as ΔCEV (Equation 5). By assigning the costs of implementation to this value, the cost-efficiency rates of the system transformation could be calculated as well.

$$\Delta\text{CEV} = \text{CEV}_{\text{Scen}} - \text{CEV}_{\text{BAU}} \quad (5)$$

The final CEV_{BAU} represents the level of circularity in the system. However, the accurate definition of circular improvement points requires an individual analysis on the elements of the equation. It means the consideration of the

single input and output values of the material and energy flows. Figure 5 visualizes the attributes of a theoretical case in order to present the mechanism of the CEV. While the right side of the figure concerns absolute Circular Economic Values of BAU and Scenario conditions, the left side illustrates how the rates are built up. The final CEV must be as high as possible, as it is the complementary value of the linear patterns pictured on the left. On the web chart, the closer the elements are to zero, the better their circular performance is.

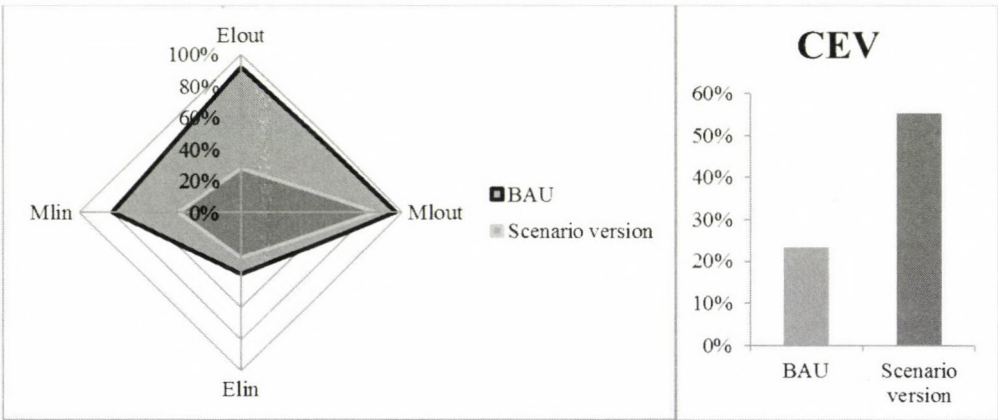


Figure 5. The illustration of differences (ΔCEV) between BAU and a possible more circular Scenario

The picture clearly indicates, that in case of the BAU, the major focus points of development should be the whole material flow and the output side of the energy processes. The input rate of energy supply already operates on a reasonable level. In comparison, the Scenario version – which consists of circular development tools – was able to tackle the input of the materials and the output of the energy flow. Although, the end of the material cycle remained a bottleneck issue and a potential room for future development. The ΔCEV was defined on 32% which is the difference in circular efficiency between the BAU and Scenario options. During the actual planning period of the Budapest 2024 Olympics, this value can be associated with cost and benefit ratios. Therefore, the ΔCEV will be the most significant outcome of the analyses employing the calculation tool presented in this paper. The cost index of the value will contribute to decision making processes at choosing the right option among several scenarios.

5. Conclusion

During the planning of circular Olympic systems, it has become clear that the traditional perspective does not contribute to the sustainable utilization of resources. In most cases, the Carbon and Resource Management Strategies – which are obligatory requirements for the organization – only maintain or strengthen the linear system patterns. For the establishment of a truly sustainable material circulation, future initiatives should focus on increasing the service content of activities, rather than the

optimization of resource usage. The preference of service flows instead of stock-based mechanisms points toward the same direction as the priorities of circular economy. Therefore, in the initial planning phase, the most effective way to measure the level of circularity is to focus on the resource intensity.

The methodology presented in this paper, illustrates the stock structure of certain initiatives through the attributes of their material and energy usage. The calculated Circular Economic Value of the BAU can be further associated with the circular priority level of the current system. This movement helps decision makers to define the most applicable tools (e. g. refurbishment, repair etc.) to enhance circular performance. This theoretical model will be applied to the future evaluation of the Budapest 2024 Olympic Games. The practical application during the planning phase will give the opportunity to restructure the equation and extend its view to a broader set of elements. Based on the experimental results, the model can be developed to cover more of the service content and measure resource productivity instead of the current resource intensity. Thus, future researches are expected to develop an accurate mechanism – based on the current model – which includes the cost-benefit ratios of circular development initiatives and contribute to the planning of circular investments.

Regarding the Budapest 2024 Olympics, the most influential attribute to assess will be the decentralized organization of the games. On the one hand, it is surely a benefit in terms of circular economy, since the diffusive

nature means less concentrated infrastructure. The major concern of previous Olympics was the enormous capacity built in a single location. Despite the great endeavours, the organizers could hardly manage the efficient utilization of these capacities in the afterlife period. On the other hand, the several locations will be a challenge to tackle in the case of Hungary. The sustainable planning must focus on the optimization of transport systems which will operate across the different placements.

However, the many years of preparation would give room for data generation and for the creation of circular best practices regarding future sport events. The initial circular examinations already stressed that the previously applied low-carbon development principles could be misleading in long-term. The sustainable, continuous flow of resources requires the elimination of linear system elements and the employment of circular solutions for future international sport events or Olympic Games.

Acknowledgements

This work was supported by The Budapest 2024 Bid Committee. The authors would like to thank the interested parties in the organization of the Budapest 2024 Olympic Games for their help and support.

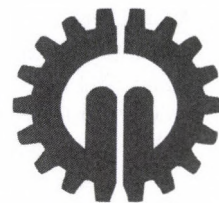
References

- [1] **Leopkey B., Parent M. M.:** 2011. Olympic Games legacy: from general benefits to sustainable long-term legacy. *The International Journal of the History of Sport*, Vol. 29 No. 6, pp. 924-943.
<http://dx.doi.org/10.1080/09523367.2011.623006>
- [2] **Preuss H.:** 2010. The conceptualisation and measurement of mega sport event legacies. *Journal of Sport & Tourism*, Vol. 12 No. 3-4, pp. 207-228.
<http://dx.doi.org/10.1080/14775080701736957>
- [3] **Veneroso C. E., Ramos G. P., Mendes T. T., Silami-Garcia E.:** 2015. Physical performance and environmental conditions: 2014 World Soccer Cup and 2016 Summer Olympics in Brazil. *Temperature*, Vol. 2 No. 4, pp. 439-440.
<http://dx.doi.org/10.1080/23328940.2015.1106637>
- [4] **Epstein D., Jackson R., Braithwaite P.:** 2011. Delivering London 2012: sustainability strategy. *Proceedings of the Institution of Civil Engineers – Civil Engineering*, Vol. 164 No. 5, pp. 27-33.
<http://dx.doi.org/10.1680/cien.2011.164.5.27>
- [5] **Samuel S., Stubbs W.:** 2012 Green Olympics, green legacies? An exploration of the environmental legacies of the Olympic Games. *International Review for the Sociology of Sport*, 48 (4), pp. 485-504,
<http://dx.doi.org/10.1177/1012690212444576>
- [6] **Mol A. P. J.:** 2010. Sustainability as global attractor: the greening of the 2008 Beijing Olympics. *Global networks*, Vol. 10 No. 4, pp. 510-528.
<http://dx.doi.org/10.1111/j.1471-0374.2010.00289.x>
- [7] **Parkes O., Lettier P., Bogle I. D. L.:** 2015. Life cycle assessment of integrated waste management systems for alternative legacy scenarios of the London Olympic Park. *Waste Management*, Vol. 40, pp. 157-166.
<http://dx.doi.org/10.1016/j.wasman.2015.03.017>
- [8] **Kim H. D.:** 2012. The 2012 London Olympics: commercial partners, environmental sustainability, corporate social responsibility and outlining the implications. *The International Journal of the History of Sport*, Vol. 30 No. 18, pp. 2197-2208.
<http://dx.doi.org/10.1080/09523367.2013.845171>
- [9] **Genovese A., Acquaye A. A., Figueroa A., Koh S. C. L.:** 2017. Sustainable supply chain management and the transition towards a circular economy: Evidence and some applications. *Omega*, Vol. 66 (B), pp. 344-357.
<http://dx.doi.org/10.1016/j.omega.2015.05.015>
- [10] **Hu J., Xiao Z., Zhou R., Deng W., Wang M., Ma S.:** 2011. Ecological utilization of leather tannery waste with circular economy model. *Journal of Cleaner Production*, Vol. 19 No. 2-3, pp. 221-228.
<http://dx.doi.org/10.1016/j.jclepro.2010.09.018>
- [11] **Andersen M. S.:** 2007. An introductory note on the environmental economics of the circular economy. *Sustainability Science*, Vol. 2 No. 1, pp. 133-140.
<http://dx.doi.org/10.1007/s11625-006-0013-6>
- [12] **Witjes S., Lozano R.:** 2016. Towards a more Circular Economy: proposing a framework linking sustainable public procurement and sustainable business models. *Resources, Conservation and Recycling*, Vol. 112, pp 37-44.
<http://dx.doi.org/10.1016/j.resconrec.2016.04.015>
- [13] **Bocken N. M. P., de Pauw I., Bakker C., van der Grinten B.:** 2015. Product design and business model strategies for a circular economy. *Journal of Industrial and Production Engineering*, Vol. 33 No. 5, pp. 308-320.
<http://dx.doi.org/10.1080/21681015.2016.1172124>
- [14] **Bakker C., Wang F., Huisman J., den Hollander M.:** 2014a. Products that go round: exploring product life extension through design. *Journal of Cleaner Production*, Vol. 69, pp. 10-16.
<http://dx.doi.org/10.1016/j.jclepro.2014.01.028>
- [15] **Zaman A. U.:** 2015. A comprehensive review of the development of zero waste management: lessons learned and guidelines. *Journal of Cleaner Production*, Vol. 91, pp. 12-25,
<http://dx.doi.org/10.1016/j.jclepro.2014.12.013>
- [16] **Onat N. C., Kucukvar M., Tatari O.:** 2014. Scope-based carbon footprint analysis of U.S. residential and commercial buildings: An input–output hybrid life cycle assessment approach. *Building and Environment*, Vol. 72, pp. 53-62.
<http://dx.doi.org/10.1016/j.buildenv.2013.10.009>
- [17] **Song T., Wang Y.:** 2012. Carbon dioxide fluxes from an urban area in Beijing. *Atmospheric Research*, Vol. 106, pp. 139-149.
<http://dx.doi.org/10.1016/j.atmosres.2011.12.001>
- [18] **Pandey D., Agrawal M., Pandey J. S.:** 2011. Carbon footprint: current methods of estimation. *Environmental Monitoring and Assessment*, Vol. 178 No. 1, pp. 135-160,
<http://dx.doi.org/10.1007/s10661-010-1678-y>
- [19] **Carbon Footprint Management Report Rio 2016 Olympic and Paralympic Games.:** 2014. Link: <http://studylib.net/doc/18267806/carbon-footprint-management-report-rio-2016-olympic-and>

- [20] **Carbon Footprint Study – Methodology and reference footprint – London 2012.**: 2010. Link: http://www.mma.gov.br/estruturas/255/_arquivos/carbon_footprint_study_relac_255.pdf
- [21] **Peters G. P.**: 2010. Carbon footprints and embodied carbon at multiple scales. *Current Opinion in Environmental Sustainability*, Vol. 2 No. 4, pp. 245-250. <http://dx.doi.org/10.1016/j.cosust.2010.05.004>
- [22] **Andrew J., Cortese C.**: 2011. Accounting for climate change and the self-regulation of carbon disclosures. *Accounting Forum*, Vol. 35 No. 3, pp. 130-138. <http://dx.doi.org/10.1016/j.accfor.2011.06.006>
- [23] **Benjaafar S., Li Y., Daskin M.**: 2013. Carbon footprint and the management of supply chains: insights from simple models. *IEEE Transactions on Automation Science and Engineering*, Vol. 10 No. 1, pp. 99-116. <http://dx.doi.org/10.1109/TASE.2012.2203304>
- [24] **Lee K. H.**: 2011. Integrating carbon footprint into supply chain management: the case of Hyundai Motor Company (HMC) in the automobile industry. *Journal of Cleaner Production*, Vol. 19 No. 11, pp. 1216-1223. <http://dx.doi.org/10.1016/j.jclepro.2011.03.010>
- [25] **Wright A. L., Kemp S., Williams I.**: 2014. 'Carbon footprinting': towards a universally accepted definition. *Carbon Management*, Vol. 2 No. 1, pp. 61-72. <http://dx.doi.org/10.4155/cmt.10.39>
- [26] **Tukker A.**: 2015. Product services for a resource-efficient and circular economy – a review. *Journal of Cleaner Production*, Vol. 97, pp. 76-91. <http://dx.doi.org/10.1016/j.jclepro.2013.11.049>
- [27] **Downie J., Stubbs W.**: 2012. Corporate Carbon Strategies and Greenhouse Gas Emission Assessments: The Implications of Scope 3 Emission Factor Selection. *Business Strategy and the Environment*, Vol. 21 No. 6, pp. 412-422. <http://dx.doi.org/10.1002/bse.1734>
- [28] **Dodman D.**: 2011. Forces driving urban greenhouse gas emissions. *Current Opinion in Environmental Sustainability*, Vol. 3 No. 3, pp. 121-125. <http://dx.doi.org/10.1016/j.cosust.2010.12.013>
- [29] **Barrett J., Peters G., Wiedmann T., Scott K., Lenzen M., Roelich K., Le Quéré C.**: 2013. Consumption-based GHG emission accounting: a UK case study. *Climate Policy*, Vol. 13 No. 4, pp. 451-470. <http://dx.doi.org/10.1080/14693062.2013.788858>
- [30] **Webster K.**: 2015. The circular economy – a wealth of flows. *Ellen MacArthur Foundation Publishing*, UK, pp. 104-110.
- [31] **Benton D., Hazell J., Hill J.**: 2015. The guide to the Circular Economy. *Greenleaf Publishing Limited*, UK, pp. 25-40.
- [32] **Yeheyis M., Hewage K., Alam M. S., Eskicioglu C., Sadiq R.**: 2013. An overview of construction and demolition waste management in Canada: a lifecycle analysis approach to sustainability. *Clean Technologies and Environmental Policy*, Vol. 15 No. 1, pp. 81-91. <http://dx.doi.org/10.1007/s10098-012-0481-6>
- [33] **Demirbas A.**: 2011. Waste management, waste resource facilities and waste conversion processes. *Energy Conversion and Management*, Vol. 52 No. 2, pp. 1280-1287. <http://dx.doi.org/10.1016/j.enconman.2010.09.025>
- [34] **Sauvé S., Bernard S., Sloan P.**: 2016. Environmental sciences, sustainable development and circular economy: Alternative concepts for trans-disciplinary research. *Environmental Development*, Vol. 17, pp. 48-56. <http://dx.doi.org/10.1016/j.envdev.2015.09.002>
- [35] **Andrews D.**: 2015. The circular economy, design thinking and education for sustainability. *Local Economy: The Journal of the Local Economy Policy Unit*, Vol. 30 No. 3, pp. 305-315. <http://dx.doi.org/10.1177/0269094215578226>
- [36] **Sherratt A.**: 2013. Cradle to cradle. *Encyclopedia of Corporate Social Responsibility*, pp. 630-638. http://dx.doi.org/10.1007/978-3-642-28036-8_165
- [37] **Bakker C. A., Wever R., Teoh C., de Clercq S.**: 2009. Designing cradle-to-cradle products: a reality check. *International Journal of Sustainable Engineering*, Vol. 3 No. 1, pp. 2-8. <http://dx.doi.org/10.1080/19397030903395166>
- [38] **Szaky T.**: 2014. Outsmart waste: the modern idea of garbage and how to think our way out of it. *Berrett-Koehler Publishers*, California, US, pp. 126-144.
- [39] **Hertwich E. G.**: 2005. Consumption and the rebound effect: an industrial ecology perspective. *Journal of Industrial Ecology*, Vol. 9 No. 1-2, pp. 85-98. <http://dx.doi.org/10.1162/1088198054084635>
- [40] **Erkman S.**: 1997. Industrial ecology: an historical view. *Journal of Cleaner Production*, Vol. 5 No. 1-2, pp. 1-10. [http://dx.doi.org/10.1016/S0959-6526\(97\)00003-6](http://dx.doi.org/10.1016/S0959-6526(97)00003-6)
- [41] **de Jong S., van der Gaast M., Kraak J., Bergema R., Usanov A.**: 2016. The Circular Economy and developing countries – a data analysis of the impact of a Circular Economy on resource-dependent developing nations. *Centre of Expertise on Resources*, The Hague, pp. 17-19.
- [42] **Cramer J.**: 2014. Moving towards a circular economy in the Netherlands: Challenges and directions. *Utrecht University*, pp. 1-9.
- [43] **Gan Y., Zhang T., Liang S., Zhao Z., Li N.**: 2013. How to deal with resource productivity – relationships between socioeconomic factors and resource productivity. *Journal of Industrial Ecology*, Vol. 17 No. 3, pp. 440-451. <http://dx.doi.org/10.1111/j.1530-9290.2012.00547.x>
- [44] **Steinberger J. K., Krausmann F.**: 2011. Material and energy productivity. *Environmental Science & Technology*, Vol. 45 No. 4, pp. 1169-1176. <http://dx.doi.org/10.1021/es1028537>
- [45] **Szira Z., Alghamdi H., Olthmar G., Varga E.**: 2016. Analyzing waste management with respect to circular economy. *Hungarian Agricultural Engineering*, Vol. 30, pp. 75-86. <http://dx.doi.org/10.17676/HAE.2016.30.75>
- [46] **Bai A., Jobbágy P., Popp J., Farkas F., Grasselli G., Szendrei J., Balogh P.**: 2016. Technical and environmental effects of biodiesel use in local public transport. *Transportation Research Part D-Transport and Environment*, Vol. 47, pp. 323-335. <http://dx.doi.org/10.1016/j.trd.2016.06.009>
- [47] **Fogarassy Cs., Horvath B.**: 2016. Low-carbon building innovation trends and policy perspectives in Hungary between 2020 and 2030. *YBL Journal of Built Environment*, Vol. 3 No. 1-2, pp. 42-54. <http://doi.org/10.1515/jbe-2015-0005>

- [48] **Sorrell S.:** 2009. Jevons' Paradox revisited: The evidence for backfire from improved energy efficiency. *Energy Policy*, Vol. 37 No. 4, pp. 1456-1469. <http://dx.doi.org/10.1016/j.enpol.2008.12.003>
- [49] **Alcott B.:** 2005. Jevons' paradox. *Ecological Economics*, Vol. 54 No. 1, pp. 9-21. <http://dx.doi.org/10.1016/j.ecolecon.2005.03.020>
- [50] **Jevons W. S.:** 1865. *The coal question*. Macmilland & Co., UK, pp. 13-19.
- [51] **O'Neill D. W.:** 2012. Measuring progress in the edgrowth transition to a steady state economy. *Ecological Economics*, Vol. 84, pp. 221-231. <http://dx.doi.org/10.1016/j.ecolecon.2011.05.020>
- [52] **Kallis G.:** 2011. In defence of degrowth. *Ecological Economics*, Vol. 70 No. 5, pp. 873-880. <http://dx.doi.org/10.1016/j.ecolecon.2010.12.007>
- [53] **Kerschner C.:** 2010. Economic de-growth vs. steady-state economy. *Journal of Cleaner Production*. Vol. 18 No. 6, pp. 544-551, <http://dx.doi.org/10.1016/j.jclepro.2009.10.019>
- [54] **Pearce D.:** 1992. *Green Economics*. Environmental Values, Vol. 1 No. 1, pp. 3-13. doi:10.3197/096327192776680179
- [55] **Stahel, W. R.:** 2010. *The Performance Economy*. Palgrave Macmillan Publishers Ltd, UK, pp. 269-287. <http://dx.doi.org/10.1057/9780230274907>
- [56] **Belk R.:** 2014. You are what you can access: sharing and collaborative consumption online. *Journal of Business Research*, Vol. 67 No. 8, pp. 1595-1600. <http://dx.doi.org/10.1016/j.jbusres.2013.10.001>
- [57] **Cohen B., Kietzmann J.:** 2014. Ride On! Mobility business model for the sharing economy. *Organization & Environment*, Vol. 27 No. 3, pp. 279-296. <http://dx.doi.org/10.1177/1086026614546199>
- [58] **Greenwald B., Stiglitz J. E.:** 1987. Keynesian, new Keynesian and new classical economics. *Oxford Economic Papers*, Vol. 39 No. 1, pp. 119-133.
- [59] **Agrawal V. V., Kavadias S., Toktay L. B.:** 2015. The limits of planned obsolescence for conspicuous durable goods. *Manufacturing & Service Operations Management*, Vol. 18 No. 2, pp. 216-226. <http://dx.doi.org/10.1287/msom.2015.0554>
- [60] **Bulow J.:** 1986. An economic theory of planned obsolescence. *The Quarterly Journal of Economics*, Vol. 101 No. 4, pp. 729-749. <https://doi.org/10.2307/1884176>
- [61] **Ellen MacArthur Foundation.:** 2015a. *Towards the Circular Economy. Business rationale for an accelerated transition*. Ellen MacArthur Foundation Publisher, UK, pp. 5-9.
- [62] **Bakker C., Zijlstra Y., van Hinte E., den Hollander M. C.:** 2014b. Products that last – product design for circular business models. TU Delft Library, pp. 48-75.
- [63] **Spitzeck H.:** 2011. TerraCycle – A business founded for societal benefit generation. *Humanistic Management in Practice*, Part of the series Humanism in Business, pp. 266-276, http://dx.doi.org/10.1057/9780230306585_18
- [64] **Ellen MacArthur Foundation.:** 2014. *Towards the Circular Economy: Accelerating the scale-up across global supply chains*. Ellen MacArthur Foundation Publisher, UK, pp. 39-50.
- [65] **Grosso M., Motta A., Rigamonti L.:** 2010. Efficiency of energy recovery from waste incineration, in the light of the new Waste Framework Directive. *Waste Management*, Vol. 30 No. 7, pp. 1238-1243. <http://dx.doi.org/10.1016/j.wasman.2010.02.036>
- [66] **Hawken P., Lovins A., Lovins H. L.:** 1999. *Natural Capitalism: creating the next industrial revolution*. Little, Brown and Company, US, pp. 1-21.
- [67] **Ritthoff M., Rohn H., Liedtke C.:** 2002. Calculating MIPS: resource productivity of products and services. Wuppertal Institute for Climate, Environment and Energy, Wuppertal, pp. 9-12.
- [68] **Spangenberg J. H., Hinterberger F., Moll S., Schutz H.:** 1999. Material flow analysis, TMR and the MIPS concept: a contribution to the development of indicators for measuring changes in consumption and production patterns. *International Journal of Sustainable Development*, Vol. 2 No. 4, pp. 491-505. <http://dx.doi.org/10.1504/IJSD.1999.004339>
- [69] **Finnveden G., Moberg A.:** 2005. Environmental systems analysis tools – an overview. *Journal of Cleaner Production*, Vol. 13 No. 12, pp. 1165-1173. <http://dx.doi.org/10.1016/j.jclepro.2004.06.004>
- [70] **Bardhi F., Eckhardt G. M.:** 2012. Access-based consumption: the case of car sharing. *Journal of Consumer Research*, Vol. 39 No. 4, pp. 881-898. <http://dx.doi.org/10.1086/666376>
- [71] **Katzev R.:** 2003. Car sharing: a new approach to urban transportation problems. *Analyses of Social Issues and Public Policy*, Vol. 3 No. 1, pp. 65-86. <http://dx.doi.org/10.1111/j.1530-2415.2003.00015.x>
- [72] **Balogh P., Bai A., Popp J., Huzsvai L., Jobbágy P.:** 2015. Internet-orientated Hungarian car drivers' knowledge and attitudes towards biofuels. *Renewable and Sustainable Energy Reviews*, Vol. 48, pp. 17-26. <http://dx.doi.org/10.1016/j.rser.2015.03.045>
- [73] **Boyaci B., Zografos K. G., Geroliminis N.:** 2015. An optimization framework for the development of efficient one-way car-sharing systems. *European Journal of Operational Research*, Vol. 240 No. 3, pp. 718-733. <http://dx.doi.org/10.1016/j.ejor.2014.07.020>
- [74] **Intlekofer K., Bras B., Ferguson M.:** 2010. Energy implications of product leasing. *Environmental Science & Technology*, Vol. 44 No. 12, pp. 4409-4415. <http://dx.doi.org/10.1021/es9036836>
- [75] **Meijkamp R.:** 1998. Changing consumer behaviour through eco-efficient services: an empirical study of car sharing in the Netherlands. *Business Strategy and the Environment*, Vol. 7 No. 4, pp. 234-244, [http://dx.doi.org/10.1002/\(SICI\)1099-0836\(199809\)7:4<234::AID-BSE159>3.0.CO;2-A](http://dx.doi.org/10.1002/(SICI)1099-0836(199809)7:4<234::AID-BSE159>3.0.CO;2-A)
- [76] **Ellen MacArthur Foundation.:** 2015b. *Circularity indicators – an approach to measuring circularity. Methodology description*. Ellen MacArthur Foundation Publishing, pp. 19-25.
- [77] **Korse M.:** 2015. A business case model to make sustainable investment decisions - adding circular economy to asset management. University of Twente, NL, pp. 47-51.

- [78] **Korse M., Ruitenburg R. J., Toxopeus M. E., Braaksma A. J. J.:** 2016. Embedding the circular economy in investment decision-making for capital assets – a business case framework. *Procedia CIRP*, Vol. 48, pp. 425-30. <http://dx.doi.org/10.1016/j.procir.2016.04.087>
- [79] **Su B., Heshmati A., Geng Y., Yu X.:** 2013. A review of the circular economy in China: moving from rhetoric to implementation. *Journal of Cleaner Production*, Vol. 42, pp. 215-227. <http://dx.doi.org/10.1016/j.jclepro.2012.11.020>
- [80] **Geng Y., Fu J., Sarkis J., Xue B.:** 2012. Towards a national circular economy indicator system in China: an evaluation and critical analysis. *Journal of Cleaner Production*, Vol. 23 No. 1, pp. 216-224. <http://dx.doi.org/10.1016/j.jclepro.2011.07.005>
- [81] **Fogarassy Cs., Orosz Sz., Ozsvári L.:** 2016. Evaluating system development options in circular economies for the milk sector – development options for production systems in the Netherlands and Hungary. *Hungarian Agricultural Engineering*, Vol. 30, pp. 62-74. <http://dx.doi.org/10.17676/HAE.2016.30.62>
- [82] **European Commission.:** 2015. Closing the loop – An EU action plan for the Circular Economy. pp. 21.
- [83] **Kraaijenhagen C., van Open C., Bocken N.:** 2016. Circular Business – Collaborate and Circulate. *Ecodrukkers*, pp. 5-30.
- [84] **Thomas V. M.:** 1997. Industrial Ecology: towards closing the materials cycle. *Journal of Industrial Ecology*, Vol. 1 No. 2, pp. 149-151. <http://dx.doi.org/10.1162/jiec.1997.1.2.149>
- [85] **International Olympic Committee.:** 2012. Sustainability through sport – implementing the Olympic movement's Agenda 21, pp. 38-48.



THE SUSTAINABILITY AND USAGE EFFICIENCY OF CONVECTIONAL GEOTHERMIC ENERGY PRODUCTION

Author(s):

J. Nagygál – L. Tóth

Affiliation:

Szent István University, Faculty Mechanical Engineering, Péter K. street 1., H-2100 Gödöllő, Hungary

Email address:

nagygj@arpad.hu, toth.laszlo@gek.szie.hu

Abstract

The use of geothermal energy in Hungary has decades of history, most notably in the area of direct usage. In the last ten years, both experts and the common people got to know this technology due to the disadvantageous legal changes. Most of the domestic energetic users are involved in agriculture. Extracting and using energy, different technologies, and the location of water are all different scientific areas. The entire system's success is based on the inter-disciplinary relations of many scientific scopes and sciences. The cooperation of the most notable practitioners of various sciences, professors, building engineers, architects, geologists, geophysicists, drilling engineers can mean the development of the sector, and the efficient solution for the problems which come with it.

In our study, we tried to find the answer to a sustainable thermal water production's most efficient method by analysing 20 currently operating thermal water wells, and did not forget to make use of the heat extracted, and the final water placement. During my work, I placed importance on getting to know the connections between thermal water and geology, on mapping the geological conditions, and on knowing the questions of digging wells. All these together make it possible to create a pre-plannable drilling, training, production and usage system's creation, which can adequately handle both ecological and economical questions. The geothermal fluid produced has to be placed somewhere, which was a question of faith for a long time. This was also further influenced by how the experts were never capable of sitting down, and conducts a discussion using actual facts and reasons. As the users cannot be expected to develop refilling techniques, it falls on the experts to plan and parameter a well construction which poses small drilling and management risks.

Keywords

Geothermal energy, renewable energy, usage efficiency

1. Introduction

The geothermic gradient of Hungary is significantly above the world average, which is why there is a notable potential

in the usage of geothermal energy. Which is already widespread method of heating in some areas (f. e. gardening, living quarters, thermal baths) of Hungary. Apart from the direct costs of digging of wells and refilling water, the most notable problem is posed by the establishment of facilities due to the costs of creating the entire system.

Thermal water without any kind of modification can be used to transport thermal energy, and to exchange it either in a direct, or in an indirect way. The operation costs of the thermal well are low when compared to the harvestable thermal energy, which is why the heating based on thermal water has strong competitiveness when compared to other methods. It is advantageous that it's in reach in our country's areas dealing in agriculture - mostly flatlands. The thermal energy can be produced locally, and there is no need to transport, it does not depend on import, season, time of day or weather conditions [1, 2].

It is a fundamental goal to use this national treasure in an environmentally friendly and sustainable manner.

Goals

The goal of this study is to highlight connections which have to be analysed in order to assure that currently used excavation and usage technological solutions are sustainable in the long-term.

1. Checking the production parameters of the thermal wells near Szentes. The detailed analysis of twenty thermal wells situated upon sandstone deposits, and the results of the in situ measurements are used to check the water level compared to ground level. The research of the conditions related to the check.
2. Overview of the current domestic experiences amassed related to refilling. Deducing if there is a "fluid layer exchange" between the water yielding layers during the wells' rest period. We have to determine if the monitoring well works properly, that proves the adequate state of the layers yielding and absorbing the water, opened and filtered for the planning of refilling. Does the low tide influences the measurement results.

3. Checking if greenhouse heating is economically profitable using energy procured from geothermal fluid, and comparing it to energy resources in use, in light of current market prices.
4. Heat pumping the fluid of lower enthalpy before refilling, and determining if the procured excess energy compensates for the costs of the heat pump, and the new well pair's digging and management. Based on the current CO₂ emission of the current electricity production, what COP value is needed by natural gas heating for an advantageous effect.
5. Does the buffer container installed in greenhouses' heating systems aid the production?

2. Material and Method

Unique well inspections

In order to get to know the data of the well, we have to do a well inspection. The measurement of the wells happens

with static and dynamic analyses [3]. The static measurement happens when the well does not produce, in a way that the well is freed of all machinery required for its usual operations. During the dynamic measurement, the well is operated with a compressor or a diving pump according to its operational parameters (Figure 1). The samplings are done after the well reaches its operational temperature. The machinery used for measurements are:

- Well consistence check, static analyses
- Dynamic analyses
- Samplings, laboratory analyses

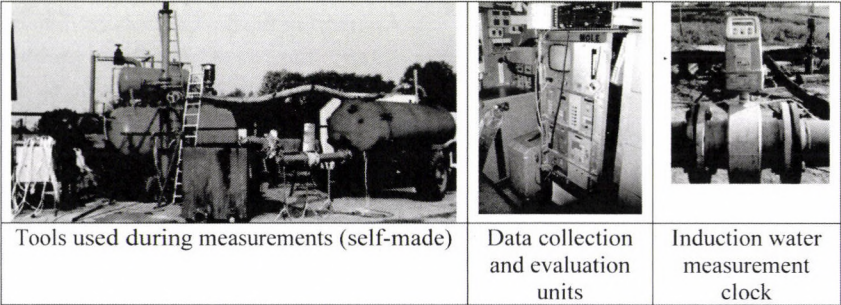


Figure 1. Surface measurements

The reference point for depth attributes was the ground level, which can be considered constant.

- Measured attributes:
1. water level and well pressure
 2. air pressure
 3. temperature of water flowing out
 4. gas content (with sampling)
 5. water yield

Water level and well pressure

In order to conduct the unique well inspections, both in its resting and operational time, the individual, long-term data recording Levelogger pressure- and temperature measurement unit was used. During the analysis of the cross-effects, multiple wells were watched at the same time, which was done with MicroDiver water level measurement units, which have similar attributes and operational method. The Levelogger and MicroDiver water level measurement units were not used to measure water level, but pressure, and they recalculate it to water height. Analogue manometers always measure water pressure compared to air pressure. The values measured by the pressure units watched two values: the pressure of the water above the unit, and the air pressure. The two combined gives us the absolute pressure as follows:

$$p = p_{\text{water}} + p_{\text{air}} \tag{1}$$

In order to calculate the pressure of the water, air pressure has to be subtracted from the absolute pressure.

Air pressure measurement

In order to collect the calculations with air pressure, Barologger was used as a data source. Gas separation, gas yield calculation During the well inspection measurements, we have to separate gases, as gas phase falsifies the data of water measurement clocks, but the calculation of this is also necessary in order to determine gas yield and gas composition. The fluid was first lead into the separator container, where the gas evaporates from the water. The gas leaving the water via the top of the container has to be cooled down for dew to manifest. The cold gas is usable for correct measurement by membrane and turbine gas measurement clocks.

Yield measurement

The water flowed from the separator containers through the water measurement clock attached to the data collection unit. This high salt-content fluid is refilled into the network via pumps.

Temperature measurement of the water flowing out

A Pt100-type temperature measurement unit was built into the pipes after the separator container, while the data were registered by the LogBox data collector.

Structural analysis of the wells

This type of measurement is a natural gamma, diameter and temperature measurement conducted via a combined unit within the closed well.

Data discovered:

- accessible base depth,
- piping diameters,
- stack exchanges,
- locations and closure of sealing,
- locations of opened areas,
- and the quality of cement works in the circular areas.

The natural gamma tunnel made it possible to check the cross-drive layer row (differentiate between permeable - impermeable areas), which is how we can check if the opened areas are capable of yielding water, and to determine where covered pipe clams are.

Flow profile

These measurements were conducted with the combined FRTmOP unit (flow, temperature, fluid resistance, optical transparency and pressure measurement unit). In the case of depth-based calculations, the unit moves in the well, and registers the data in 10 cm sampling increments, thereby pressure gradient and flow measurements determining the active areas of the filters can be conducted. The recorded pressure data is used to calculate gradient, which is in proportion to the density of the context, it's role is to show the bubbling point. Measured data was corrected by the temperature values.

Time-based depth pressure and temperature measurements

In order to conduct the depth pressure measurement - during the unique well inspections - the FTRMOP acoustic units were used, which sends the depth data real-time through a cable.

Organising measurements

The "timetable" set up for the analyses: building the pumps, static analyses, structural analysis of the well, rebuilding the well for compressor-aided production, building the lubricator, building the water measurement system, building the refilling unit, installing the compressor, prior production (24-48 hours), dynamic analyses.

Effects of the low tide

We analysed data measured by high-definition measurement tools, by taking the moon phase into consideration. Technically, we looked for the pulsating production change's effects of the active well and the pressure changes via the inspection well.

Possible agricultural heating systems, and comparison with geothermal heating

In Hungary, winter production is impossible without greenhouses. In practice, there are various energy resources, but due to the economic parameters, only a few can actually be realised [4].

Combustion heat production:

- firewood, wood chips
- pellet
- coal
- natural gas or PB gas

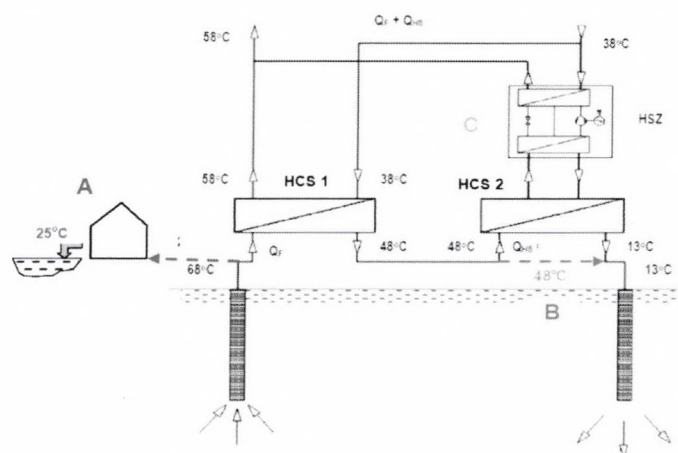


Figure 2. Options of using thermal water [6]

- A= direct heating coming from the well with the thermal water, leading the cooled (f. e. 25 °C) into a resting lake
- B= leading the thermal water coming from the well into a heat exchanger (HCS-1), and refilling the less hot (f. e. 48 °C) water, cooler due to the extracted heat
- C= leading the thermal water coming from the well into a heat exchanger (HCS-1), and leading the less hot (f. e. 48 °C) water into a heat exchanger (HCS-2), heat pumping it, then refilling the cooled (f. e. 13 °C) water, and leading the extracted heat into the heating system.

–heating oil..

Without combustion:

–heat production from thermal water.

Using heat from the environment with energy aid (electricity, natural gas, pyrolysis gas):

–heat pumping (air-air, soil-air, or used water-air).

In practice, we calculate heat requirement as follows:

$$Q = K' (t_b - t_k) F_{\text{ü}} \quad (2)$$

Based on the data received from the designers and the managers, and the offers from the websites, we determined the costs of the various heating systems for 1600 kW heat performance requirement. We did similarly when calculating the fuels' costs.

Greenhouse development for sustainability

Placing thermal water above ground causes environmental problems due to its high salt content, which is why there is an environmental load fee. Refilling it into the water yielding layer causes problems due to the drinking water base, but those can be solved, and the usage will be compulsory due to sustainability reasons [5]. In any case, refilling is an option, while another one is placement above ground after using heat pumping to extract the thermal energy from the high enthalpy fluid (Figure 2).

Thereby, the total amount of heat extracted: where:

$$Q_{FC} = \dot{m}c(T_{fo} - T_{fh}) \frac{\varepsilon_f}{\varepsilon_f - 1} \quad (3)$$

T_{fo} = average temperature of the leaving (for heating) water (K),

T_{fh} = average temperature of the fluid lead into the heat pump (K).

Our heating system is efficient exergetically if we use exactly as much exergy as we need. In practice, we have to carefully select the heat pump for this.

Measurement results in the buffer container

The heating systems of greenhouses have to constantly substitute for the heat exchanged into the environment through the material of the greenhouse and the ventilation [7]. If the greenhouses' structure is homogeneous in 90-95%, and the heat leaving through it (Q_o) and the heat leaving through it is considered a base heat loss, then we can calculate from the heat exchanging surfaces' heat loss:

$$Q_o = A_h \cdot k_o (t_i - t_e), \quad [W \cdot m^{-2} \cdot K^{-1}] \quad (4)$$

where:

– A_h – surface area of the greenhouse [m^2],

– k_o – heat permeability of the greenhouse's surface area [$W \cdot m^{-2} \cdot K^{-1}$],

– t_i – internal temperature of the greenhouse [$^{\circ}C$],

– t_e – external temperature of the greenhouse [$^{\circ}C$].

We measured the mass flow and temperature of the water flowing into the container in three time intervals, and the environment's and the greenhouse's average temperature (Figure 3). The data is required to determine the container's capacity.

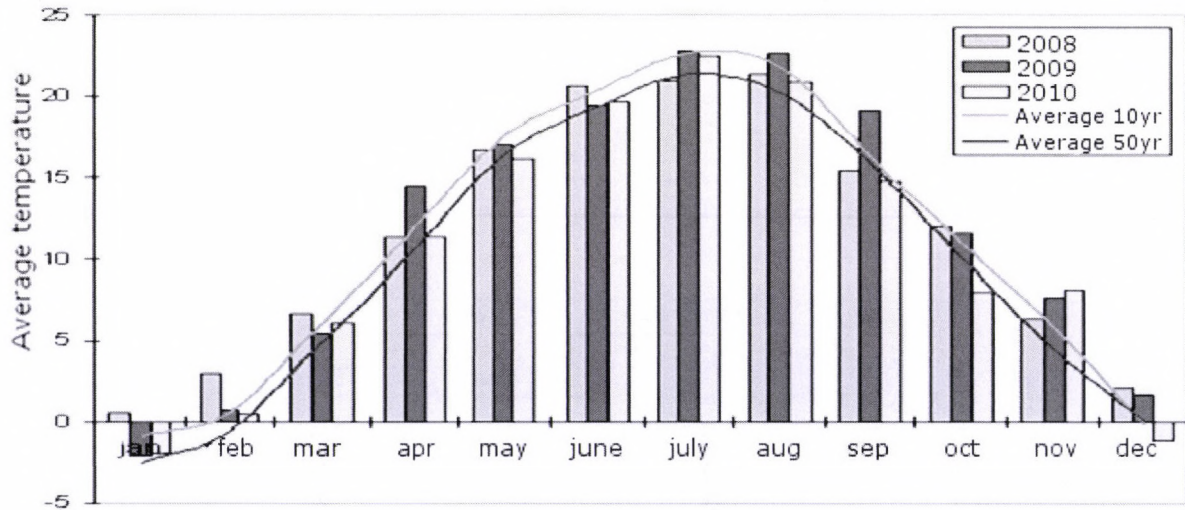


Figure 3. The monthly temperature average for a year around Szentes

3. Results

Geological and hydro-geological conditions, attributes of the area in question, details of the layers

As the depth increases, so does the pressure. In the upper Pannon's lower area, the hydrostatic pressure is about 40 meters below the potentiometric level (Figure 4).

In order to determine the regional hydro-dynamic attributes of the wells in question, the cross-effects and capacity analysis and refill measurement of the 3. well of the Árpád VII well group was applicable. The essence of this is the data from the inspection wells, during the well's operations. The various (numbered 14) but inter-connected wells yield more water as the base depth increases (Figure 5).

Determining the connections of water exchange between layers

Currently, there are 34 thermal water wells in the region around Szentes, of these, I analysed and modelled 20 currently operating wells (Table 1). The ground formation consists of sandstone, aleurolite and clay limestone, most of which is sandstone. The channel filling and aber reef deposits dominate, which have a good containing capacity, and limited horizontal spread, but the multiple avulsions and overlays are connected from a hydro-dynamic perspective. Therefore, many 5-25 metres sandy layers with good flow permeability change with clay-aleurite formations with bad permeability, as f. e. the acoustic logs from around Szentes also prove (Figures 6-7).

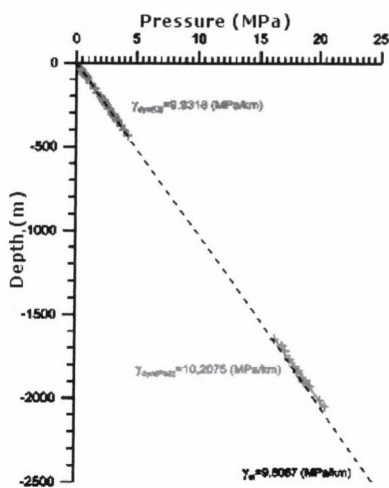


Figure 4. Pressure and depth data of the wells of Szentes

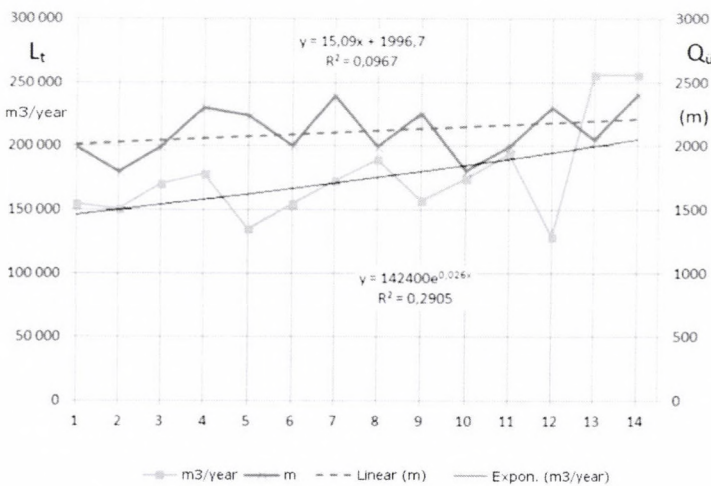


Figure 5. The connection between the wells' depths (L_t) and yield (Q_u)

Table 1. Average data of 20 wells from Szegvár and Szentes

	Base depth	Filtering (lower)	Filtering (upper)	Q max.	Water temperature
	(m)	(m)	(m)	(l/min)	(°C)
Average	2165,4	1873,75	2119,1	1488,45	86,5
Deviation	236,0	175,6	227,2	370,2	7,7

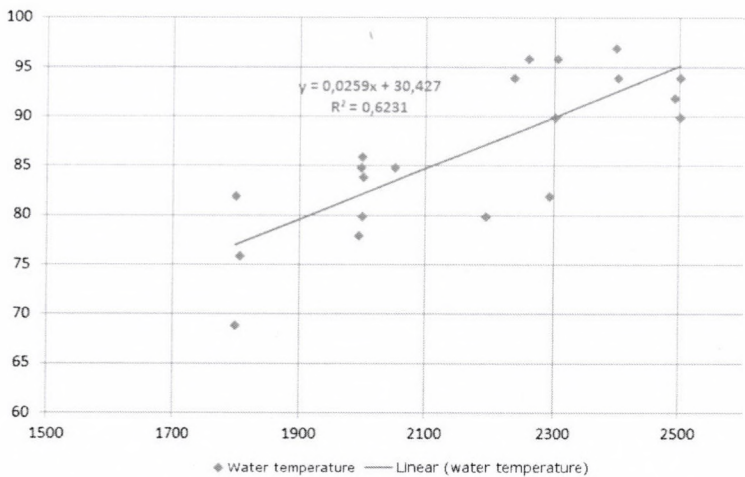


Figure 6. Connection between base depth (m) and water temperature

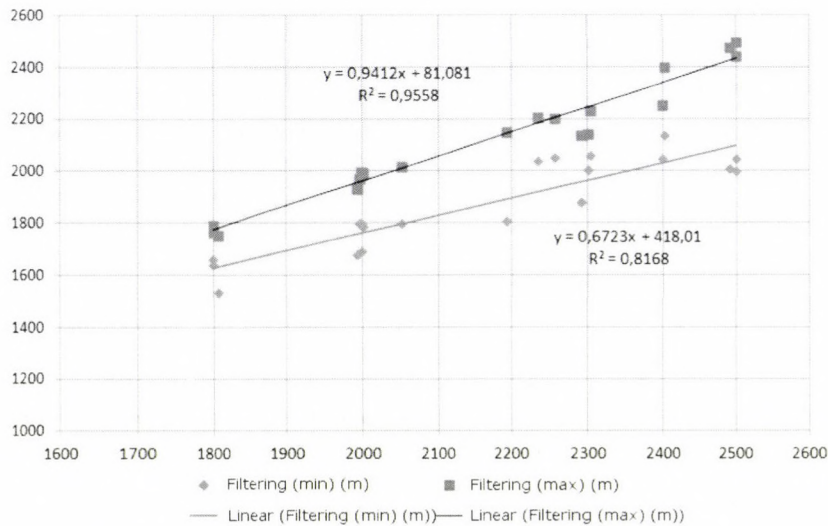


Figure 7. Connection between filtering max and min, and base depth (m)

Figure 8 contains a visual representation of the data gained from two wells of Szentes, made in order to find connections. The data set is as follows:

- natural gamma log (red)
- flow measurement curve (black)
- filtered areas (purple)
- non-reachable well areas (grey)
- active areas (green)
- route of cross-filling (black arrows)
- base of reachable areas (yellow)
- geothermic gradient's calculated reciprocal (on the bottom)

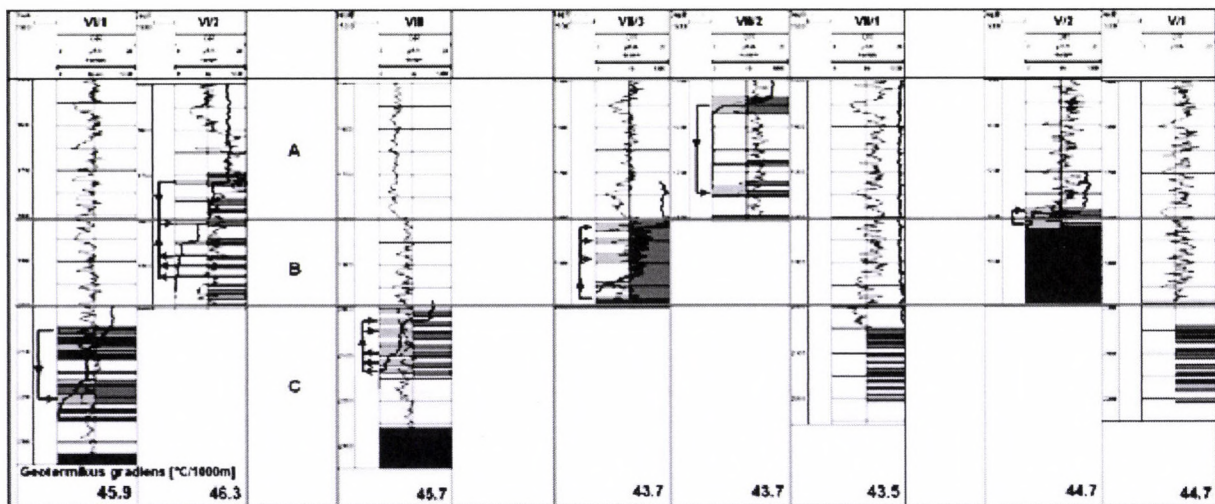


Figure 8. Internal cross-fillings between filtered layers within the wells of Szentes (for group I)

Illustrating the measurements conducted in the wells, and detailed analysis (we merely illustrate the attributes observed for the various wells):

Markings:

- blue curve – temperature log measured in the closed well
- red curve – temperature log measured during production
- blue curve upper – flow measurement log
- red columns – active filters
- blue arrows – internal water flow's route in closed wells
- above the figures: temperature gradient (green line)

In the example on Figure 8, all filters produce in the closed well. Areas I and II (from top to bottom) produce, but the water is drained into areas III, and mainly IV. It is important

to note that filters VI and V also produce in a closed situation towards area IV, as much as during operation.

According to the evaluations, we determined that [8]:

- temperature gradients match for the wells close to each other
- among the gradients, we can identify area differences
- the routes of cross-fillings are varied, in many wells, the cross-filling happens towards the middle layer from both the top and bottom layers
- the routes of cross-feedings give useful information about the pressure conditions of the yielding layers, which should be taken into consideration for both well production planning and new well planning

–when planning a refilling well, it is important to know the location and temperature of the absorbing layer, and the route of cross-filling.

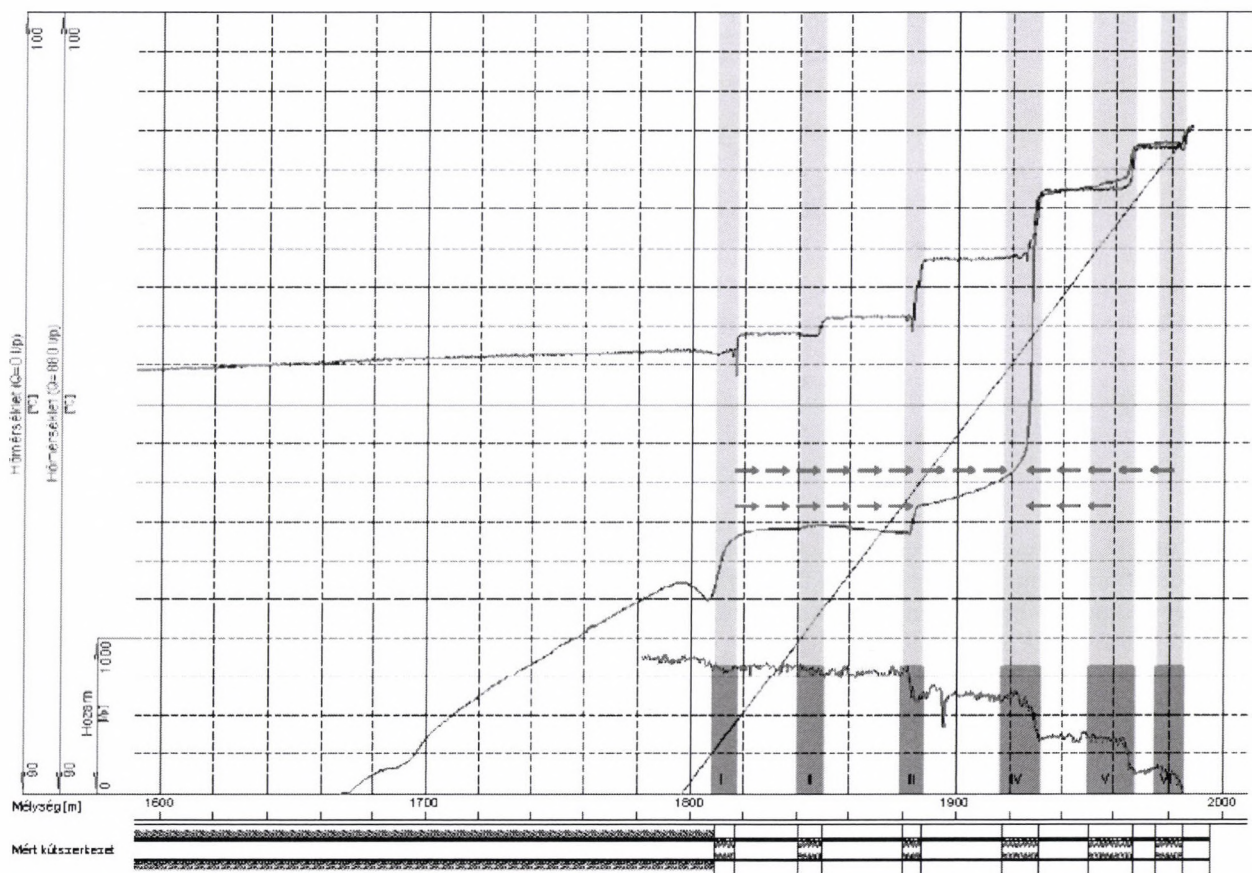


Figure 9. Szentes, Árpád-Agrár Co. Ltd., thermal well I (2000m), calculated geothermic gradient is 44,9 [°C/1000m]
A two-way flow was created

In wells which have multiple filters, cross-feeding and the absorption of some layers can always be observed, which means refilling can theoretically be realised always, to some degree at least (Figure 9). These analyses helped me get familiar with the area's hydro-geological attributes, and the more concrete technical and hydro-dynamic parameters of the wells in operation.

Low tide's effect on the measurements of thermal wells

During the calculations, using high-definition units in the inspection well showed the pulsating production changes' effect in the active well. The Moon caused the greatest effect when in line with the Sun during the analyses, which were the phases of New moon on 8. September, 2010, and Full moon, on 23. September, 2010. Of the two dates, the registered time of our analyses includes the New moon date. If we highlight a 12-hour from the periodic changes, we can observe the state seen on Figure 10.

The average process of this 12-hour pressure change can be seen on Figure 11. The trend shows a parabolic connection ($R^2 = 0,8519$).

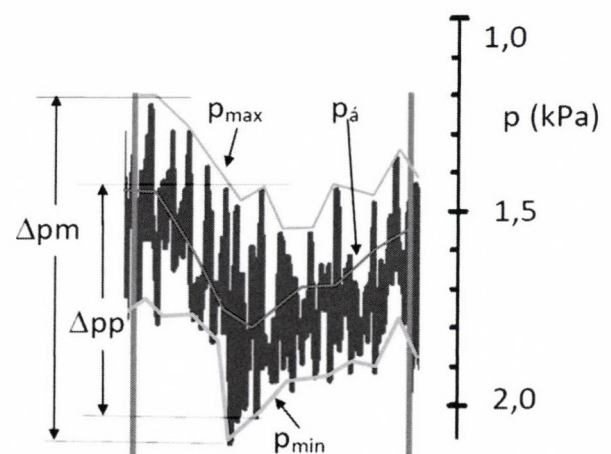


Figure 10. Maximum, minimum and average values' changes during the 12 hour period
 Δp_m = max change in 12 hours
 Δp_p = 0,6 kPa change during an hour
 $\Delta p_{\acute{a}}$ = 0,35 kPa highest change of the average of 12 hours

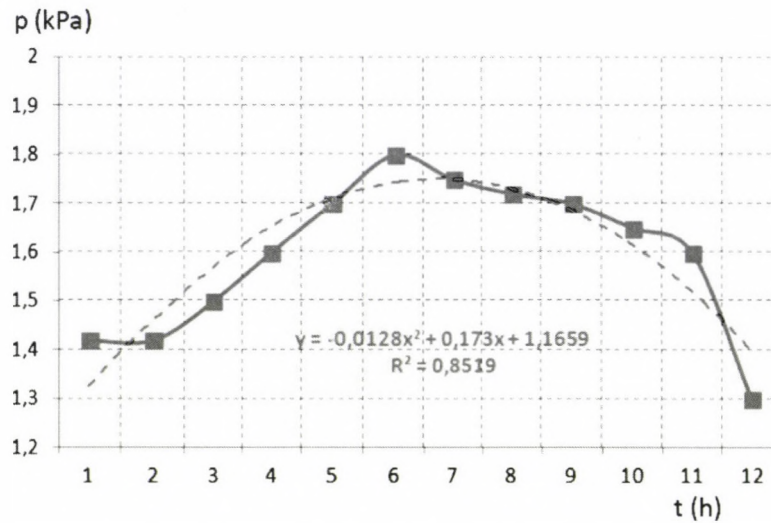


Figure 11. Average process of 12-hour pressure decrease

Based on the measurement results, we can state that if certain conditions are met, the positions of the Sun and the Moon can influence the rest and operation water level values of subterranean water bodies – the wells, in our case. During the analyses, the changes of water level show a 70 cm monthly, and ~15 cm daily in a cycle, even without any influencing factors.

Comparison of possible agricultural heating systems and the geothermal heating

As the heating requirements can change for any national areas due to different external factors, the values taken

from charts cannot be used in general for any area, and are mostly usable for comparison. When determining the prices of energy resources, we relied on the average value of prices for Hungarian industrial users. When determining the prices of machinery, we aimed to select those of good quality and price to value ratio.

As we can see on the data of Figure 12, the most advantageous is the thermal well heating system, followed by coal and lignite, and heat pumping in 4.th place. The calculation is applicable to the given situation, but the heat pumping systems have a determining effect when looking at the heat considered waste.

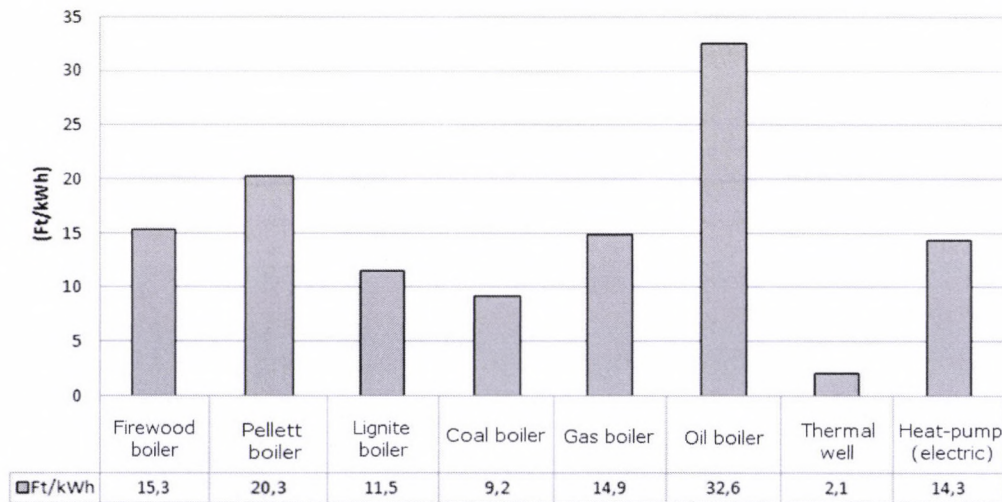


Figure 12. Total price of 1,0 kWh heat for a 15 year return on the system [9]

Greenhouse development for sustainability

Usage, economic benefits and environmental questions of using a heat pump

Using the most modern, large airspace greenhouses, the most developed construction techniques, and the best

technical solutions, experts forecast a huge leap in the sector's development. In modern agricultural production systems, geothermal fluids' energy content is used in multiple steps, and they do not forget to take sustainability into consideration either (Figure 13).

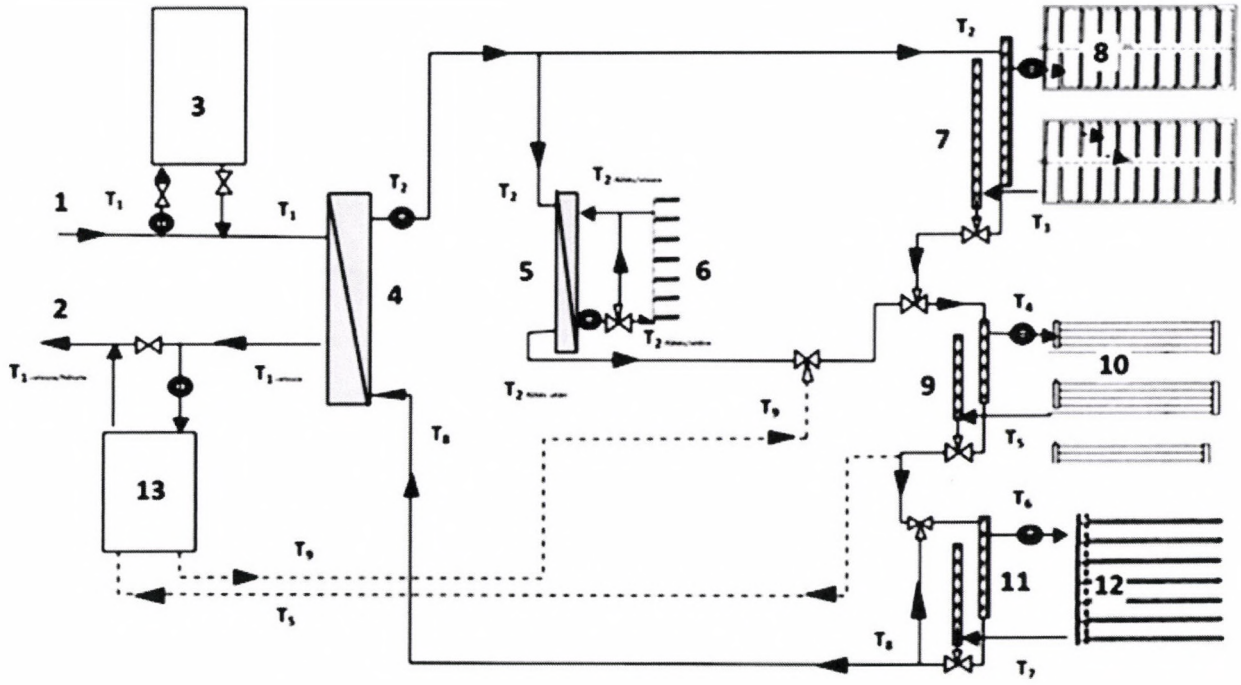


Figure 13. Theoretical heating system of a modern greenhouse [3]

Signs on the figure: 1 – production well, 2 – absorbing well, 3 – buffer container, 4 – main flow heat exchanger / heat centre, 5 – heat exchanger of social buildings, 6 – heating of social building, 7 – spread-collect units of vegetation heating, 8 – vegetation heating, 9 – spread-collect units of bloom heating, 10 – bloom heating, 11 – spread-collect units of soil heating, 12 – soil heating, 13 – heat pump

The heat performance obtainable via the heat pump is related to the mass flow and the ΔT value at the heat exchanger (temperature difference between inbound and outbound fluid):

Case A

$$Q_{FA} = \dot{m}c(T_{68} - T_{25}) \quad (5)$$

Case B

$$Q_{FB} = \dot{m}c(T_{68} - T_{48}) \quad (6)$$

Case C – via heat pump

$$Q_{FC} = \dot{m}c(T_{48} - T_{13}) \frac{\varepsilon_f}{\varepsilon_f - 1} \quad (7)$$

Case B and C combined:

$$Q_{F(C-B)} = Q_{FB} + Q_{FC} \quad (8)$$

If we take a look at the above, we can say that heat pumping before either refilling or letting the water off can produce energy close to 60-80% of the energy coming from direct usage. If we calculate properly, this energy, and the costs of using heat pumping has to be compared to the investment costs of a new pair of wells, and in the case of

letting the water off, the environmental load fee. The calculation shows positive results even for a new well. This system is especially advantageous in case we increase the plantation, and the energy requirement increases too, but we do not want to make a new geothermal investment.

In summary: in places, where refilling can be realised without problems, the system has a competitive edge against direct heat extraction using a new pair of wells. The heat pump serves sustainability best if assisted with renewable-source electricity. Figure 14 below shows an exergy-based analysis of a heating system including a heat pump. In the T diagram, to make sure we get T_{vf} temperature, the required heat is signified by points 1-2-7-8. In the environment, we have the amount of heat signified by points 3-4-7-8. From the perspective of exergetics, if the reference temperature equals the environmental temperature, area 1-2-3-4 (which can be gotten by subtracting the V2 loss) is the efficiently used energy (Ex). The temperature of vegetation heating (T_5) (heat amount) is aided from the secondary (condensation) side of the heat pump, which is subtracted from the heat not let out towards the environment. On the figure, the two areas of 3-4-7-8 and a-b-9-10 are equal (naturally, if we include losses, the latter is bigger). The exergy content (a-b-c-d) of this equals the heating requirement of vegetation heating. Our heating system is efficient exergetically, in case we use as much exergy as we require. In practice, we have to carefully choose the heat pump for this.

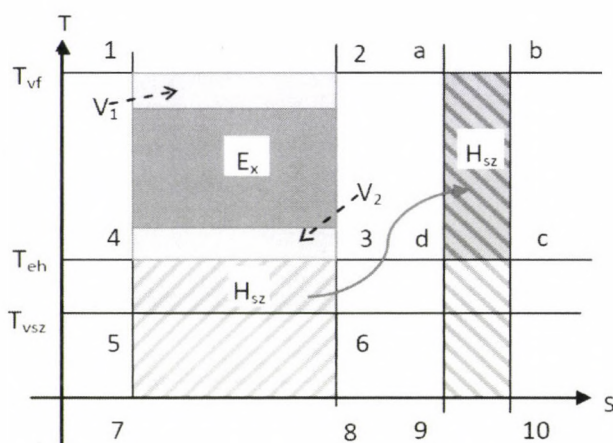


Figure 14. The exergy of the system increases by using the heat pump

In conclusion, using a heat pump increases the exergy in the system, and the heating water is substantially different in its attributes from the environment. This persists for both the internal and the external environments, but it's important that in the more critical winter season, it has a higher exergy content than on a hot summer day.

Buffer container measurement results

The heating systems of greenhouses have to complement the heat which the greenhouse emits through the surface area and the ventilation. In the hourly average temperature of January, the difference during 4 days reached 24 °C, which has to be compensated by the heating performance,

which is made even harder by how weather is sunny (with high radiation), or foggy-cloudy, when there is a weaker, more spread radiation. These extremities cause the system to require bivalent heating, if the well(s)' heating performance is inadequate (f. e. gas heating). Quick changes can be reacted to easily by spare heat containers, but well-side errors may also offer them some use. In case the well produces excess, the container is filled, and in case there is excess energy, the heat container offers extra heating. I analysed three specific time periods (Figure 15), and determined that extreme weather conditions and haviaria cold can both be averted for 6-8 hours when using a buffer.

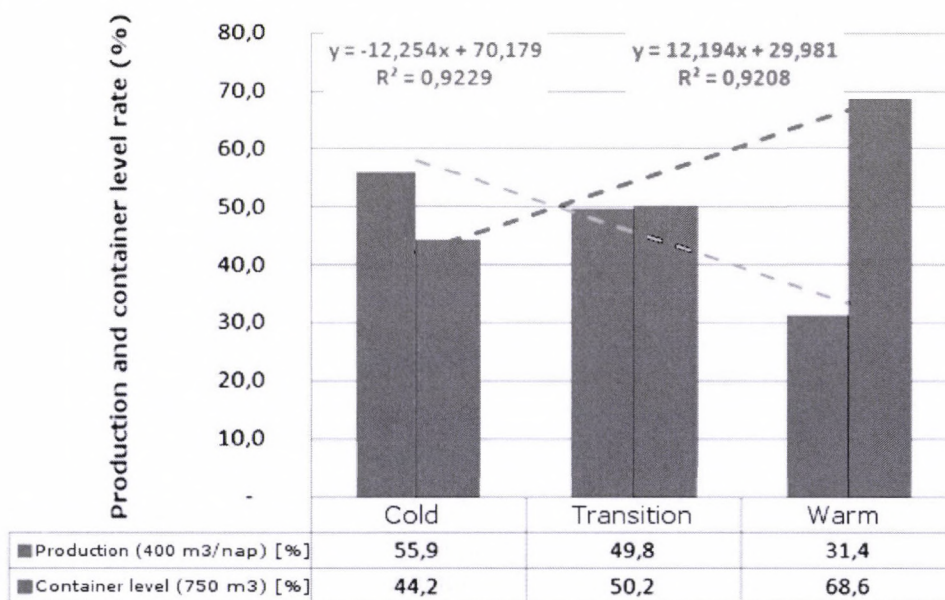


Figure 15. Conditions of the container's level and continuous water supply (production) ratio, in more general environmental temperature timeframes.

4. Conclusions

The detailed analysis of the 20 wells in the area around Szegvár and Szentés, and the results of the in situ measurements made me conclude that the resting water level compared to ground level has decreased by 25-30 mm

in the last 40 years. We proved that during the wells' rest period, a "fluid layer exchange" happens via cross-filling between water yielding layers. Therefore, the different water yielding layers are connected, which causes the resting wells to also have fluid movement, which also means that the water yielding layers can also act as water

absorbing layers during production. Generally in the resting period, when the period starts, filling goes towards the previously water yielding layer, which causes the flow in the well body to go vertically up or down between the filtered layers.

By analysing the measurement data, we were able to prove that the water level of porous-based thermal wells resting, and situated on the Southern Great Plains is influenced not only by the cross-fillings, but periodically (both daily and monthly) the Moon's low tide phenomenon as well.

We proved that a correct well measurement and comparison can only be done with measurements done within the same Moon cycle.

We proved that for wells maintained on the Southern Great Plains - even though the water level decreased, and production persisted for ~40-45 years – do not have a significant decrease in production. The water yielding layers of the Southern Great Plains' wells show a correlation of different flow and temperature, and depth gradients, and the absorbing layers, which shows they affect each other. I proved that refilling used (lowered enthalpy) water is possible, which means the base requirement is met. However, its success is greatly dependent on the attributes of the stone bed (size of grains, pore tunnel size, migrating material content, etc.). We proved that for planning refilling, only the monitoring well which proves the state of the water yielding and absorbing layers opened and filtered is usable.

We were able to prove that out of all the energy resources used for heating greenhouses (by the current market prices) the geothermal energy produced via convection is the most economically sound option. The three temperature level heating is the most advantageous, due to the different requirements caused by weather conditions, using a buffer container, and increasing the exergy of the "waste heating" remaining in the fluid, and the obtained heat content followed by rerouting it into the system's vegetation phase. Even in the case where the water which had its exergy removed after using the heat pump, and we also increase the specific energy costs with those of the refilling well.

We proved that the costs of establishing a heat pumping system, and the costs of establishing and maintaining a new pair of wells is covered by the excess energy produced (due to advantageous COP and SPF) in 2,5-3 years. Using the enthalpy of the "used water" only has an advantage above a COP value of 6,0 in spite of its economic advantage, due to the electricity production's CO₂ emission using natural gas heating (direct gas heating). We proved that using a heat pump can only be better environmentally when using renewable resources, when compared to natural gas heating. The optimal solution - if enough methane is at hand - is to use either separated and dried methane combustion, or mechanical heat pumping.

We proved that installing a buffer container into agricultural greenhouses' heating systems assures the safety of production (in case of significant and fast changes in weather and system errors), reduces the investment and management costs of necessary spare requirements (well capacity at hand) and spare energy resources. Depending on warm and cold weather, the level in containers is

inversely proportional to the fluid production ($R^2 = 0,92$). We proved that refilling and the usage of a heat pump and buffer containers are advantageous from both sustainability, environmental protection and agricultural economical benefits' perspective.

References

- [1] **Ádám B.:** 2008. Hőszivattyús földhő hasznosítás aktuális helyzete Magyarországon az EU helyzet tükrében, Kistelek, Geotermia a XXI. században szakmai fórum, 2008.
- [2] **Bobok E., Takács G., Turzó Z.:** 1998. Present status of geothermal energy production in Hungary (A geotermális energiatermelés jelenlegi helyzete Magyarországon), Proceedings of Geothermal Resources Council, San Diego, 1998.
- [3] **Strober I., Bucher K.:** 2013. Geothermal energy: from theoretical models to exploration and development, Springer, London, eBook, pp. 252-254.
<http://dx.doi.org/10.1007/978-3-642-13352-7>
- [4] **Nagygal J., Tóth L., Horváth B., Bártfai Z., Szabó I.:** 2015. Enhancing The Effectiveness of Thermal Water Consumption Via Heat Pumping. Applied Studies in Agribusiness and Commerce, Vol. 11 No 4, pp. 53-99.
<http://dx.doi.org/10.19041/APSTRACT/2015/4/7>
- [5] **Dincer I., Rosen M. A.:** 2007. Exergy: Energy, Environment and Sustainable Development, Elsevier, Oxford (UK), p. 13.
- [6] **Nagygal J., Tóth L., Horváth B., Fogarassy Cs.:** 2017. Thermal water utilization in the hungarian greenhouse practice. Thermal Science Vol. OnLine-First (00) <https://doi.org/10.2298/TSCI160831011N>
- [7] **Ásbjörnsson E. J.:** 2016. Renewable energy and carbon reduction, Reykjavik University. Slideshow, pp. 2-6.
- [8] **Nagygal J.:** 2014. Experiences of the Geothermal Project in Szentes, in: Hungary IGC, Freiburg, Germany, pp. 1-13.
- [9] **Nagygal J., Tóth L., Beke J., Szabó I.:** 2015. Comparison Of Possible Greenhouse Energy Sources. Hungarian Agricultural Engineering Vol. 26, pp. 47-53.
<http://dx.doi.org/10.17676/HAE.2014.26.47>

Notations

T_t	temperature of the container	°C
T_r	temperature of the refilled water	°C
T_0	temperature above ground	°C
\dot{m}	mass flow of the heating water	kg/h
q_0	heat performance procured	J
w	compressor work put in (energy)	kWh
COP	specific cooling (Coefficient Of Performance)	-
ε	specific cooling	-
e	specific exergy	kWh/kg
a	specific aenergy	kWh/kg
\dot{E}	exergy	J
$t_b - t_k = \Delta t$	difference between external and internal temperature	°C
F_u	size of the greenhouse surface area	m ²
Q_{FC}	effective heat energy	J

E_o	energy consumed by the system	J	t_e	external temperature of	
Q_{FC}	effective heat energy	J,		the greenhouse's atmosphere	$^{\circ}C$
E_o	energy consumed by the system	J.	k	Permeability	μm^2
ηE	P/Qfg efficiency of producing used electricity	-	$G_{rad} T$	Temperature gradient	$^{\circ}C/km$
$Q_{\text{össz}}$	total energy of the fluid	J	L_t	Base depth	m
Q_{VSZ}	total energy of the refilled fluid	J	SPF	Seasonal Performance Factor	-
P_{VE}	(electric) energy used to propel the heat pump	kWh	<i>Abbreviation</i>		
Q_{EXE}	efficient heat energy (exergy)	J	TL	Temperature measurement	-
k_o	thermal transmittance coefficient of the greenhouse	$W\ m^{-2}\ K^{-1},$	FLOW	Flow measurement	-
t_i	internal temperature of the greenhouse's atmosphere	$^{\circ}C$	REF	Refilling	-
			P_{rise}	Pressure increase	-
			P_{grad}	Pressure gradient	-
			H	Water level	-



DRYING CHARACTERISTICS AND QUALITY OF PEAR UNDER HYBRID DRYING (MID-INFRARED-FREEZE DRYING)

Author(s):

T. Antal

Affiliation:

University of Nyíregyháza, Institute of Engineering and Agricultural Sciences,
 Department of Vehicle and Agricultural Engineering, Kótaji Str. 9-11.,
 H-4400 Nyíregyháza, Hungary.

Email address:

antal.tamas@nye.hu

Abstract

This article provides results of an experimental investigation of hybrid- (MIR-FD), mid-infrared- (MIR) and freeze drying (FD) on the drying characteristics, energy consumption and quality parameters of pear. Rehydration ratio, color, texture were measured to evaluate the quality of dried pear products. Mid-infrared-freeze drying (MIR-FD) had the higher drying rate, which reduced the drying time by 14.3-42.9% compared with FD method. Two empirical models were chosen to fit the drying curves. The MIR-FD pear had darker color, better rehydration capacity and lower hardness than single stage of FD products. Above all, the MIR50-60°C-FD was suggested as the best drying method for pear in this study.

Keywords

combined drying, freeze drying, drying kinetics, energy uptake, quality

1. Introduction

The pears (*Pyrus communis* L.) are pomace fruit-tree species of the Rosaceae family. The pear is a fruit much appreciated for its characteristic flavor, crispness and sweetness. Most pears are eaten fresh and in processed forms: purées, juice, jams, dried, and in other forms [1].

Freeze-drying (FD), also denoted as lyophilization, has long been known as the best drying method for preserving the high-price products, the heat-sensitive materials [2, 3]. The FD is a dehydration process in which the solvent and/or suspension medium is crystallized at a low temperature and then sublimated from the solid state directly into the vapor phase [4]. FD has been reported to be an ideal method due to minimal shrinkage resulting in a porous product with excellent rehydration capacity, soft texture, bright color, superior taste, while the low temperatures used ensures good retention of nutrients [5]. However, the FD has long drying time, high energy uptake and costly process, a judicious combination with other dehydration methods. According to [6] the cost of FD has

been found to be at least one order of magnitude higher than conventional drying system.

Infrared drying (IR) supplies energy directly to the surface of the material and thus causes its rapid heating. The heat is transferred further towards the material inside by heat conduction [7]. The depth of penetration of radiation depends upon the characteristics of the sample and wavelength of radiation [8]. IR has many advantages compared to the widely used hot air drying. Such as, high heat transfer coefficients, short process time, quick response time, faster drying rate, uniform product heating and low energy cost are the characteristic properties of IR [6]. Moreover, drying of food products by IR enhances the quality of the dried products. According to [9] the wavelength of medium-wave- or mid-infrared radiation drying (MIR) is in the range of 1-4 μm which covers the maximum absorption wavelength of water molecule. The high heating speed is one of the most apparent advantages of MIR. The MIR is often employed to control the final moisture content of industrial product, mainly because MIR is heat-efficient, convenient and safe. For the penetrability of MIR is strong and it would be more effective in drying products. Therefore, the MIR can decrease a duration of drying [10].

The infrared drying has other advantages, for example the easy combination of the IR with convective, vibration, vacuum, freeze and microwave technologies; simplicity of the equipment and versatility [11]. The minimizing the energy consumption and enhancing the product quality of FD by combination of infrared or microwave drying were investigated by many researchers [12].

Hybrid drying (IR-FD) is a modern technique that combines all of the advantages of different drying methods, in terms of enhanced product quality and reduction in operational time and in energy consumption [6].

The mathematical model of drying kinetics is an important tool used to optimize management of operating parameters and to predict performance of a drying system. Numerous mathematical models, theoretical, empirical and semi-empirical, have been proposed to estimate the drying

characteristics of food products. These mathematical models, allow prediction of simultaneous heat and mass transfer during drying and are applied to simulate the drying curves [13, 14]. Several empirical models for drying kinetics in falling rate drying period are available in the scientific literature [15].

Product color is one of the most important sensory attributes of dried food. The mechanism of browning for many agricultural and horticultural products can be enzymatic and non-enzymatic (Maillard browning) source [16].

Texture, defined as a sensory property is perceived by humans using senses of touch and pressure, is a multi-parameter attribute related to the structure of the biomaterial [17].

The rehydration characteristics of a dried biomaterial are used as a quality index. According to [18] the degree of rehydration is dependent on the degree of cellular and structural disruption of treated material by different drying methods.

To our knowledge, no work is available the effect of mid-infrared-freeze drying on dehydration and quality characteristics of pear. Therefore, this present study was undertaken to investigate the MIR, FD and MIR-FD drying characteristics of pear, to determine the effect of hybrid-, FD and MIR drying on the specific energy consumption. In addition, the aim of our work is to evaluate the effect of different drying technology on the physical and mechanical parameters of pear dice.

2. Material and method

Sample preparation

The raw pear Packham's Triumph species (*Pyrus communis* L.) employed in the experiments were purchased from the grower (Apagy, Hungary) and stored in a refrigerator (5°C). The pears were washed with tap water, hand-peeled and cored with a knife, and then cut into cubes of 5 mm thickness using a hand-operated slicer. The free water on the surface of samples was removed with an absorbent filler paper. They were stored at a temperature of 5°C until the drying experiments.

The samples were divided into ten groups, each group of samples weighed 100 g. The initial mass of pear cubes was measured using a balance (model JKH-500, Jadever Co., New Taipei, Taiwan) with 0.1 g precision. The prepared pear samples were put into dryers after cutting to avoid surface enzymatic browning.

Determination of moisture content

Moisture content of the raw and dried pear dices was determined by the gravimetric method (model LP306, LaborMIM, Budapest, Hungary). At regular time intervals (30 min) during the drying process, samples were taken out and dried in the oven for 8 h at 105°C until constant weight. Weighing was performed on a digital balance (JKH-500, Jadever Co., New Taipei, Taiwan) and then moisture content was calculated.

Moisture content was expressed in wet matter (g 100 g fresh matter⁻¹, %) and in dry matter (kg moisture kg dry

matter⁻¹). The initial moisture content of the pear was found to be 81.03% (wet basis: w.b.), 4.271 kgH₂O kg dry matter⁻¹ (dry basis: d.b.). The tests were performed in triplicate.

Drying experiments

The pear cubes were dried by different drying methods with the optimal drying technology until the final moisture content (2-2.5%, wet basis: w.b.). The applied drying methods are described below-mentioned. The drying process was continued until a constant moisture content was recorded (The samples was dried until it reached the equilibrium moisture content). The moisture loss was recorded at 1 min intervals during the drying process in order to determine the drying curves. The experimental data sets from the different drying runs were expressed as moisture ratio (MR) versus drying time (t).

All the experiments were repeated thrice and the average of three results for each treatment was used in this paper. The dried products – before quality assessment – were cooled and packed in low-density polyethylene (LDPE) bags that were heat-sealed.

1. Mid-infrared drying (MIR). A quartz infrared heater, with nearly 80% efficiency in converting electrical energy to infrared energy was used for effective drying. The chamber wall was formed from aluminized steel, with a length of 15 cm, a breadth of 15 cm, and a height of 25 cm, equipped with a single door opening at the top, which allowed insertion and removal of the sample. In the drying chamber, a pair of quartz glass emitters (220 V, maximum power of per lamp 300 W) was positioned above the sample support. Infrared radiation, with wavelengths expressed in microns, can be accurately measured, controlled, and applied to the product. The wavelength of radiation between 2.4-3.0 μm and the heating intensity were maintained between 3-5.5 kW m⁻². The quartz glass emitter is located at a distance of 15 cm from the pear cubes surface. The sample tray was supported on a balance (a precision of ± 0.1 g, model Precisa, Precisa Instruments AG, Dietikon, Switzerland) to monitor the sample weight change during drying. The samples were spread uniformly in a monolayer on the aluminum tray. A vent was provided at the top of the chamber for the exit of moist air.

The experiments were carried out for 40-70°C drying temperatures. The emitter temperature and relative humidity were measured by Testo 4510 type meter (Testo GmbH, Lenzkirch, Germany) in the drying chamber. Another temperature probe was inserted into the sample to measure the product temperature (K-type thermocouple, Testo GmbH, Lenzkirch, Germany). However, the relative humidity was not controlled during the laboratory test. The samples were dehydrated until they reached the final moisture content (2.1-2.5%, w.b.).

2. Freeze drying (FD) was performed in a laboratory-scale Armfield FT-33 freeze-dryer (Armfield Ltd., Ringwood, UK). In the FD process, the pear dices were spread uniformly in a single layer on a stainless steel tray. The pear samples (100 g) were frozen at -24°C in a freezing/heating chamber and freeze dried to a moisture content of 2.06% (w.b.) at an absolute pressure of 85-95

Pa with a chamber temperature of 23°C and a condenser temperature of -47°C. In all experiments, temperature of the condenser and the chamber pressure were maintained at constant parameter. Thermocouples (four pieces) of freeze drier were inserted into the pear cubes.

The weight loss of the samples was followed by a data logger (ES-138, Emalog, Budapest, Hungary) and a RS-232 attached to a PC computer, acquired the data readings from platform cell (PAB-01, Emalog, Budapest, Hungary), which is placed within the sample chamber.

3. Hybrid or combined drying (MIR-FD): The pear samples were dried by FD drier by coupling with the MIR devices before the freeze drying step until the final moisture content was between 2.18-2.45% (w. b.). The samples after pre-drying procedure (MIR) were immediately placed into the FD, this is the so-called change point. The change points were placed in drying curve before reach to inflexion point of MIR curve. After the achievement of the inflexion point the color of the samples changed darkening – this phenomenon was determined using ColorLite sph900 colorimeter (ColorLite GmbH, Katlenburg-Lindau, Germany).

The experimental samples dried by MIR at 40°C for 5 min (MIR40°C-FD), MIR at 50°C for 5 min (MIR50°C -FD), MIR at 60°C for 5 min (MIR60°C -FD) and MIR at 70°C for 5 min (MIR70°C -FD) then dried by FD were chosen for further quality evaluation. The drying parameters are in agreement with above-mentioned ones (points of 1-2).

Mathematical models

There are several empirical approaches for modeling the drying kinetics. Henderson and Pabis (exponential) and third-degree polynomial models were used to fit the drying curves (MR versus drying time) in this study.

The Henderson and Pabis model was developed based on approximation that diffusion controls the drying process. This model has been used to describe various food and agricultural materials [19] (Eq. 1).

$$MR = a \cdot e^{-kt} \quad (1)$$

Another model, which is used for thin-layer drying studies, is the third-degree polynomial (Eq. 2). The model was successfully used to describe the freeze-drying characteristics of fruits and vegetables [20].

$$MR = a \cdot t^3 + b \cdot t^2 + c \cdot t + d \quad (2)$$

where MR is the dimensionless moisture ratio, a, b, c, d is the drying coefficients, k is the drying constant, t is the drying time (min, h).

The moisture content of samples is defined by (Eq. 3):

$$M_t = \frac{m_t - m_f}{m_f} \quad (3)$$

where M_t is the moisture content at time t on dry basis (kg H₂O kg dm⁻¹), m_t is the weight of material at specific t

(kg), and m_f is the dry matter weight of the material (kg).

The dimensionless moisture ratio (MR) was calculated as (Eq. 4):

$$MR = \frac{M_t - M_e}{M_0 - M_e} \quad (4)$$

where M_t is the moisture content at time t on dry basis (kg H₂O kg dm⁻¹), M_e is the equilibrium moisture content (kg H₂O kg dm⁻¹), and M_0 is the initial moisture content (kg H₂O kg dm⁻¹).

The moisture ratio (MR) was simplified to M_t/M_0 instead of $(M_t - M_e)/(M_0 - M_e)$ since M_e is relatively small as compared with M_0 – in case of all drying methods.

The coefficient of determination (R^2) and root mean square error (RMSE) were calculated to evaluate the fitting of two models to experimental data. The higher values of the R^2 and the lower values of the RMSE were chosen for goodness of fit. These statistical parameters can be calculated as (Eqs. 5, 6):

$$R^2 = 1 - \left[\frac{\sum_1^n (MR_{exp_i} - MR_{pre_i})^2}{\sum_1^n (MR_{ave} - MR_{pre_i})^2} \right] \quad (5)$$

$$RMSE = \sqrt{\frac{1}{n} \cdot \sum_{i=1}^N (MR_{exp_i} - MR_{pre_i})^2} \quad (6)$$

where n is the number of observations, exp is the experimental data, pre is the predicted data, ave is the average data, and MR is the moisture ratio.

Specific energy consumption

The total electrical power consumption (E , kWh) during FD, MIR and MIR-FD was measured by an energy-cost-checker (model EKM 265, Conrad Electronic GmbH, Hirschau, Germany).

Analysis was performed in triplicate. The specific energy consumption (SEC) expressed electrical power consumption requires for evaporation of one kilogram of water from specimen and was calculated according to Eq. 7.

$$SEC = \frac{E \times 3600}{W_0 - W_f} \quad (7)$$

where SEC is the specific energy consumption (MJ kg H₂O⁻¹), E is electrical power consumption from the energy-cost-checker (kWh), W_0 is the initial mass of the raw material (kg) and W_f is the final mass of the dried sample (kg).

Hardness test

The texture characteristics of the fresh and dehydrated pear were measured using a CT3-4500 (Brookfield Engineering

Laboratories, Middleboro, USA) texture analyzer fitted with a spherical probe. Compression test was carried out to generate a plot of force (N) vs. time (s). This plot was used to determine the value of hardness. The parameters that have been used were the followings: 8 kg force load cell, 2 mm s⁻¹ test speed, 20 mm travel distance and 4 mm diameter of cylindrical probe. The maximum depth of penetration was 3 mm and trigger force was 4.5 g. A 115 mm diameter plate (rotary base table) was used as a base while compressing the pear samples.

The samples were kept in a room temperature at 21°C until analysis. The penetrometer measurements are reported in Newton's (N).

Ten samples were tested and the average values were reported.

Color of products

The color of pear cubes was measured just before and immediately after drying treatment using a ColorLite sph900 colorimeter (ColorLite GmbH, Katlenburg-Lindau, Germany). The colorimeter (illuminant D65, 10° observer angle) was calibrated against a standard ceramic white tile. For each drying experiment the color measurement was performed on ten dried samples and the color values were compared with those of fresh samples (control). The powder obtained by grinding the dried material in a domestic mixer was used for color estimation. The spectrophotometer was supplied with special adapter. MA38 adapter converts the scanning spot from 3.5 to 38 mm. This device can be used to measure pear powders (the samples were examined from different points).

An important factor characterizing the variation of color in the test sample is total color difference. The total color change (ΔE) was evaluated as (Eq. 8):

$$\Delta E = \sqrt{(L_0 - L)^2 + (a_0 - a)^2 + (b_0 - b)^2} \tag{8}$$

where L^* is the degree of lightness (100) and darkness (0), a^* is the degree of redness (+) and greenness (-) and b^*

is the degree of yellowness (+) and blueness (-). Subscript 'zero' refers to the color reading of fresh pear cubes. This is my basis for comparison. A larger ΔE value denotes greater color change from the control (fresh) sample.

All experiments were performed in triplicate and the average values were reported.

Rehydration ratio

The measurement of the water rehydration ratio was based on the following procedure. 100 ml of distilled water was brought to a temperature of 30°C in a constant temperature water bath. Then a precisely weighed 0.5 g sample of the dried material was placed in a plastic vessel and immersed for 90 min. Afterwards the samples were taken out (when the time reached 5, 10, 30, 60 and 90 min) and blotted with tissue paper to eliminate excess water on the surface.

The weights of dried and rehydrated specimens were measured with an electronic digital balance (model JKH-500, Jadever Co., New Taipei, Taiwan) having a sensitivity of 0.1 g. The RR values were determined in triplicate.

$$RR = \frac{W_r}{W_d} \tag{9}$$

Rehydration ratio (RR) of dehydrated samples was estimated using the equation given below (Eq. 9).

where W_r is the drained weight of the rehydrated sample (g), and W_d is the weight of the dry sample used for rehydration (g).

Statistical analysis

Data analyses were determined using the PASW Statistics 18 software (IBM Corp., Armonk, USA), and analyses of variance were conducted by ANOVA procedure, Duncan test. Mean values were considered to be significantly different when $P < 0.05$.

Formal statistical analyses on all collected data were performed via Microsoft Excel v. 2013 (Microsoft Corporation, Redmond, USA) software.

Table 1. Effect of drying methods on moisture content of product and operational time

Drying method (Symbol)	Infrared pre-drying period [min]	Freeze finish-drying period [h]	Product moisture content [%, w.b.]	Total drying time [min]	Reduction in FD drying time [%]
FD	-	21	2,06	1260 ^h	-
MIR40°C-FD	5	17,92	2,21	1080 ^g	14,28 ^d
MIR50°C-FD	5	15,92	2,18	960 ^f	23,81 ^c
MIR60°C-FD	5	12,92	2,22	780 ^e	38,1 ^b
MIR70°C-FD	5	11,92	2,45	720 ^d	42,85 ^a
MIR40°C	20	-	2,34	20 ^c	-
MIR50°C	19	-	2,22	19 ^c	-
MIR60°C	16	-	2,49	16 ^b	-
MIR70°C	14	-	2,11	14 ^a	-

Means with different letters in the same column were significantly different at the level ($P < 0.05$)
FD, freeze-drying; MIR-FD, mid-infrared-assisted freeze-drying; MIR, mid-infrared drying.

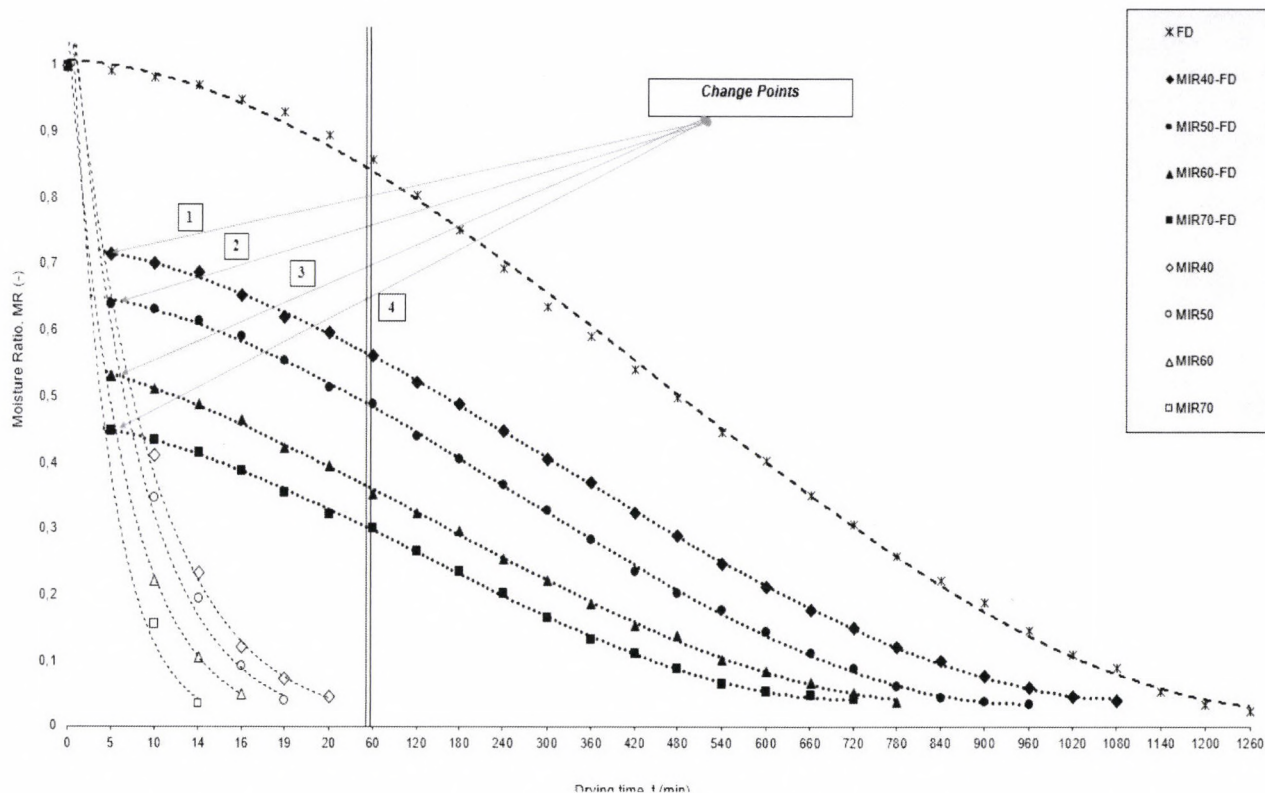


Figure 1. Drying curve of pear cubes

3. Results and discussion

Drying kinetics of different drying methods

Pear cubes with initial moisture content of 81.03% (w.b.) or 4.271 kgH₂O kg dry matter⁻¹ (d.b.) were dried following three different drying methods i.e. mid-infrared (MIR), freeze-drying (FD) and combined mid-infrared-freeze drying (MIR-FD) to a final moisture content of 2.06-2.49% (w.b.) or 0.09-0.21 kgH₂O kg dry matter⁻¹ (d.b.) (Table 1).

Drying curves of samples dried using MIR, FD and MIR-FD are compared in Figure 1.

The moisture content decreased continuously with drying time. This figure shows the drying values observed and estimated by the Henderson-Pabis and the third-degree polynomial models. The change points were placed in drying curve before reach to inflexion point of curve and the falling rate period.

As shown in Figure 1, the drying time to reach the final moisture content (2.11-2.49%, w.b.) using MIR at 40°C, 50°C, 60°C and 70°C was 20 min, 19 min, 16 min and 14 min, respectively. Therefore, the MIR operational time of the pear was very short.

In the early stage of MIR, the moisture content decreased more rapidly and subsequently slowly reduced with increase in drying time. This was due to the high drying rates in the early stages. During pear drying with MIR, no constant rate period was observed. From Figure 1, it can be observed that the moisture content decreases with drying time following an exponential decay. A similar trend was seen in studies grape [21].

It is observed that the total drying time required for FD is the longest (1260 min), followed by MIR40°C-FD (1080

min), MIR50°C-FD (960 min), MIR60°C-FD (780 min), and MIR70°C-FD (720 min), which yielded the shortest time (Table 1). Figure 1 showed that drying was completed after 720 min for MIR70°C-FD, and this represents a 42.85% reduction of drying time in comparison with FD. Thus, the MIR pre-drying lessened the drying time significantly ($P < 0.05$). Drying time used in MIR-assisted FD drying was 57.14-85.71% of that in FD drying (Table 1).

The MIR-FD drying curves can be divided into two drying stages, i.e. mid-infrared and freeze-drying parts. In the first stage, the dimensionless moisture ratio (MR) of pear decreased sharply, while reached the change point (at 5 min), for example at MIR40°C pre-drying (from 1 to 0.71), at MIR50°C pre-drying (from 1 to 0.64), at MIR60°C pre-drying (from 1 to 0.53) and at MIR70°C pre-drying (from 1 to 0.45) – i.e. MIR pre-drying described with a high drying rate. The change point shows where joined the various drying methods in succession. It can be observed that if the change points – at MIR-FD – decreases, the drying time decreases significantly ($p < 0.05$) (Table 1).

In the second stage, the drying rate of FD finish-drying exhibited a slow decrease to equilibrium moisture content of dried samples – i.e. FD finish-drying described with a low drying rate. Therefore, freeze-drying was applied after change point, when the moisture content of pear was reduced to 3.05 (1), 2.73 (2), 2.27 (3) and 1.91 kgH₂O kg dry matter⁻¹ (4), respectively (Figure 1). Overall, MIR-FD had a significantly higher drying rate than FD, but were significantly lower than MIR drying. These results were also observed by [22]. The decrease in the total drying time with increase of IR intensity from 3 to 5.5 kW m⁻² was associated with an increase in water migration inside the pear caused by MIR pre-drying.

Changes in the drying rate (DR is expressed as the amount of the evaporated moisture over time: $\text{kg water} \cdot \text{kg solid}^{-1} \cdot \text{min}^{-1}$) with drying time for different drying methods are shown in Figure 2.

The critical point (peak) divides the drying curves into two parts at FD curve. At the beginning of the drying process, the DR was progressively increased while

reached the critical point (so called initial heating period). The drying rate gradually decreased with drying time after the critical point (540 min), and kept almost constant at the end of the dehydration process (so called falling rate period).

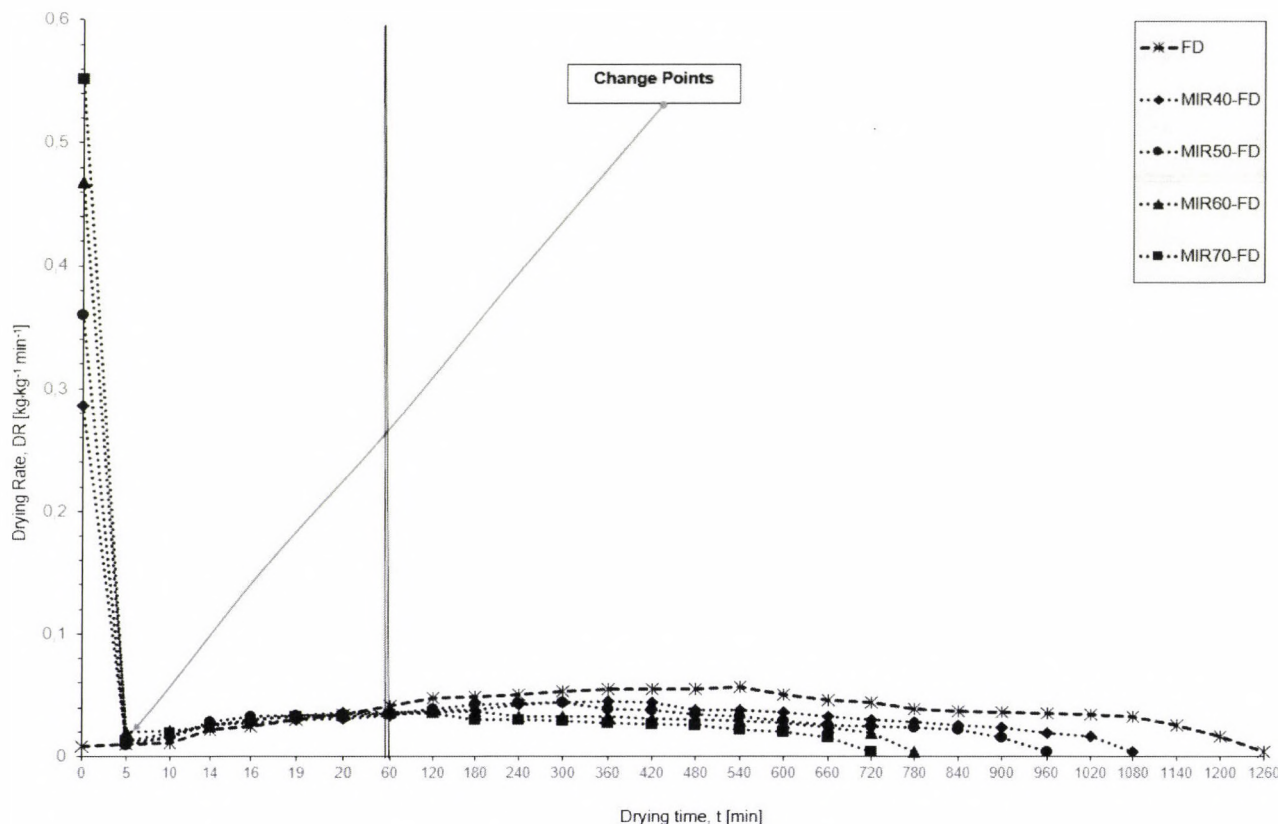


Figure 2. Drying rate curve of pear cubes

Compared with MIR-FD, a drying stage of constant rate period in FD can be observed (between 300 and 480 min). The drying rate of MIR-FD was obviously higher than that of FD. It was observed that the highest drying rate of MIR 70°C-FD was $0.552 \text{ kg} \cdot \text{kg}^{-1} \cdot \text{min}^{-1}$ (at the initiation of MIR pre-drying), while that of FD was $0.057 \text{ kg} \cdot \text{kg}^{-1} \cdot \text{min}^{-1}$ (at the 540 min drying time of FD), indicating that the MIR70°C-FD drying rate was about 9.7 times higher than FD drying rate. This phenomenon due to drying temperature (infrared intensity) of MIR. It was found that the drying rates increased from 0.28 to $0.55 \text{ kg} \cdot \text{kg}^{-1} \cdot \text{min}^{-1}$ with an increase in IR intensity at MIR pre-drying. The results were in conjunction with [23], in which the drying rate increased with the increase of drying temperature, and consequently reduced the operational time.

The increased molecular vibration in the exposed material due to absorption of radiation generates heat simultaneously at the surface and in the inner layers of the product. The rapid heating of the sample increased the rate of water removal [24].

A big fluctuation was observed in the MIR-FD drying curve and this might be due to the intermittent working mode of the combined mid-infrared pre-drying and freeze finish-drying method. During the drying, DR were high

($0.28\text{--}0.55 \text{ kg} \cdot \text{kg}^{-1} \cdot \text{min}^{-1}$) at the beginning of the process, and after that they intensely decreased approx. $0.01\text{--}0.02 \text{ kg} \cdot \text{kg}^{-1} \cdot \text{min}^{-1}$ at the change point.

The DR decreases continuously with drying time in falling rate period (This is a first falling rate period.). Drying rate under MIR-FD conditions increased from change points, this is a heating period. The values of critical point (peak) of MIR40-70°C-FD at the second stages of drying: $0.045 \text{ kg} \cdot \text{kg}^{-1} \cdot \text{min}^{-1}$ (360 min), $0.044 \text{ kg} \cdot \text{kg}^{-1} \cdot \text{min}^{-1}$ (300 min), $0.037 \text{ kg} \cdot \text{kg}^{-1} \cdot \text{min}^{-1}$ (180 min), $0.035 \text{ kg} \cdot \text{kg}^{-1} \cdot \text{min}^{-1}$ (120 min), respectively. The DR of MIR-FD was very low, gradually declined after critical point of the drying process (This is a second falling rate period). When the moisture content of pear cubes reached to final values, the values of DR at FD, MIR40°C-FD, MIR50°C-FD, MIR60°C-FD, and MIR70°C-FD were 0.0032, 0.004, 0.0038, 0.004 and $0.0044 \text{ kg} \cdot \text{kg}^{-1} \cdot \text{min}^{-1}$, respectively.

Taking it all round, the MIR-assisted FD drying is considered to be more efficient than FD drying alone, because of a synergistic effect. For MIR drying, the heat efficiency is high, the rate of heat loss is low, and the DR is quicker than that of FD drying.

The variation of dimensionless moisture ratio (MR) with drying time was fitted using two models, including Henderson and Pabis and third-degree polynomial models. The statistical parameters which estimated the model performance and the model constants are shown in Table 2.

The coefficient of determination (R^2) and root mean square error (RMSE) were used to assess how well the models characterized the drying kinetics. The R^2 values for all models were above 0.98. According to the statistical analysis, it was observed that the Henderson and Pabis and third-degree polynomial models presented high values of R^2 and low values of RMSE. The Henderson and Pabis model clearly fitted experimental data of MIR. The values of R^2 and RMSE of the Henderson and Pabis model for MIR dehydrated pear were in the range of 0.9807 to 0.9982, 0.0175 to 0.0465 which indicates the model

suitable for describing the drying characteristics of the pear during MIR drying.

A higher drying constant (k) demonstrates a higher drying rate at MIR drying. The values of k and a of the Henderson and Pabis model is higher with increasing in drying temperature (from 40°C to 70°C).

It was observed that the R^2 and RMSE of the third-degree polynomial were in the range of 0.9991 to 0.9998, 0.0067 to 0.0143. Thus, it adequately fit the experimental data for the freeze-drying of the pear cubes.

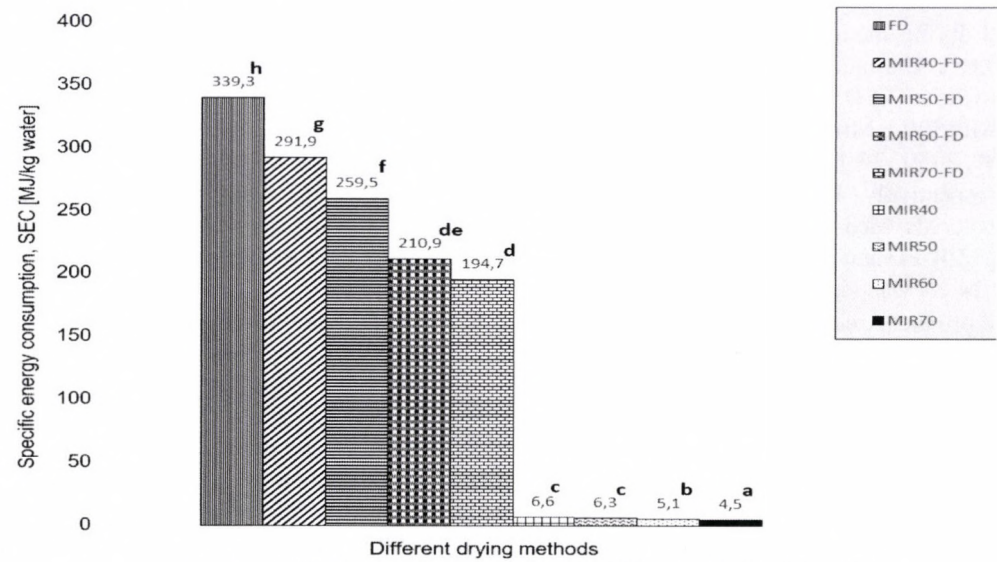
The thin-layer drying models, i.e. Henderson and Pabis and third-degree polynomial models were found to represent the drying kinetics of pear cubes with high R^2 and low RMSE values for all drying conditions.

The model's predicted data were described as curves in Figure 1 and these predicted curves fitted the experimental values very well.

Table 2. Model constants and statistical results obtained from the drying models

Drying method (Symbol)	Model constants					Evaluation criteria	
	k	a	b	c	d	R^2	RMSE
FD	-	0,000085	-0,003736	0,003312	1,008756	0,999102	0,014366
MIR40°C-FD	-	0,000079	-0,002938	-0,003406	0,735488	0,999852	0,006789
MIR50°C-FD	-	0,000103	-0,003547	-0,000284	0,660602	0,999513	0,009134
MIR60°C-FD	-	0,000086	-0,002444	-0,011792	0,567067	0,999428	0,010235
MIR70°C-FD	-	0,000123	-0,003439	-0,001170	0,464552	0,999469	0,010156
MIR40°C	0,539804	1,925862	-	-	-	0,995577	0,029865
MIR50°C	0,642646	2,208593	-	-	-	0,989468	0,042268
MIR60°C	0,761415	2,241401	-	-	-	0,998230	0,017542
MIR70°C	1,111216	3,577709	-	-	-	0,980729	0,046543

FD, freeze-drying; MIR-FD, mid-infrared-assisted freeze-drying; MIR, mid-infrared drying



Means with different letters were significantly different at the level ($P<0.05$)

Figure 3. Specific energy consumptions of pear under various dehydration conditions

uptake of different dryers

The specific energy consumption (SEC) during different drying processes are summarized in Figure 3. The SEC values were varied between 4.5 and 339.3 MJ·kg water⁻¹ for all drying conditions. The maximum SEC occurred at the FD drying (339.3 MJ·kg water⁻¹ –

FD had the longest drying time). In the case of the FD process, the longest drying time resulted the highest SEC.

It can be seen from Figure 3 that the SEC linearly increased with the drying temperature decreased in MIR (pre-drying). It was observed that the SEC of MIR-FD was significantly lower ($P<0.05$) than that of the FD. The SEC

in the MIR70°C-FD was 194.7 MJ·kg water⁻¹, which was lower than of 42.62% in pure FD drying.

Among all of the drying operations, the SEC of MIR70°C was 4.5 MJ·kg water⁻¹, which was the lowest – it was less, than of 98.67% in single stage of FD dehydration. The MIR drying had significantly lower ($P<0.05$) drying time and energy consumption compared with other drying methods. These results are in agreement with those reported by [25].

It was stated that increasing mid-infrared radiation or drying temperature reduced the operational time, thereby reducing the specific energy consumption. Similar results have also been reported by [26].

Hardness of pear product

The effects of MIR, FD and MIR-FD drying methods on the texture of pear cubes are reported in Figure 4.

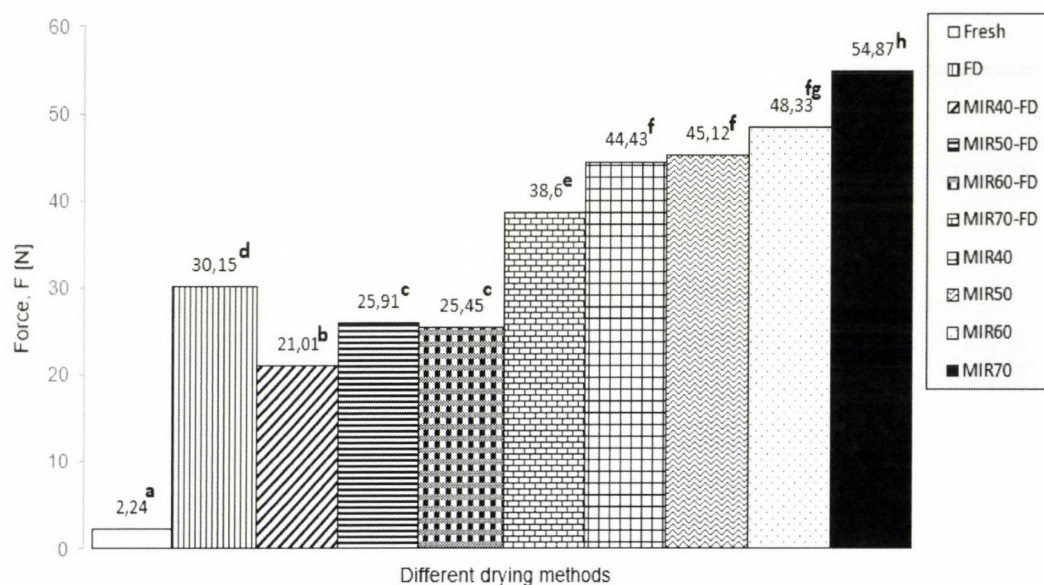


Figure 4. Effect of different drying methods on the hardness of pear cubes

The statistical analysis showed that the effects of drying temperature and drying methods on the firmness were significant ($P<0.05$). The hardness force values for FD, MIR40°C-FD, MIR50°C-FD, MIR60°C-FD, MIR70°C-FD, MIR40°C, MIR50°C, MIR60°C and MIR70°C pears were 30.15, 21.01, 25.91, 25.45, 38.6, 44.43, 45.12, 48.33 and 54.87 N, respectively. It was evidenced that the hardness of biomaterials dried by MIR was higher than for those dried using MIR-FD and FD. Moreover, the hardness of fresh pear (2.24 N) was significantly lower ($P<0.05$) than that of dried products treated by all drying methods.

The pear dehydrated by MIR40-60°C-FD methods show significantly lower ($P<0.05$) firmness values than FD dried sample. This fact can be explained by the drying uniformity and short drying time.

The shorter operational time of MIR pre-drying might have contributed to the better texture quality of the finish product. According to [27] in case of the MIR pre-drying the surface moisture evaporates faster and the inside of the biomaterial retains a porous honeycomb structure. This fact leads to softening of the texture.

The statistical analysis of the biomaterial showed no significant differences ($P>0.05$) between MIR50°C-FD and MIR60°C-FD dried pears.

It can be observed that the FD product result in a clearly porous structure, which explain relatively low firmness of freeze-drying (30.15 N) [28].

The results showed that the higher drying rate and IR power during MIR70°C resulted in significantly higher ($P<0.05$) firmness of the products compared to MIR40-60°C. The results of hardness at MIR40°C, MIR50°C and MIR60°C products showed no significant ($P>0.05$) differences in texture between drying methods. It can be observed, that increasing drying temperature and IR intensity, the hardness values increased ($P>0.05$) at MIR-FD and MIR drying (except of MIR60°C-FD).

Effect of drying on product color

Table 3 presents the color parameters of MIR, FD and MIR-FD dried and fresh pear samples. Color of fresh pear cubes before processing is: $L^*=73.59$, $a^*=0.22$, $b^*=16.86$, respectively. Compared to the control (raw material), the L^* and b^* values decreased and the a^* values increased significantly for MIR and MIR-FD dried products. Preferred colors are those closest to the original color of fresh pear cubes.

In general, MIR-FD dried pears were darker ($+L^*$), redder ($+a^*$) and less yellow ($+b^*$) in color than the undried pears. The FD dried product were lighter ($+L^*$), slightly redder ($+a^*$) and less yellow ($+b^*$) than fresh pear cubes.

The L^* values were ranged between 56.97 and 78.18 and a^* values between 2.05 and 8.97 and b^* values between 11.65 and 16.67 for dried pear cubes. The total color

change (ΔE) of pear cubes, calculated from Eq. 8 is variation of colors in foods during drying. The ΔE of dried pear was in a range between 4.95 and 19.49.

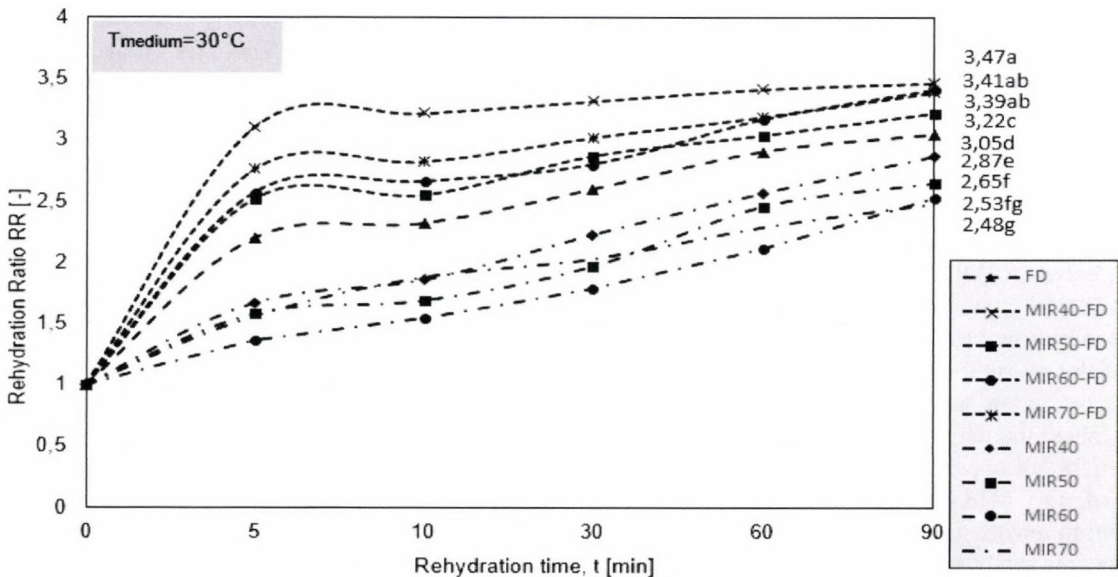
Table 3. Color values of the pear samples produced by using different drying methods

Description	Color parameters			
	L	a	b	ΔE
Fresh material	73,59	0,22	16,86	---
FD	78,18	2,05	16,60	4,95 ^a
MIR40°C-FD	71,73	5,29	16,67	5,4 ^{ab}
MIR50°C-FD	66,82	6,45	15,83	9,25 ^d
MIR60°C-FD	67,71	4,91	15,82	7,59 ^c
MIR70°C-FD	63,83	6,01	14,60	11,56 ^e
MIR40°C	60,66	7,23	13,40	15,11 ^f
MIR50°C	58,67	7,56	12,52	17,18 ^h
MIR60°C	59,23	7,13	12,98	16,40 ^{fg}
MIR70°C	56,97	8,97	11,65	19,49 ⁱ

Means with different letters in the same column were significantly different at the level ($P<0.05$)
 FD, freeze-drying; MIR-FD, mid-infrared-assisted freeze-drying; MIR, mid-infrared drying.

The FD dried pear exhibited the highest L^* value and the lowest ΔE value, followed by MIR-FD and MIR pear showed the lowest L^* value and the highest ΔE value. High L^* value (78.18) of FD pear indicated that the brightness coordinate faded due to freezing process in FD drying. Freezing rate during FD drying is one of the causes of significant ΔE (4.95) changes in FD products. The b^* values of the samples (16.60 and 16.67) showed that the FD and MIR40°C-FD pear cubes resembled the fresh product. This can be explained by the sensitivity of pear to temperature. The FD and MIR40°C-FD drying caused little

color change compared with the raw pear cubes. During the FD process, the Maillard reaction was inactivated.
 The color of MIR40°C-FD product was the closest to that of the FD samples. There were no significant differences ($P>0.05$) observed in the total color difference (ΔE) among the two drying methods. It is clear that lower drying temperature (IR intensity) and longer operational time of FD finish-drying maintained the original color of fresh pear cubes better. This can be explained by the short drying times and relatively low temperatures in case of MIR pre-drying which did not promote browning reactions.



Means with different letters were significantly different at the level ($P<0.05$)

Figure 5. Effect of different drying methods on the rehydration characteristics of pear

It can be seen that the L^* value (71.73) of dried product by MIR40°C-FD is very similar to fresh material. Drying temperatures were above 40°C at MIR-FD, rendering the possibility to the Maillard browning (so called non-

enzymatic browning). It was observed that the L^* value is relevant to browning in the products. In the case of L^* value, it was found that drying temperature and drying methods were the significant factors influencing the changes in brightness.

However, at the end of the drying the total color difference for MIR-FD at 40°C-70°C was the significantly ($P<0.05$) less than that for MIR drying at same drying temperature. The higher drying temperature (higher emission peak wavelength) may be the reason for deterioration of color of pear during MIR from 40°C to 70°C. The present color results indicated that the MIR products were darker (brownier and redder) than those of the FD and MIR-FD samples. The MIR products provided the highest a^* and lowest L^* and b^* values due to charring. The Maillard reaction and caramelization, may also occur due to heat during the MIR drying process. As the IR power increased, the ΔE values of the MIR and MIR-FD samples increased significantly ($P<0.05$) – except of MIR60°C and MIR60°C-FD.

Rehydration capacity

The Rehydration Ratio (RR) values of pear cubes dried by MIR, FD and MIR-FD are shown in Figure 5.

The end of the rehydration process the RR values for pear cubes dried with MIR40°C-FD, MIR60°C-FD, MIR70°C-FD, MIR50°C-FD, FD, MIR40°C, MIR50°C, MIR60°C and MIR70°C were 3.47, 3.41, 3.39, 3.22, 3.05, 2.87, 2.65, 2.53 and 2.48, respectively. The RR of the biomaterial dried by MIR-FD was the highest, followed by FD and MIR dried pear dices, and there was significant difference ($P<0.05$) between each methods. Opposite trend was observed in the previous study [25]. The MIR-FD was found to be inferior compared to the FD-MIR as the former tended to produce products with a collapse surface layer and poor rehydration capacity.

From Figure 5 we can see that the highest RR values in dried pear cubes by MIR-FD was because fewer physical and chemical changes occurred in the MIR-FD process due to shorter drying time and uniform heating compared to FD. The MIR pre-drying shows great promise in this respect. There were no significant differences ($P>0.05$) observed between MIR40°C-FD, MIR60°C-FD and MIR70°C-FD dried products. The water uptake curve of MIR-FD samples was suddenly jumped during the first 5 minutes of the rehydration procedure. This is because of the fast rehydration achieved with MIR-assisted FD materials. When the rehydration time was increased from 5 to 60 min, the RR of pear cubes was rose slightly at MIR-FD. All of the MIR-FD and FD samples showed stabilization in rehydration curve from 60 to 90 min – the samples became saturated.

Faster drying with IR and quicker diffusion of water vapor from the pear might help the sample retains its porous, less dense structure, increasing its ability to absorb more water during rehydration process [29]. Roknul et al. [30] was observed some porous spaces in the tissue cells of the material dried by IR. This phenomenon can be explained by the fact that during IR,

some swelling occurs in the tissue cells due to the absorbance of IR radiation, especially in a thin-layer on the sample surface.

The relatively higher rehydration capacity of FD products ($RR=3.05$) might be the result of such enhanced porous structures and prevention of tissue collapse. It was observed that the RR of FD after relatively rapid water uptake (at the beginning of rehydration process) gradually increased until reached the constant state at 60 min.

The pear cubes dried by MIR showed the significantly ($P<0.05$) lowest RR (between 2.48 and 2.87), but the values of RR is not negligible. The RR of MIR-FD sample almost doubled than the MIR samples when the rehydration process was reached 5 and 10 min. In addition, when the soaking time was increased from 10 min to 90 min, the RR of samples was increased slightly at MIR. The RR was found to decrease with increasing IR intensity levels (drying temperature) at MIR drying. Data indicated that increasing IR intensity level from 3 to 5.5 kW m⁻² exhibited a decline in RR of MIR40°C-70°C from 2.87 to 2.48.

The difference in rehydration attribute was related to surface hardening and the degree of structural damage which occurred during dehydration.

4. Conclusion

Three drying methods, i.e. mid-infrared-freeze drying (MIR-FD), freeze-drying (FD) and mid-infrared drying (MIR) were used in the preparation of pear cubes at four different drying temperatures (40, 50, 60 and 70°C) and the drying kinetics, the specific energy consumption (SEC), physical and mechanical properties of product (rehydration, color and texture) was investigated.

Application of mid-infrared-freeze drying enhanced the drying rate and significantly reduced ($P<0.05$) the operational time and SEC for pear samples. The dehydration rate (DR) of MIR-FD for pear cubes was higher than FD and was lower than MIR. The total drying time required for MIR-FD methods was 720-1080 min, reduced by 43-14% compared to pure FD (1260 min). Moreover, the operational time of MIR70°C-FD was the shortest, followed by MIR60°C-FD, MIR50°C-FD and MIR40°C-FD. It was found that the drying rate increases substantially with the increase in infrared drying temperature (intensity level).

In order to explain the drying behavior of pear, two thin-layer drying models were used. The drying kinetics were well-fitted by Henderson and Pabis model and third-degree polynomial model could adequate describe the dehydration behavior of pear under MIR, FD and MIR-FD conditions.

The MIR-FD products had softer texture (except of MIR70°C-FD) and better rehydration capacity than the FD and MIR samples. In terms of physical attributes of product, FD showed the better color. Pears dried by MIR had the worst quality, but cost the lowest SEC.

Hence, taking into account the drying characteristics and the product quality attributes, the combined mid-infrared pre- and freeze finish-drying (optimum condition: MIR50-60°C-FD) was the best method for industrial processing of

pear and commercial-scale application. On the basis of our results, it can be recommended that the MIR pre-drying temperature of pear should not exceed 60°C during the dehydration process.

References

- [1] **Kolniak-Ostek J.:** 2016. Identification and quantification of polyphenolic compounds in ten pear cultivars by UPLC-PDA-Q/TOF-MS. *Journal of Food Composition and Analysis*, Vol. 49, pp. 65-77. <http://dx.doi.org/10.1016/j.jfca.2016.04.004>
- [2] **Wojdyło A., Figiel A., Oszmiański J.:** 2009. Effect of drying methods with the application of vacuum microwaves on the bioactive compounds, color, and antioxidant activity of strawberry fruits. *Journal of Agricultural and Food Chemistry*, Vol. 57, Issue 4, pp. 1337-1343. <http://dx.doi.org/10.1021/jf802507>
- [3] **Kerekes B., Antal T.:** 2006. Drying methods of fruits and vegetables. *Hungarian Agricultural Engineering*, Vol. 19, pp. 43-45. Published online: ISSN 0864-7410
- [4] **Ciurzynska A., Lenart A.:** 2011. Freeze drying – application in food processing and biotechnology – a review. *Polish Journal of Food and Nutrition Science*, Vol. 61, Issue 3, pp. 165-171. <http://dx.doi.org/10.2478/v10222-011-0017-5>
- [5] **Ratti C.:** 2001. Hot air and freeze-drying of high-value foods: a review. *Journal of Food Engineering*, Vol. 49, Issue 9, pp. 311-319. [http://dx.doi.org/10.1016/S0260-8774\(00\)00228-4](http://dx.doi.org/10.1016/S0260-8774(00)00228-4)
- [6] **Chou S. K., Chua K. J.:** 2001. New hybrid drying technologies for heat sensitive foodstuffs. *Trends Food Science and Technology*, Vol. 12, Issue 10, 359-369. [http://dx.doi.org/10.1016/S0924-2244\(01\)00102-9](http://dx.doi.org/10.1016/S0924-2244(01)00102-9)
- [7] **Lechtanska J. M., Szadzinska J., Kowalski S. J.:** 2015. Microwave- and infrared-assisted convective drying of green pepper: Quality and energy considerations. *Chemical Engineering and Processing: Process Intensification*, Vol. 98, pp. 155-164. <http://dx.doi.org/10.1016/j.cep.2015.10.001>
- [8] **Hebbbar H. U., Rastogi N. K.:** 2001. Mass transfer during infrared drying of cashew kernel. *Journal of Food Engineering*, Vol. 47, Issue 1, pp. 1-5. [http://dx.doi.org/10.1016/S0260-8774\(00\)00088-1](http://dx.doi.org/10.1016/S0260-8774(00)00088-1)
- [9] **Chen Q., Bi J., Wu X., Yi J., Zhou L., Zhou Y.:** 2015. Drying kinetics and quality attributes of jujube (*Zizyphus jujube* Miller) slices dried by hot-air and short- and medium-wave infrared radiation. *LWT – Food Science and Technology*, Vol. 64, Issue 2, pp. 759-766. <http://dx.doi.org/10.1016/j.lwt.2015.06.071>
- [10] **Wang L., Zhang M., Fang Z., Xu, B.:** 2014. Application of intermediate-wave infrared drying in preparation of mushroom chewing tablets. *Drying Technology* Vol. 32, Issue 15, pp. 1820-1827. <http://dx.doi.org/10.1080/07373937.2014.949347>
- [11] **Riadh M. S., Ahmad S. A. B., Marhaban M. H., Soh, A. C.:** 2015. Infrared heating in food drying: An overview. *Drying Technology*, Vol. 33, Issue 3, pp. 322-335. <http://dx.doi.org/10.1080/07373937.2014.951124>
- [12] **Chong C. H., Figiel A., Law C. L., Wojdyło A.:** 2014. Combined drying of apple cubes by using of heat pump, vacuum-microwave, and intermittent techniques. *Food Bioprocess Technology*, Vol. 7, Issue 4, pp. 975-989. <http://dx.doi.org/10.1007/s11947-013-1123-7>
- [13] **Poós T., Örvös M.:** 2012. Heat and mass transfer in agitated, co-, or countercurrent conductive-convective heated drum dryer. *Drying Technology*, Vol. 30, Issue 13, pp. 1457-1468. <http://dx.doi.org/10.1080/07373937.2012.689402>
- [14] **Mészáros Cs., Farkas I., Bálint Á.:** 2001. A new application of percolation theory for coupled transport phenomena through porous media. *Mathematics and Computers in Simulation*, Vol. 56, pp. 395-404. [http://dx.doi.org/10.1016/S0378-4754\(01\)00310-X](http://dx.doi.org/10.1016/S0378-4754(01)00310-X)
- [15] **Beke J., Kurják Z., Bessenyei K.:** 2012. Konvekciós szárítási modellek alkalmazási lehetőségei a mikrohullámú szárítási folyamatokban. *Mezőgazdasági Technika*, Vol. 53, Issue 7, pp. 30-32.
- [16] **Pekke M. A., Pan Z., Atungulu G. G., Smith, G., Thompson J. F.:** 2013. Drying characteristics and quality of bananas under infrared radiation heating. *International Journal of Agricultural and Biological Engineering*, Vol. 6, Issue 3, pp. 58-70. <http://dx.doi.org/10.3965/j.ijabe.20130603.008>
- [17] **Szczesniak A. S.:** 2002. Texture is a sensory property. *Food Quality and Preference*, Vol. 13, Issue 4, pp. 215-225. [http://dx.doi.org/10.1016/S0950-3293\(01\)00039-8](http://dx.doi.org/10.1016/S0950-3293(01)00039-8)
- [18] **Krokida M. K., Marinos-Kouris D.:** 2003. Rehydration kinetics of dehydrated products. *Journal of Food Engineering*, Vol. 57, Issue 1, pp. 1-7. [http://dx.doi.org/10.1016/S0260-8774\(02\)00214-5](http://dx.doi.org/10.1016/S0260-8774(02)00214-5)
- [19] **Henderson S. M., Pabis S.:** 1961. Grain drying theory II: Temperature effects on drying coefficients. *Journal of Agricultural Engineering Research*, Vol. 6, Issue 3, pp. 169-174.
- [20] **Antal T., Kerekes B.:** 2015. Investigation of hot air- and infrared-assisted freeze-drying of apple. *Journal of Food Processing and Preservation*, Vol. 40, Issue 2, pp. 257-269. <http://dx.doi.org/10.1111/jfpp.12603>
- [21] **Celma A.R., López-Rodríguez F., Blázquez F. C.:** 2009. Experimental modelling of infrared drying of industrial grape by-products. *Food and Bioprocess Technology*, Vol. 87, Issue 4, pp. 247-253. <http://dx.doi.org/10.1016/j.fbp.2008.10.005>
- [22] **Lin Y. P., Tsen J. H., King V. A. E.:** 2005. Effects of far-infrared radiation on the freeze-drying of sweet potato. *Journal of Food Engineering*, Vol. 68, Issue 2, pp. 249-255. <http://dx.doi.org/10.1016/j.jfoodeng.2004.05.037>
- [23] **Sharma G. P., Verma R. C., Pathare P. B.:** 2005. Thin-layer infrared radiation drying of onion slices. *Journal of Food Engineering*, Vol. 67, Issue 3, pp. 361-366. <http://dx.doi.org/10.1016/j.jfoodeng.2004.05.002>
- [24] **Puente-Díaz L., Ah-Hen K., Vega-Gálvez A., Lemus-Mondaca R., Di Scala K.:** 2013. Combined infrared-convective drying of Murta (*Ugni molinae* Turcz) Berries: Kinetic Modelling and quality assessment. *Drying Technology*, Vol. 31, Issue 3, pp. 329-338. <http://dx.doi.org/10.1080/07373937.2012.736113>

- [25] Wang H., Zhang M., Adhikari B.: 2015. Drying of shiitake mushroom by combining freeze-drying and mid-infrared radiation. Food and Bioproducts Processing, Vol. 94, pp. 507-517.
<http://dx.doi.org/10.1016/j.fbp.2014.07.008>
- [26] Ning X., Lee J., Han C.: 2015. Drying characteristics and quality of red ginseng using far-infrared rays. Journal of Ginseng Research, Vol. 39, Issue 4, pp. 371-375.
<http://dx.doi.org/10.1016/j.jgr.2015.04.001>
- [27] Wang H., Zhang M., Mujumdar A. S.: 2014. Comparison of three new drying methods for drying characteristics and quality of shiitake mushroom (*Lentinus edodes*). Drying Technology, Vol. 32, Issue 15, pp. 1791-1802.
<http://dx.doi.org/10.1080/07373937.2014.947426>
- [28] Ferenczi S., Czukor B., Cserhalmi Zs.: 2014. Evaluation of microwave vacuum drying combined with hot-air drying and compared with freeze- and hot-air drying by the quality of the dried apple product. Periodica Polytechnica. Chemical Engineering, Vol. 58, Issue 2, pp. 111-116. <http://dx.doi.org/10.3311/PPch.7082>
- [29] Nasiroglu S., Kocabiyik H.: 2009. Thin-layer infrared radiation drying of red pepper slices. Journal of Food Process Engineering, Vol 32, Issue 1, pp. 1-16.
<http://dx.doi.org/10.1111/j.1745-4530.2007.00195.x>
- [30] Roknul A. S. M., Zhang M., Mujumdar A. S., Wang Y.: 2014. A comparative study for four drying methods on drying time and quality characteristics of stem lettuce slices (*Lactuca sativa* L.). Drying Technology, Vol. 32, Issue 6, pp. 657-666.
<http://dx.doi.org/10.1080/07373937.2013.850435>



THE COST-BENEFIT ANALYSIS OF APPLICATION OF VITAMIN AND MINERAL SUPPLEMENTS IN BROILER CHICKEN PRODUCTION

Author(s):

L. Ózsvári¹ – R. Tisóczki¹ – Á. Bartha² – M. K. Horváth²

Affiliation:

¹University of Veterinary Medicine Budapest, Department of Veterinary Forensics, Law and Economics, István street 2, H-1078 Budapest, Hungary

²Szent István University, Faculty of Economics and Social Sciences, Climate Change Economics Research Centre, Péter Károly street 1, H-2100 Gödöllő, Hungary

Email address:

ozsvari.laszlo@univet.hu, renato.tisoczki@gmail.com, akos.bartha@gmail.com, horvathmonikakitti@gmail.com

Abstract

Out of all food of animal origin, the demand for poultry meat increases the most dynamically - the poultry sector can only satisfy this demand by introducing more and more intensive raising technology. The goal of this study is to measure the positive impact on production parameters (mortality, live weight gain, feed conversion ratio) of vitamins and nutrient supplements (Gastroferm M+C®, Jolovit®, Norovit-Amino Forte®, Phylamic®, Tetraselene-400-E®, Tetravit AD3E Forte® and Vitaplan DCP®) in raising broiler chickens, and to conduct an economic analysis of their application. In the study, we measured the effects on production indices of a special feed additive mix that contains vitamin- and nutrient supplements, which were compared to those in the control group having no extra supplements. Based on the differences in the production parameters, we conducted the cost-benefit analysis of this special feed supplement mix. The Ross 308 hybrids in the experimental group were fed with supplements and produced 0.6% percentage point lower mortality rate, 0.11 kg more slaughter weight, and 0.13 kg/kg smaller feed conversation ratio on average compared to the control group. Based on the analysed production indeces, the use of the vitamin and mineral supplements had a 10.9 return on investment (ROI), and yielded 41.5 HUF extra profit per chicken in the experimental group compared to the control group.

Keywords

cost-benefit analysis, broiler chicken production, nutrient supplements

1. Introduction

The poultry sector has a very significant role within the agriculture sector, not only in Hungary, but all around the world [1]. Producing poultry meat is faster, and more cost-

efficient than that of mammals. As the less-developed countries gradually close the economic distance, their population gradually changes their eating habits which requires a larger amount of meat being produced globally. Out of all food of animal origin, the demand for poultry meat increases the most dynamically, and the poultry sector can only satisfy this demand by introducing more and more intensive raising technology.

In Hungary, an average of 70% of total production costs of broiler raising are made up of the feeding costs [2]. As the livestock farmers have no way of influencing grain prices, they try to decrease other costs [3]. The goal of this study is to measure the positive impact on production parameters of vitamins and nutrient supplements in raising broiler chickens and to conduct an economic analysis of their application.

2. Overview of the global and Hungarian poultry sector

Global market outlook of the poultry sector

The poultry sector has undergone a more rapid development than other animal husbandry sectors in the XX. century, most notably in its second half. Even the economic crisis that we had to deal with in the first decade of the XXI. century, and the decrease in demand and the increase in feeding costs could not diminish this sector. Even though it doesn't show the same dynamism as before, it's still expanding steadily. The global annual poultry meat production reached 100 million tons by 2011. Based on the forecasts, this amount may go up to 122 million tons by 2020 [4]. Due to the biological traits of poultry species, poultry is the husbandry sector that adapts most easily to the consumer demands [5]. Therefore, the poultry meat production and trade is expected to grow further on a global level [6]. Based on Rabobank's [7] forecast, the global poultry meat production may even surpass the pork production by 2030.

The chicken meat production of the European Union exceeded the consumption by 181.000 tons in 2000, which is expected to be 125.000 tons more by 2025. This means that the European Union won't become a net importer by then [8]. However, the costs related to the stricter administrative, animal welfare, environmental protection and animal transport regulations, and to the more often authority checks and laboratory tests will increase [9]. This increase in production cost can be expected in both the member states that joined the EU in the last 10-15 years with less developed economies, and the older member states [2].

Production costs of the Hungarian boiler chicken sector

In broiler chicken production the feed costs are the most significant, as they give nearly three fourths of the total production cost (Figure 1). In recent years, we saw these costs fluctuated greatly year by year, but eventually increased (Figure 2). For the production the feed was generally purchased, therefore, the broiler chicken farmers are very dependent on the feed distributors.

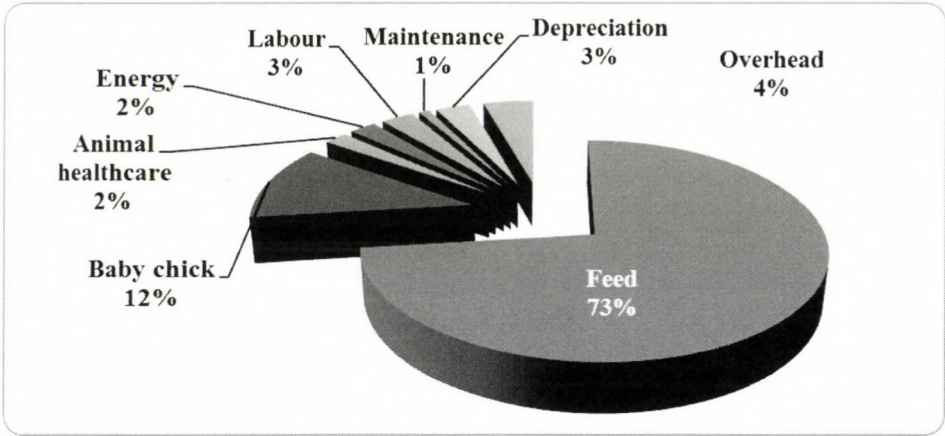


Figure 1. Distribution of broiler chicken production cost in 2012 [6]

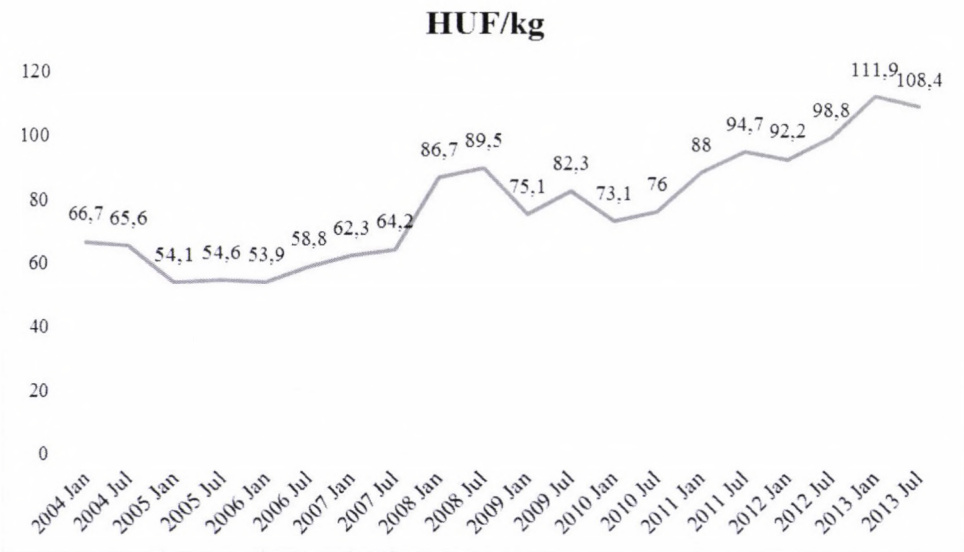


Figure 2. Monthly sale prices for broiler starter feed (2004-2013) [5]

Based on the change in feed prices in the last 10 years, we can conclude that the prices are closely related to the procurement of soya, which is a weakness for the Hungarian animal husbandry in general [11]. The changes of global market prices are fundamentally influenced by three factors; the decrease of production in some major production areas, the increasing demand for feed due to the expansion of animal husbandry, and the increasing bio-

ethanol production [12]. Feed prices were between 70 and 75 HUF/kg in 2004, whereas nowadays, they're above 100 HUF/kg [8].

Sale prices of chickens for slaughter follow the changes in feed prices a little bit later. Figure 3. shows that after the avian flu outbreak in 2006, sale prices were constantly on the rise until 2008, when the global financial crisis hit in, but afterwards began to rise again.

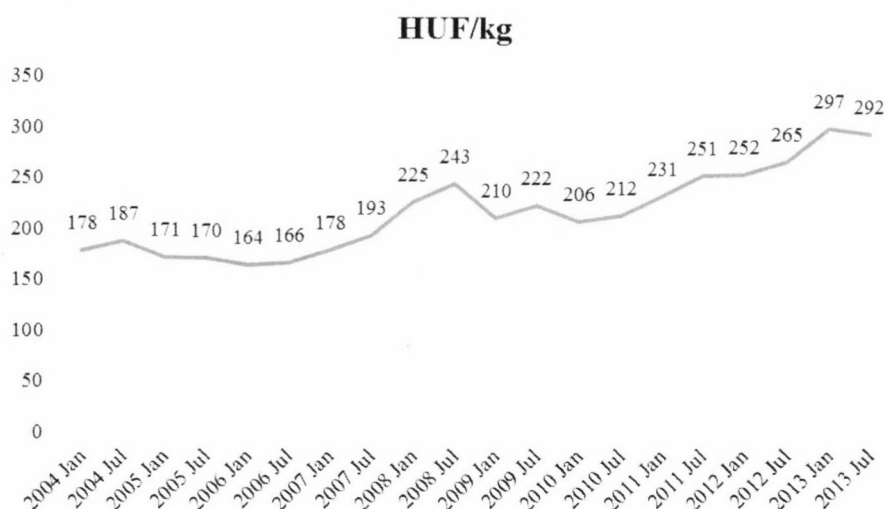


Figure 3. Monthly sale prices of chickens for slaughter in Hungary (2004-2013) [5]

3. Materials and methods

The goal of the research was to measure the effects on production indexes (mortality, live weight gain, feed conversion ratio) of a special feed additive mix containing vitamins [13, 14] and nutrient supplements [15, 16, 17] (Gastroferm M+C®, Jolovit®, Norovit-Amino Forte®, Phylamic®, Tetraselene-400-E®, Tetravit AD3E Forte® and Vitaplan DCP®), which were compared to those in the control group having no extra supplements. Based on the differences in the production parameters, we conducted the cost-benefit analysis of this special feed supplement mix. The research was done on a poultry farm in Bács-Kiskun county between June 2012 and March 2013.

The chickens were raised in four pens on the closed intensive poultry farm, each measuring 1000 m², and there were other service buildings. The pens had automatic feeding, drinking, heating and ventilation systems with a total capacity of 70,000 broiler chickens and all-in-all-out technology was applied. Mixed gender Ross 308 hybrids were raised to be ready for slaughter in 5 and half weeks, and after the second day of Week 5, the chickens were started to be transported to the slaughterhouse, and by Week 6, the pens became empty. This was followed by a week of cleaning, and another two weeks of the service period. Thus, the rearing period was 9 weeks altogether.

The day-old chicks in the trial were settled on the 29th of November 2012, and were transported for slaughter on the 7th of January 2013, when they were 38 days old. One of the four pens was used for the experimental group, another for the control group. Up to 17,800-18,200 birds were kept in one building. In the trial, we observed 17,965 experimental and 18,078 control animals which were sorted to two separate pens, but their housing and feeding conditions were identical. The stocking density was 17 chickens/m². In the flock an ad libitum feeding protocol for 6 weeks was applied.

In the trial, the control group didn't receive any vitamin or mineral supplements. The experimental group received

the vitamin- and nutrient supplements through the drinking system. The drinking protocol in the experimental group can be seen in Table 1. The average water consumption for 17,000 chickens in the flock was as follows: 2,200 litres on Week 2, 3,700 litres on Week 3, 5,000 litres on Week 4, 5,500 litres on Week 5. During the experiment, neither the experimental, nor the control group received antibiotics for curative or preventative reasons.

Evaluation of the production and economic indices

In the trial we used those production indices that can also be expressed in monetary units in order to conduct the economic analysis. Therefore, we analysed the slaughter weight, the feed conversion ratio and the mortality - as the length of the fattening was identical for both the experimental and the control groups. We conducted representative body weighings weekly to follow the live weight gain, and measured the total weight of broiler chickens marketed. We registered the total feed consumption for the entire fattening period. The number of mortalities and that of culled chickens and their live weight were also registered. We did pathology examinations for the chickens that died in order to determine the cause of death.

Based on the aforementioned recorded data we calculated the disposal rate (%) by summing the mortalities and cullings, which was divided by the number of day old chicks settled, and afterwards multiplied by 100. We calculated the number of broilers ready to slaughter by subtracting the sum of mortalities and cullings from that of day old chicks which were settled. We divided the total slaughter weight by the number of birds marketed (slaughtered), which led to the average slaughter weight. We calculated the feed conversion ratio via dividing the total feed consumption by the total slaughter weight.

We also calculated the broiler index in order to evaluate the efficacy of broiler chicken raising better. The broiler

index (EPEF - European Production Efficiency Factor) is a relative index without unit and being related to the profitability of broiler chicken production, which is calculated by using the following formula [10]:

$$\text{Broiler index: } \frac{\text{survival rate (\%)} \times \text{slaughter weight(kg)}}{\text{fattening period (days)} \times \text{feed conversation ratio}} \times 100.$$

Table 1. Drinking protocol in the experimental broiler chicken group

Age (days)	Product	Dose/1000 l water	Age (days)	Product	Dose/1000 l water
1.	Jolovit [®]	1000 ml	20.	Norovit-Amino Forte [®]	500 ml
2.	Jolovit [®]	1000 ml	21.	<i>Vaccination against Newcastle disease</i>	-
3.	Vitaplan DCP [®]	200 ml	22.	Norovit-Amino Forte [®]	500 ml
4.	Vitaplan DCP [®]	200 ml	23.	-	-
5.	Vitaplan DCP [®]	200 ml	24.	-	-
6.	Gastroferm M+C [®]	250 g	25.	-	-
7.	Gastroferm M+C [®]	250 g	26.	Tetravit AD3E Forte [®]	1000 ml
8.	Norovit-Amino Forte [®]	500 ml	27.	Tetravit AD3E Forte [®]	1000 ml
9.	Norovit-Amino Forte [®]	500 ml	28.	Tetravit AD3E Forte [®]	1000 ml
10.	Norovit-Amino Forte [®]	500 ml	29.	Tetravit AD3E Forte [®]	1000 ml
11.	Tetraselene -400-E [®]	1000 ml	30.	Gastroferm M+C [®]	500 g
12.	<i>Vaccination against contagious bursitis</i>	-	31.	Gastroferm M+C [®]	500 g
13.	Tetraselene -400-E [®]	1000 ml	32.	Gastroferm M+C [®]	500 g
14.	Tetraselene -400-E [®]	1000 ml	33.	-	-
15.	Tetraselene -400-E [®]	1000 ml	34.	-	-
16.	Gastroferm M+C [®]	250 g	35.	Jolovit [®] + Phylamic [®]	1000+2000ml
17.	Gastroferm M+C [®]	250 g	36.	Jolovit [®] + Phylamic [®]	1000+2000ml
18.	Gastroferm M+C [®]	250 g	37.	Phylamic [®]	2000 ml
19.	-	-	38.	-	-

In our financial analysis, the partial budgeting method which takes into account only those costs and revenues that change after administering the feed supplements. In the calculations, we multiplied the total slaughter weight by the market price in order to get total income. The total feed costs were calculated by multiplying the costs of the given diets (e.g. pre-starter, starter, grower, finisher) per unit by their quantities consumed, and summed them up. The price of day old chicks was multiplied by the number of birds settled, which resulted in the total cost of day old chicks. We calculated the gross margin as the margin between total income and the total cost of day old chicks and feeding [10].

The difference between the gross margin of the experimental group and that of the control group gave us the extra margin for the experimental group, and afterwards, having known the price and cost data of vitamin and nutrient supplements, we were able to calculate the benefit-cost ratio (B/C) and the return of the investment (ROI) of the application of the feed additive mix [Ózsvári].

Price and cost data

In the financial analysis, we used the procurement prices of the different – pre-starter, starter, grower and finisher - feeding diets and the slaughter price of the broiler chickens (Table 2).

Table 2. Cost and price data

ITEM	HUF/kg
Old day chicken price (HUF/chicken)	94.0
Pre-starter feeding diet price (HUF/kg)	121.0
Starter feeding diet price	118.6
Grower feeding diet price	114.2
Finisher feedign diet price	112.0
Broiler chicken slaughter price	295.0

The procurement prices of vitamin and nutrient supplements administered in the experiment were calculated as the average of the sale prices of three distributors - two private veterinary pharmacies and one big veterinary wholesaler and retailer corporation. The costs of feed supplements were calculated by multiplying their average price by their quantity used up.

4. Results and discussion

Return of the vitamin- and nutrient supplements used in broiler raising

The average length of broiler fattening was 38 days in both the experimental and the control groups. The vitamins and nutrients which were given as supplements in the experimental group via drinking water during the fattening

resulted in better production indices, compared to the control group (Figure 4).

Substantial improvement could be observed for cullings (experimental: 42, control: 74 animals) which together with the number of deaths diminished the disposal rate (%). The disposal rate was nearly 1 percentage point higher in the control group than in the experimental group. The mortality of chickens decreased significantly from Week 2 in the experimental group, compared to the control group. Furthermore, at the end of the 38-day fattening time, the slaughter chickens in the experimental group weighted 10 grams more on average, however their feed conversation rate was 13 grams lower. The broiler index was also significantly better, as it was 352 for the experimental group, and only 309 for the control group.

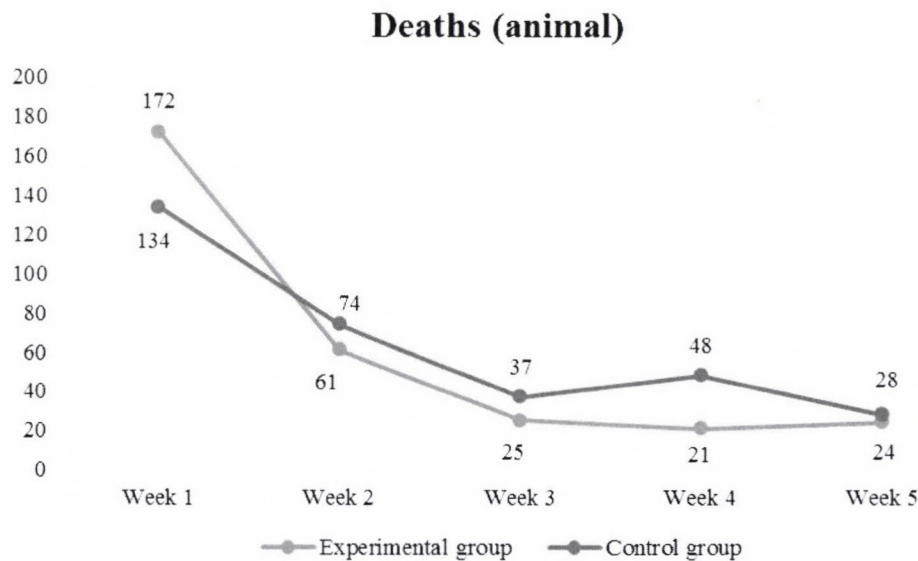


Figure 4. Mortality rate

The gross margin analysis for the control broiler chicken group can be seen in detail below:

Day old chicken price:	94 HUF/chicken
Day old chicken costs:	18,078 chickens x 94 HUF = 1,699,332 HUF
Total feed costs:	5,620 kg x 121 HUF/kg = 680,020 HUF (pre-starter diet)
	9,990 kg x 118.6 HUF/kg = 1,184,814 HUF (starter diet)
	27,100 kg x 114.2 HUF/kg = 3,094,820 HUF (grower diet)
	29,140 kg x 112 HUF/kg = 3,263,680 HUF (finisher diet)
Slaughter price:	295 HUF/kg
Total income:	295 HUF/kg x 39,077 kg = 11,527,715 HUF
Total gross margin:	11,527,715 HUF - (1,699,332 HUF + 680,020 HUF + 1,184,814 HUF + 3,094,820 HUF + 3,263,680 HUF) = 11,527,715 HUF - 9,922,666 HUF = 1,605,049 HUF
Average gross margin:	1,605,049 HUF/ 17,291 chickens = 92.8 HUF/ slaughter chicken

The gross margin analysis for the experimental broiler chicken group can be seen in detail below:

Day old chicken price:	94 HUF/chicken
Day old chicken costs:	17,965 chickens x 94 HUF = 1,688,710 HUF
Total feed costs:	5,500 kg x 121 HUF/kg = 665,500 HUF (pre-starter diet) 10,000 kg x 118.6 HUF/kg = 1,186,000 HUF (starter diet) 26,800 kg x 114.2 HUF/kg = 3,060,560 HUF (grower diet) 27,900 kg x 112 HUF/kg = 3,124,800 HUF (finisher diet)
Slaughter price:	295 HUF/kg
Total income:	295 HUF/kg x 41,093 kg = 12,122,435 HUF
Total gross margin:	12,122,435 HUF - (1,688,710 HUF + 665,500 HUF + 1,186,000 HUF + 3,060,560 HUF + 3,124,800 HUF) = 12,122,435 HUF - 9,725,570 HUF = 2,396,865 HUF
Average gross margin:	2,396,865 HUF/ 17,339 chickens = 138.2 HUF/ /slaughter chicken

The total vitamin- and nutrient supplements costs amounted to 72,650 HUF in the experimental group.

Due to the better production parameters, the experimental broiler chicken group generated 45.4 HUF/head extra gross margin and 41.5 HUF/head extra profit compared to the control group. The benefit-cost ratio (B/C) of application of vitamin and nutrient supplements was 10.8. In other words, on every HUF invested 10.9 HUF income was generated, that is, 9.9 HUF profit. The return on investment was 990%, which means a much higher yield than the current financial investment options (Annex 1).

The results of the experiment show that the application of feed additive mix containing Gastroferm M+C®, Jolovit®, Norovit-Amino Forte®, Phylamic®, Tetraselene-400-E®, Tetravit AD3E Forte® and Vitaplan DCP® makes broiler chicken production more profitable.

5. Conclusions

Based on the cost-benefit analysis it can be stated that for broiler chicken production, it is economically beneficial to apply mixtures of vitamin and nutrient supplements administered in the drinking water, but further experiments are required to find the optimal feed additive mixture.

References

- [1] **EFSA.**: 2015. The European Union summary report on trends and sources of zoonoses, zoonotic agents and food-borne outbreaks in 2013. EFSA Journal, Vol. 13 No. 1, pp. 3991. <http://dx.doi.org/10.2903/j.efsa.2015.3991>
- [2] **OECD, FAO.**: 2011. Agricultural Outlook 2011. http://dx.doi.org/10.1787/agr_outlook-2011-en
- [3] **González-García S., Gomez-Fernández Z., Dias A. C., Feijoo G., Moreira M. T., Arroja L.**: 2014. Life Cycle Assessment of broiler chicken production: a Portuguese case study. Journal of Cleaner Production, Vol. 71, pp. 125-134. <http://dx.doi.org/10.1016/j.jclepro.2014.03.067>
- [4] **Kállay B.**: 2012. Töretlen a baromfiipar globális fejlődése. Baromfiágazat, Vol. 12 No. 4, pp. 6-14.
- [5] **Hoinville L. J., Alban L., Drewe J. A., Gibbens J. C., Gustafson L., Häsler B., Saegerman C., Salman M., Stärk K. D. C.**: 2013. Proposed terms and concept for

describing and evaluating animal-health surveillance systems. Preventive Veterinary Medicine, Vol. 112 No. 1-2, pp. 1-12.

<http://dx.doi.org/10.1016/j.prevetmed.2013.06.006>

[6] **FAPRI, ISU.**: 2011. 2011 World Agricultural Outlook. Food and Agricultural Policy Research Institute, Iowa State University.

[7] **Rabobank.**: 2011. Global Meat Demand 2010–2030. Presentation by Nan-Dirk Mulder, Rabobank International. International poultry Council Meeting, Rome, April 2011.

[8] **Blaskó B., Cehla B., Kiss I., Kovács K., Papis M., Madai H., Nagy A. Sz., Nábrádi A., Pupos T., Szöllősi L., Szűsz I.**: 2011. Állattenyésztési ágazatok ökonómiája. Debreceni Egyetem, Nyugat-Magyarországi Egyetem, Pannon Egyetem.

[9] **Finkensiep A.**: 2012. Leistungsteigern statt Kosten senken. (Increase the performance instead of reducing the costs: vet fees as high-yield investment in animal health.) Praktische Tierarzt Hannover: Schlütersche Verlagsgesellschaft GmbH & Co. KG

[10] **Ózsvári L.**: 2016. Mennyi veszteséget okoznak a betegségek a baromfitartásban? Baromfiágazat, Vol. 16 No. 1, pp. 70-75.

[11] **Feldman Zs.**: 2013. Szakminisztériumi előadás. III. Tejágazati Konferencia, Budapest, november 21.

[12] **Bakosné Böröcz M., Fogarassy C.**: 2011. A hazai húsmarhatartás környezeti értékelése és externáliáinak vizsgálata benchmarking módszerrel. Gazdálkodás, Vol. 55 No. 2, pp. 181-185.

[13] **Leshchinsky T. V., Klasing K. C.**: 2001. Relationship Between the Level of Dietary Vitamin E and the Immune Response of Broiler Chickens. Poultry Science, Vol. 80 No. 11, pp. 1590-1599. <http://dx.doi.org/10.1093/ps/80.11.1590>

[14] **Habibian M., Ghazi S., Moeini M. M., Abdolmohammadi A.**: 2013. Effects of dietary selenium and vitamin E on immune response and biological blood parameters of broilers reared under thermoneutral or heat stress conditions. International Journal of Biometeorology, Vol. 58 No. 5, pp. 741-752.

<http://dx.doi.org/10.1007/s00484-013-0654-y>

[15] **Saripinar A. D., Aksu T., Özsoy B., Baytok E.**: 2010. The Effects of Replacing Inorganic with a Lower

Level of Organically Complexed Minerals (Cu, Zn and Mn) in Broiler Diets on Lipid Peroxidation and Antioxidant Defense Systems. Asian-Australasian Journal of Animal Sciences, Vol. 23 No. 8, pp. 1066-1072.
<http://dx.doi.org/10.5713/ajas.2010.90534>

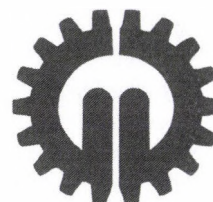
[16] Saripinar A. D., Aksu T., Özsoy B.: 2010. The Effects of Lower Supplementation Levels of Organically Complexed Minerals (zinc, copper and manganese) Versus

Inorganic Forms on Hematological and Biochemical Parameters in Broilers. Kafkas Üniversitesi Veteriner Fakültesi Dergisi, Vol. 16 No. 4., pp. 553-559.

[17] Stef D. S., Gergen I.: 2012. Effect of mineral-enriched diet and medicinal herbs on Fe, Mn, Zn, and Cu uptake in chicken. Chemistry Central Journal, Vol. 6 No. 1, pp. 19. <http://dx.doi.org/10.1186/1752-153X-6-19>

Annex 1. Economic analysis of the application of broiler chicken vitamin and nutrient supplements

Parameters	Control group	Experimental group	Difference
<i>Number of settled birds</i>	18 078	17 965	-113
<i>Deaths (birds)</i>	713	584	-129
<i>Deaths (kg)</i>	438.2	262.7	-175.5
<i>Mortality (%)</i>	3.9	3.3	-0.6
<i>Cullings (birds)</i>	74	42	-32
<i>Cullings (kg)</i>	162.8	96.6	-66.2
<i>Disposal rate (%)</i>	4.4	3.5	-0.9
<i>Number of ready to slaughter birds</i>	17 291	17 339	+48
<i>Total slaughter weight (kg)</i>	39 077	41 093	+2 016
<i>Average slaughter weight (kg/chicken)</i>	2.26	2.37	+0.11
<i>Total feed consumption (kg)</i>	71 850	70 200	-1 650
<i>Feed conversion ratio</i>	1.84	1.71	-0.13
<i>Broiler index</i>	309	352	+43
<i>Total income (HUF)</i>	11 527 715	12 122 435	+594 420
<i>Total feed costs (HUF)</i>	9 922 666	9 725 570	-197 196
<i>Day old chicken costs (HUF)</i>	1 699 332	1 688 710	-10 622
<i>Total gross margin (HUF)</i>	1 605 049	2 396 865	+791 816
<i>Average gross margin (HUF/slaughter chicken)</i>	92.8	138.2	+45.4
<i>Total vitamin- and nutrient supplement costs (HUF)</i>	0	72 650	+72 650
<i>Average supplement costs (HUF/slaughter chicken)</i>			4.2
<i>Average profit (HUF/slaughter /chicken)</i>			41.5
<i>Benefit-cost (B/C) ratio</i>			10.9
<i>Return on investment (ROI, %)</i>			990



THE EFFECT OF ATMOSPHERIC DBD PLASMA ON SURFACE ENERGY AND SHEAR STRENGTH OF ADHESIVELY BONDED POLYMER

Author(s):

H. Al-Maliki – G. Kalácska

Affiliation:

Szent István University, Institute for Mechanical Engineering Technology, Páter Károly street 1, H-2100 Gödöllő, Hungary

Email address:

haidrlatif@gmail.com, kalacska.gabor@gek.szie.hu

Abstract

Virgin and surface treated polymers are often used in food-processing and packaging industry. Atmospheric cold plasma treatment can effectively modify the adhesive behaviour of the surfaces. An extruded (smooth) surface of PA6 E and UHMW-PE HD1000 have been treated by DBD plasma under air atmosphere conditions. The major objectives of the present study are exploring the effect of DBD plasma on the surface energy and adhesive bonding capability of the polymer. Where the surface energy has calculated, based on Owens-Wendt method and the adhesive (lap-shear) test carried out DIN EN 1465 standard with applying different adhesive types. The results expose that the DBD plasma treatment enhances the adhesive bonding capability due to increased surface energy and modified the topography and the chemical composition of the surface. However, PA6 E shows higher tensile shear strength compared to UHMW-PE HD1000 because of the higher polarity of PA6 E after treatment.

Keywords

DBD cold plasma treatment, surface energy, wettability, shear strength, polymer adhesive bonding

1. Introduction

Nonpolar material and polymers (in particular) have low surface energy thus low adhesion force. A hydrophilic surface is required to obtain adequate adhesion to other material types. On the other hand, the superhydrophobic surface is required for several applications [1]. The development in the testing of sticking technologies of machine parts made of engineering plastics comes into the foreground rather continually [2]. Vehicle industry is a good example of importance to explore quick high strengths and elastic component contacts [3], this made the surface treatment required to promote surface properties. Many different methods have been developed for polymer

modification, such as chemical vapor deposition, soft lithographic imprinting, sol-gel method, etc. [1]. However, there are many current and emerging wetting and adhesion issues which require an additional surface processing to enhance interfacial surface properties [4]. Plasma treatment has become the best method to improve the surface wettability of polymers [5]. Among studies have been extensively investigated low-pressure plasma techniques (plasma immersion ion implantation) and their effects on the surface modification of various polymers [6, 7]. Recently, atmospheric-pressure plasma has been rising interest to use for surface modification of polymeric materials instead of low-pressure plasma in the academic research and industrial applications, due to its vacuum less system, operable under atmospheric pressure and its effects of ablation crosslinking and activation.

In the present study, two commercial polymers most commonly used in the industrial, agricultural and medical applications have been selected: Polyamide 6 Extruded (PA 6 E) and Ultra High Molecular Weight Polyethylene High Density 1000 (UHMW-PE HD1000).

In literature, the results showed that atmospheric cold plasma treatment in a low-pressure increase the surface energy of PE and they found that plasma improves the using of PE in the medical applications [8] and it enhances the shear strength of adhesive bonding also [9]. In parallel, PA 6 illustrated better surface energy and adhesive bonding over plasma treatment [10].

The main aim is finding a correlation between pristine and treated surface properties from the point of surface energy, thus adhesion and shear strength of adhesive bonding for polymer/polymer and polymer/ steel pairs for the selected polymers.

2. Materials and methods

Materials and preparation

Two types of commercially available engineering polymers (distributed by Quattroplast Ltd., Hungary and produced by Ensinger GmbH, Germany), were used in bulk

conditions: Polyamide 6 Extruded or PA6 E grade Docamid-6-E and Ultra High Molecular Weight Polyethylene High Density 1000 or UHMW-PE HD1000 grad Docalene-HD1000. The mechanical properties of the materials are as follows: PA6 E (elastic modulus $E = 3300$ MPa, tensile strength $\sigma = 79$ MPa, glass transition temperature $T_g = 45$ °C), UHMW-PE HD1000 (elastic modulus $E = 680$ MPa, tensile strength $\sigma = 22$ MPa, Melting temperature= 135 °C). Structural steel (S 235 JR N) was used as counterfaces for the adhesive test, it is one of the most common type of the general-purpose, non-alloy steels with low carbon content (0.17 %). In general, its $R_m = 400\text{-}500\text{N/mm}^2$ (Ferroglobus Ltd, Hungary). Different adhesives (Henkel Loctite, Hungary) were applied with bond line (thickness) 0.1 mm: Loctite 406 (Ethyl cyano-Acrylate), Loctite 3035 (Methacrylate-

Acrylic), Loctite 9466 (Two-component Epoxy), Loctite 330 (Urethane metacrylate ester- Acrylic) and Loctite 770 (Aliphatic amine-Primer, Cyanoacrylate) as primary activator, detailed technological steps specified and properties of each glue are available in (Technical Data Sheet (TDS) of Loctite) [11]. The polymer applied very smooth (extruded) surfaces. Before testing, the samples were cleaned in an ultrasonic bath with distilled water and 96% ethanol (Reanal, Hungary). The surface energy evaluation samples were prepared in disc-shaped samples with a diameter of 10 mm and thickness of 2 mm. For adhesive test the samples (polymer and steel) were prepared in a rectangular shape with dimensions: 25.4 mm x 100.0 mm x 2.0 mm as shown in Figure 1. The polymer samples were cut from extruded plate.

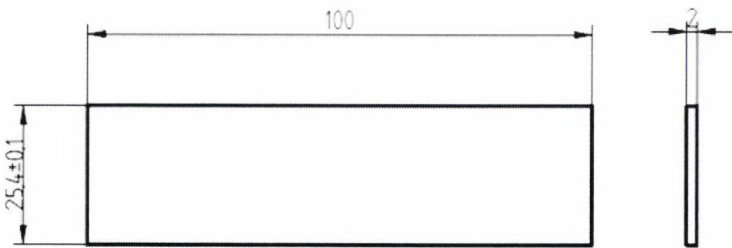


Figure 1. Sample dimensions of adhesive test

Table 1. illustrates the materials and used adhesives (the Loctite made a choice based on Technical Data Sheet (TDS) recommendation) [11].

Table 1. The planning material and adhesives for the bonding test

Bonded materials	Adhesive	Primary activator
PA6E – PA6E	Super glue: Loctite 406	-
	Two-component Epoxy: Loctite 9466	-
	Structural adhesive: Loctite 330	-
PA6E – S235 Steel	Super glue: Loctite 406	-
	Two-component Epoxy: Loctite 9466	-
	Structural adhesive: Loctite 330	-
HD1000- HD1000	Super glue: Loctite 406	Primary: Loctite 770
	Structural adhesive: Loctite 3035	-
HD1000– S235 Steel	Super glue: Loctite 406	Loctite 770 only for HD1000
	Structural adhesive: Loctite 3035	-

Plasma treatment

The atmospheric pressure ambient air plasma was generated by DCSBD plasma source. The principle of DCSBD plasma is based on a coplanar DBD where comb-shape electrodes are embedded in a dielectric. The diffuse plasma is generated in thin 0.3 mm thick flat layer on alumina ceramic which designates the DCSBD to be used especially for treatment of flat surfaces. The DCSBD electrode system was powered by AC HV source of

frequency approx. 14 kHz and voltage approx. 20 kV peak-to-peak and the total power in plasma during the experiments was 400 W. The area of generated plasma of DCSBD is 170 cm², thus the surface energy density and volume energy density at power of 400 W are approximately 2 W cm² and 80 W cm³, respectively. The DCSBD plasma is described in detail [12]. The plasma treatment was performed in dynamic treatment mode and the distance between the treated polymer surface and DCSBD ceramic was 0.3 mm. The treatment has been done

under air atmosphere conditions ($T = 23^{\circ}\text{C}$, $H = 50\%$), the apparatus shown in Figure 2. The treatment time for each specimen was 1 min.

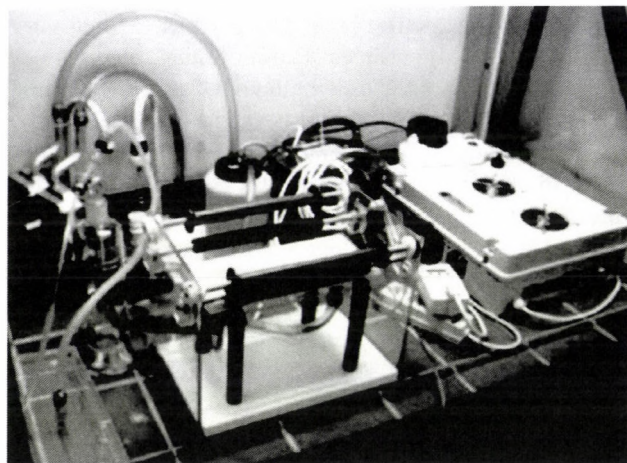


Figure 2. DBD laboratory test equipment used for polymer surface

The marking system of bonded specimens

The different combination of specimens must be distinguished, therefore the following identification has been introduced.

PA6 example:

0_PA6_PA6_406_11_1

- 1. marking: It indicates the condition of the surface (0-pristine surface without plasma treatment, 1-with cold plasma (DBD) treated surface).
- 2. and 3. marking: refer to the conjugate materials.
- 4. marking: refers to the type of adhesive.
- 5. marking: refers to the use of the activator. If 11 means activator was used for both surfaces, 00 not one of them, 10, 01 – only one surface.
- 6. marking: refers to the serial numbers of the specimen in the bonding test (from 1 to 5).

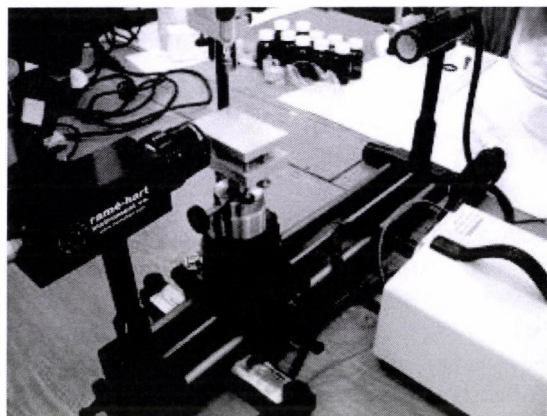


Figure 3. SEE System apparatus which used to evaluate the contact angle of polymer

Contact angle measurements

Contact angle measurements were done by the static sessile drop method at 23°C , with double distilled water and diiodomethane (Sigma–Aldrich, Reagent Plus 99% grade), applying the SEE System apparatus (Ramé hart 100-00) as shown in Figure 3. A Hamilton syringe was used to inject $2\ \mu\text{l}$ droplets. Each result of the contact angle is an average of 5 measurements, performed always on previously non-wetted parts of the samples. The surface energy component calculations based on Owens-Wendt method.

Adhesive test

The tensile test was carried out the ISO 527-1 standard, the overlap joints made according to the DIN EN 1465 standard with a lap-shear test.

The requirements for bonding of the specimens:

- 5 repeated bonding at the same time with a given materials.
- Overlapping has to be $12.5 \pm 0.1\ \text{mm}$.
- The same normal force (5 N) applied during curing.
- Stick-free bonding-jig to prepare the bond.

The experiments were carried out according to the glue producer's (Henkel Loctite, Hungary) recommendations (Technical Data Sheet – TDS – of Loctite):

- Rough cleaning with water.
- Degreasing of the surfaces with Loctite SF 7063.
- Creating the bonds in the jig.

The two plates were bonded to each other by using the apparatus which made from PTFE to reduce the specimens sticking (knowing, hydrophobic surface of PTFE) as in Figure 4. The specimens prepared adequately on a tensile test machine, according to DIN EN 1465 standard (as mentioned). Although the standard mentions more solutions onto the forming of the specimens, the simple overlap joining was selected. The adhesive test was done within 24 hours after the plasma treatment, To ensure a full effect of DBD plasma. Where the best results of plasma surface modification were performed immediately after treatment, then the surface starts recovering to the reference state after 24 hours [13, 1]. The overlap area of the polymer plates (immediately after plasma treatment) coated with a primary activator (for the glues that have been recommended to use them with primary activator) before adding the adhesives. The glue amounts are 0.035 ml of Loctite 406 and 0.1 ml for the other structural adhesives after the adhesives adding, the plates set up with each other in the apparatus. The test has been repeated 5 times for each polymer and different pairs polymer/polymer and polymer/steel. The tensile test was managed by a (Zwick Roell Z100) tensile machine as shown in Figure 5, with 1.3 m/min pulling speed and 100kN maximum tensile load. The shear strength is equal to the maximum failure force dividing the bonded area.

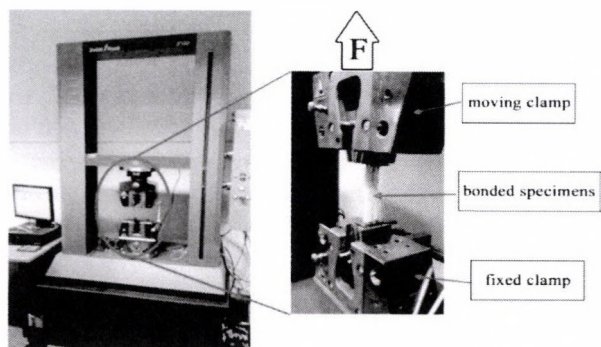


Figure 4. Zwick Roell Z100 tensile test machine

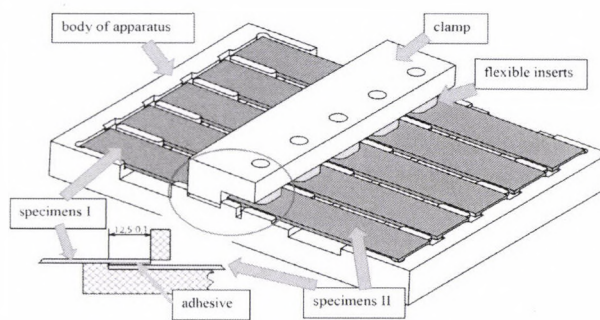
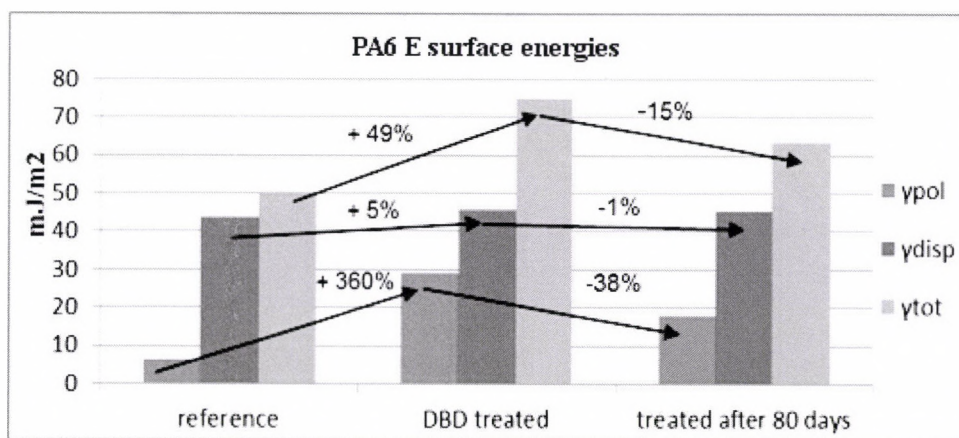


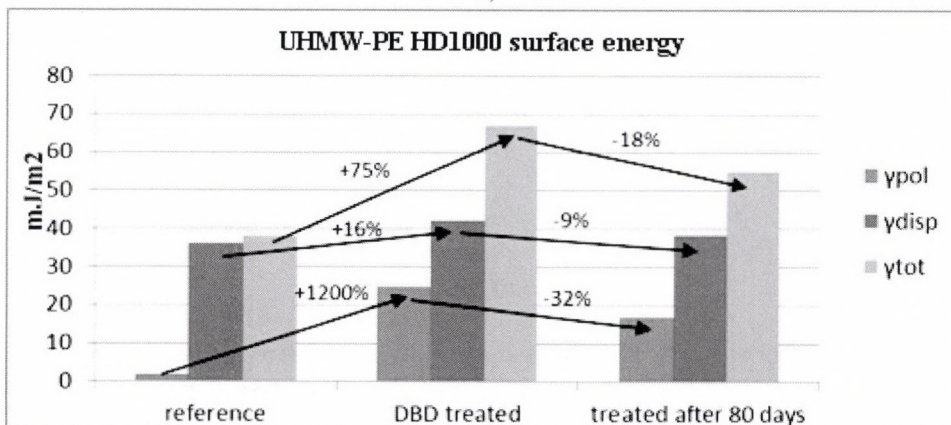
Figure 5. The apparatus which used to bond the pairs

Table 2. Contact angle and surface energy values for pristine and treated surfaces

Sample	Θ_w (deg)	Θ_{CH2I2} (deg)	$\gamma_{pol}(mJ/m^2)$	$\gamma_{disp}(mJ/m^2)$	$\gamma_{tot}(mJ/m^2)$
PA6 untreated	70 ± 7.2	32 ± 2.1	6.3	43.6	50.0
PA6 treated	21 ± 0.5	26 ± 1.5	29.1	45.8	74.9
PE1000 untreated	87 ± 0.4	47 ± 1.9	1.9	36.2	38.1
PE1000 treated	35 ± 2.3	35 ± 5.8	24.7	42.2	67



a)



b)

Figure 6. The change in the surface energy values after DBD plasma treatment with 24 hours and 80 days; (a) PA6 E and (b) UHMW-PE HD1000

3. Results and discussion

Surface energy evaluation

The Table 2. Shows the surface contact angle (water and diiodomethane) and surface energy components: polar (γ_{pol}), dispersive (γ_{disp}) and total energy(γ_{tot}) values. Where Figure 6 illustrates the surface energies change for pristine and a DBD plasma treated surface (after 24 hours and 80 days shift time). It can be seen the significant increase of wettability(decrease the contact angles), thus the surface energies. In the case of PA6 E due to DBD plasma treatment, the surface energy increased based on Owens-wendt calculation. Both the polar and disprive components increased, in particular, the polar component increased 350% more than the original state. The hydrophobic recovery decreases the polar and disprive components, thus the total surface energy with the function

of time, where the polarity decreased 38% and the total energy 15% after 80 days shift time as shown in Figure 6a.

On the other hand, UHMW-PE HD1000 surface energies also increased due to DBD treatment based on Owens-wendt calculation, but the results have Observed that the increasing percent of the surface energy was higher relative to the original surface energy values compared to PA6 E. Where the polar component increased more than 1200% after treatment, within 24 hours. Nonetheless, the action of Hydrophobic recovery decreased the polar and disprive thus total components with time function, where the polar component and total surface energy expose 32% and 18% less, respectively, after 80 days shift time as shown in Figure 6b. The change in the surface energies with the function of time is very slight (they can be described as negligible) compared to the change due to the effect of DBD plasma treatment.

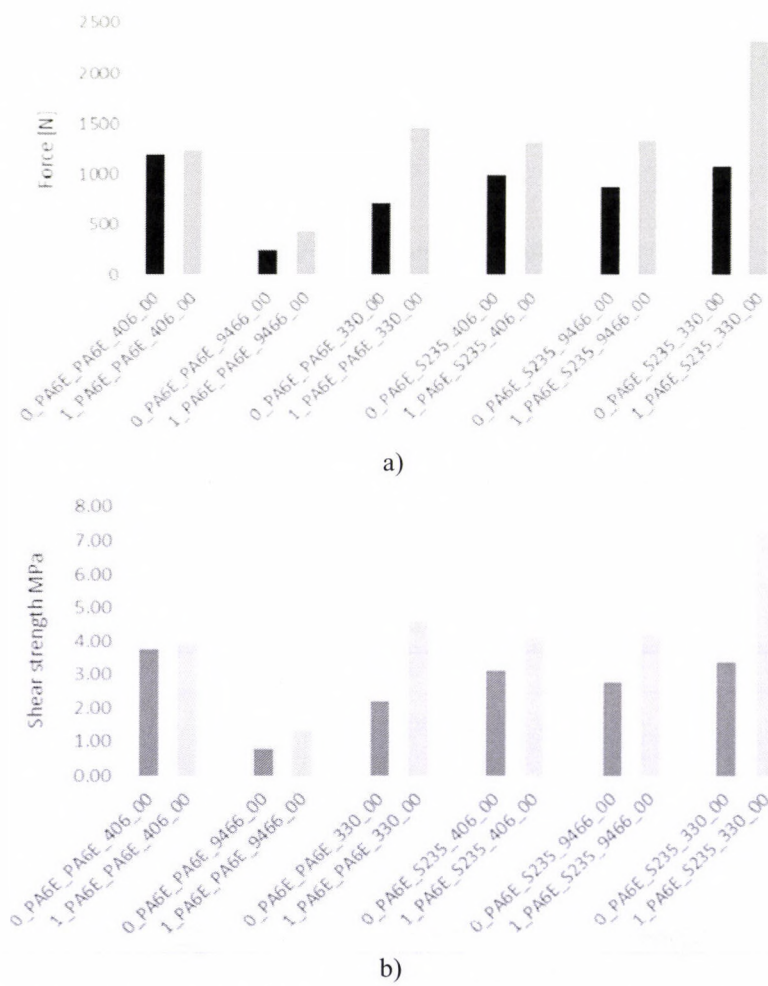


Figure 7. Lap-shear test results of PA6 E (polymer/polymer and polymer/steel pairs) with different adhesives for pristine and DBD plasma treated polymer: (a) average of maximum tensile test and (b) average tensile shear strength

Adhesive tests

The average of maximum force and average shear strength of five repetitions (polymer/polymer and polymer/steel joints) summarized in Figure 7 for PE6 E and Figure 8 for

UHMW-PE HD1000. The statistical deviation of PA6 E on the shear strength more low after DBD plasma treatment, whereas slightly reduce due to plasma treatment for UHMW-PE HD1000, irrespective the counterface. In general, the DBD plasma enhances the shear strength,

irrespective, adhesive type and counterface as a consequence to increasing the polymer polarity after plasma treatment and modified the topography and the chemical composition. Using different groups of adhesives for each polymer makes the comparison not easy. Generally, PA6 E average shear strength is higher than UHMW-PE HD1000, it is expected, according to the higher polarity which PA6 E was exposed after plasma treatment.

In the case of PA6 E, Loctite 330 shows the highest increasing in the shear strength and Loctite 406 shows the lowest change of shear strength due to plasma treatment. In spite of increased shear strength after plasma treatment for Loctite 406 and Loctite 9466, but they still show comparable shear strength to the pristine surfaces. Where the tensile shear strength of Loctite 406, Loctite 9466 and Loctite 330 increased after plasma treatment: 4%, 70%, and 110% respectively for polymer/polymer joints and:

34%, 53%, and 116% respectively for polymer/steel joint. The failure type change from adhesive failure on one or two surfaces of the pristine surface to cohesive in the adhesive layer failure or adhesive failure on one or two surfaces after plasma treatment of almost 5 repetitions expect polymer/polymer joints with Loctite 406 where kept the same failure type.

In contrast, polymer/polymer joints of UHMW-PE HD1000 expose higher shear strength compared to polymer/steel joints during lap-shear test regardless adhesive type. The increasing in the tensile shear strengths of Loctite 406 and Loctite 3035 joints are 88% and 40% respectively for polymer/polymer joints, and: 1% and 6% respectively for polymer/steel joints. The failure type of 5 repetitions is an adhesive failure on one or two surfaces of the pristine surface and it has remained the same failure type after treatment.

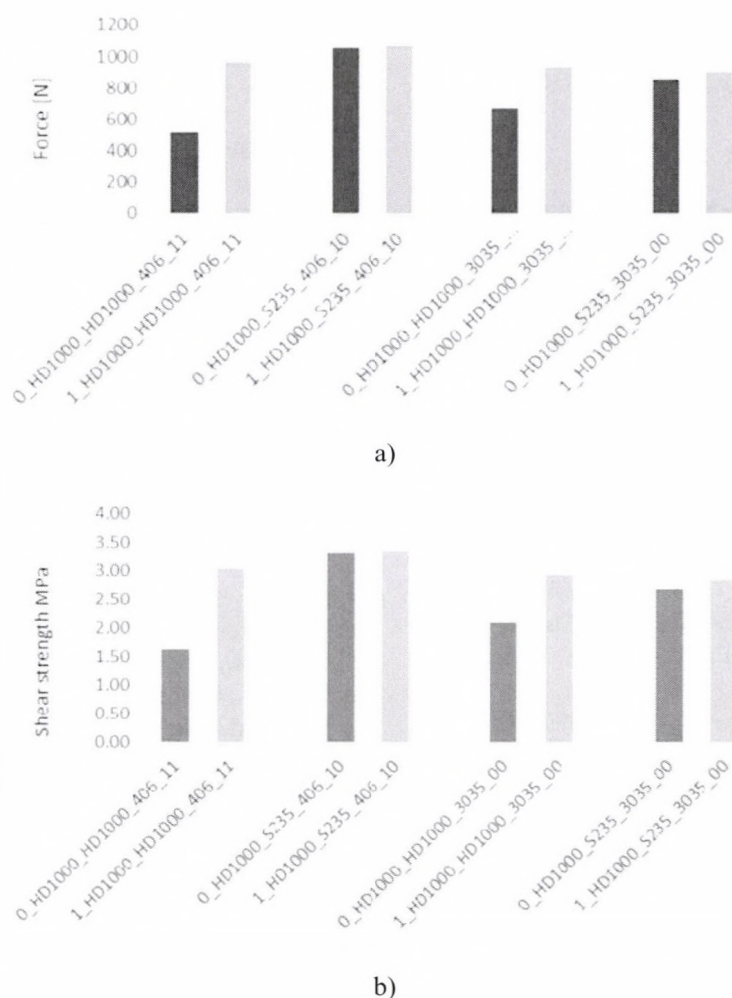


Figure 8. Lap-shear test results of UHMW-PE HD1000 (polymer/polymer and polymer/steel pairs) with different adhesives for pristine and DBD plasma treated polymer: (a) average of maximum tensile test and (b) average tensile shear strength

4. Conclusion

Atmospheric DBD plasma is a very efficient technique to modify the polymer surface. The results of PA6 E and

UHMW-PE HD1000 surface modified by DBD plasma under air conditions show:

- Increase the wettability of polymer (decrease the contact angle value) and the surface energy components based

on Owens-Wendt method, where the polar component of PA6 E increased more than 350% for PA6 E and 1200% for UHMW-PE HD1000.

- Enhance the average tensile shear strength of adhesively bonded pairs of different couples (polymer/polymer and polymer/steel) and different adhesives during lap-shear test (carried out DIN EN 1465 standard) due to DBD plasma treatment due the surface characterizations modification after plasma treatment. Generally, PA6 E shows higher change in shear strength after plasma treatment because of the high polarity of PA6 E. Regardless pairs type of PA6 E, Loctite 330 shows the highest shear strength, where increased (110-120%) after treatment compared to the pristine surface. However, UHMW-PE HD1000 exposed converse behaviour after plasma treatment, where polymer/polymer pairs showed higher shear strength compared to polymer/steel pairs irrespective the adhesive type. The increase of UHMW-PE HD1000 (polymer/polymer pairs) was (40-90%) compared to the pristine surface.

Acknowledgements

The present research is supported by OTKA K 113039.

References

- [1] **Karoly Z., Klebet Sz., Al-Maliki H., Pataki T.:** 2016. Comparison of NPIII and DBD Plasma in term of wettability of PTFE and PA6, The international conference of the Carpathian Euro-Region's specialists in industrial (CEurSIS 2016), Baia Mare, Romania, June 2-4, 2016, pp. 47-50.
- [2] **Ebnesajjad S.:** 2015. 17 - Surface Treatment of Fluoropolymers for Adhesion, Fluoroplastics (Second Edition), pp. 564-588.
<https://doi.org/10.1016/B978-1-4557-3197-8.00017-1>
- [3] **Keresztes R., Szakál Z., Kári-Horváth A., Pataki T., Sarankó Á.:** 2016. Tensile behaviour of adhesive overlap joints with PP, UHMW-PE, and PTFE polymers, The international conference of the Carpathian Euro-Region's specialists in industrial (CEurSIS 2016). Baia Mare, Romania, June 2-4, 2016, pp. 51-56.
- [4] **Wolf R., Sparavigna A. C.:** 2010. Role of Plasma Surface Treatments on Wetting and Adhesion, Engineering, Vol. 2, pp. 397-402.
<http://dx.doi.org/10.4236/eng.2010.26052>
- [5] **Takahashi T., Hirano Y., Takasawa Y., Gowa T., Fukutake N., Oshima A., Tagawa S., Washio M.:** 2011. Change in surface morphology of polytetrafluoroethylene by reactive ion etching, Radiation Physics and Chemistry, Vol. 80 No. 2, pp. 53-256.
<http://dx.doi.org/10.1016/j.radphyschem.2010.07.042>
- [6] **Mandolino C., Lertora E., Gambaro C., Bruno M.:** 2014. Improving adhesion performance of polyethylene surfaces by cold plasma treatment, Meccanica Vol. 49, pp. 2299-2306. <http://dx.doi.org/10.1007/s11012-014-9993-y>
- [7] **Kalácska G., Zsidai L., Keresztes R., Tóth A., Mohai M., Szépvölgyi J.:** 2012. Effect of nitrogen plasma immersion ion implantation of polyamide-6 on its sliding properties against steel surface, Wear, Vol. 290-291, pp. 66-73.
<http://dx.doi.org/10.1016/j.wear.2012.05.011>
- [8] **Preedy E. C., Emmanuel B., Evans S. L., Perni S., Prokopovich P.:** 2014. Adhesive forces and surface properties of cold gas plasma treated UHMWPE, Colloids and Surfaces A: Physicochem. Eng. Aspects, Vol. 460, pp. 83-89.
<http://dx.doi.org/10.1016/j.colsurfa.2014.03.052>
- [9] **Mandolino C., Lertora E., Gambaro C.:** 2014. Effect of cold plasma treatment on surface roughness and bonding strength of polymeric substrates, Key Engineering Materials, Vol. 611-612, pp. 1484-1493.
<http://dx.doi.org/10.4028/www.scientific.net/KEM.611-612.1484>
- [10] **Schäfer J., Hofmann T., Holtmannspötter J., Frauenhofer M., von Czarnecki J., Hans-Joachim G.:** 2015. Atmospheric-pressure plasma treatment of polyamide 6 composites for bonding with polyurethane, Journal of Adhesion Science and Technology, Vol. 29 No. 17, pp. 1807-1819.
<http://dx.doi.org/10.1080/01694243.2015.1037380>
- [11] **Henkel, TDS Document Search,** Online at <http://tds.henkel.com/tds5/search.asp>, accessed on 10 May 2017.
- [12] **Cernák M., Cernáková L., Hudec I., Kováčik D., Zahoranová A.:** 2009. Diffuse Coplanar Surface Barrier Discharge and its applications for in-line processing of low-added-value materials, European Physical Journal: Applied Physics, Vol. 47, pp. 1-6.
<http://dx.doi.org/10.1051/epjap/2009131>
- [13] **Novák I., Popelka A., Luyt A. S., Chehimi M.M., Špírková M., Janigová I., Kleinová A., Stopka P., Šlouf M., Vanko V., Chodák I., Valentin M.:** 2013. Adhesive properties of polyester treated by cold plasma in oxygen and nitrogen atmospheres, Surface & Coatings Technology, Vol. 235, pp. 407-416.
<http://dx.doi.org/10.1016/j.surfcoat.2013.07.057>

CONTENTS OF 31/2017

THE APPLICATION OF LIFE CYCLE ASSESSMENT IN CIRCULAR ECONOMY

K. Tóth Szita^{1,2}

¹Faculty of Economics, University of Miskolc, H-3515 Miskolc, Hungary

²LCA Centre, Iglói street 2, H-3519 Miskolc, Hungary

5

THE DEVELOPMENT OF A CIRCULAR EVALUATION (CEV) TOOL – CASE STUDY FOR THE 2024 BUDAPEST OLYMPICS

Cs. Fogarassy¹ – A. Kovacs² – B. Horvath¹ – M. Borocz¹

¹Climate Change Economics Research Centre, Szent István University, Páter Károly street 1., H-2100 Gödöllő, Hungary

²Department of Operations Management and Logistics, Szent István University, Páter Károly street 1., H-2100 Gödöllő, Hungary

10

THE SUSTAINABILITY AND USAGE EFFICIENCY OF CONVECTIONAL GEOTHERMIC ENERGY PRODUCTION

J. Nagygál – L. Tóth

Szent István University, Faculty Mechanical Engineering, Páter K. street 1., H-2100 Gödöllő, Hungary

21

DRYING CHARACTERISTICS AND QUALITY OF PEAR UNDER HYBRID DRYING (MID-INFRARED-FREEZE DRYING)

T. Antal

University of Nyíregyháza, Institute of Engineering and Agricultural Sciences, Department of Vehicle and Agricultural Engineering, Kótaji Str. 9-11., H-4400 Nyiregyhaza, Hungary.

33

THE COST-BENEFIT ANALYSIS OF APPLICATION OF VITAMIN AND MINERAL SUPPLEMENTS IN BROILER CHICKEN PRODUCTION

L. Ózsvári¹ – R. Tisóczki¹ – Á. Bartha² – M. K. Horváth²

¹University of Veterinary Medicine Budapest, Department of Veterinary Forensics, Law and Economics, István street 2, H-1078 Budapest, Hungary

²Szent István University, Faculty of Economics and Social Sciences, Climate Change Economics Research Centre, Páter Károly street 1, H-2100 Gödöllő, Hungary

45

THE EFFECT OF ATMOSPHERIC DBD PLASMA ON SURFACE ENERGY AND SHEAR STRENGTH OF ADHESIVELY BONDED POLYMER

H. Al-Maliki – G. Kalácska

Szent István University, Institute for Mechanical Engineering Technology, Páter Károly street 1, H-2100 Gödöllő, Hungary

52

The “Circular Economy scientific special issue” was supported by the HU03-0005-C1-2014 project which is part of the EEA Grants 2009-2014 Renewable Energy programme area.
www.eeagrants.org, www.egt-newenergy.szie.hu ”



